

**TKK Helsinki University of Technology
Faculty of Engineering and Architecture
Department of Structural Engineering and Building Technology**

Nicodemus Jansson

The effect of variable hydraulic pressure on a post-tensioned concrete slab

*Master's thesis submitted for the grading
as part of the degree of Master of Science
(Technology)*

Espoo, March 26, 2008

*Supervisor: Professor Jari Puttonen
Instructor: M.Sc. (Tech.) Teuvo Meriläinen*

HELSINKI UNIVERSITY OF TECHNOLOGY
ABSTRACT OF THE MASTER'S THESIS

Author:	Nicodemus Jansson
Title:	The effect of variable hydraulic pressure on a post-tensioned concrete slab
Date:	March 26, 2008
Number of pages:	85 + Appendices
Faculty:	Faculty of Engineering and Architecture
Department:	Department of Structural Engineering and Building Technology
Professorship:	Structural Engineering
Supervisor:	Professor Jari Puttonen
Instructor:	M.Sc. (Tech.) Teuvo Meriläinen
<p>The aim of this Master's thesis is to challenge the engineering problem of how to design a post-tensioned concrete slab exposed to variable hydraulic pressure and ensure the watertightness of the slab. The study is done using the Eurocodes and ADAPT-software.</p> <p>Post-tensioning designs usually involve a reversed parabola tendon profile, but due to variable hydraulic pressure, this tendon profile was not suitable for this design. Instead, a design solution involving straight tendons at the top and bottom of the slab was found with ADAPT-software. These straight tendons can resist vertical loads in both directions and are also useful for crack mitigation. The design solution obtained with ADAPT-software was manually verified by code-based methods.</p> <p>The watertightness of the slab was ensured by crack control in ADAPT-software and then double-checked by manually calculating the crack widths. All calculated crack widths were below the limitation value 0,178 mm.</p> <p>The exceptional design solution of this study revealed three bugs in ADAPT-software. These bugs would perhaps never have been detected when doing more traditional post-tensioning design. All bugs were reported to the ADAPT development team and will be corrected in future releases.</p> <p>The design solution found in this study, involving straight tendons at the top and bottom of the slab, can be used as a general solution for any post-tensioned slab exposed to variable vertical loading. The use of straight tendons at both slab surfaces also proved advantageous for crack control.</p>	

TEKNILLINEN KORKEAKOULU
DIPLOMITYÖN TIIVISTELMÄ

Tekijä:	Nicodemus Jansson
Työn nimi:	Vaihtelevan vedenpaineen vaikutus jälkijännitettyyn betonilaattaan
Päivämäärä:	26.03.2008
Sivumäärä:	85 + Liitteet
Tiedekunta:	Insinööritieteiden ja arkkitehtuurin tiedekunta
Laitos:	Rakenne- ja rakennustuotantotekniikan laitos
Professori:	Talonrakennustekniikka
Valvoja:	Professori Jari Puttonen
Ohjaaja:	DI Teuvo Meriläinen

Tässä diplomityössä on tutkittu, miten vaihteleva vedenpaine vaikuttaa jälkijännitetyn betonilaatan suunnitteluun ja miten varmistetaan laatan vedenpitävyys. Tutkimuksessa on sovellettu Eurokoodeja ja numeeriset analyysit on tehty ADAPT-ohjelmistolla.

Jälkijännitetyt laatat suunnitellaan yleensä käännetyillä paraabelijänteillä, mutta vaihtelevan vedenpaineen takia, kyseinen jännegeometria ei ollut tässä tapauksessa soveltuva. ADAPT-ohjelmistolla löydettiin suoriin jännepunoksiin perustuva suunnitteluratkaisu, asettamalla laatan molempiin pintoihin suorat jännepunokset. Tällä tavalla jännepunokset kestävät pystysuoria kuormia sekä ylhäältä että alhaalta. Sen lisäksi, suorat jännepunokset rajoittavat halkeilua molemmissa pinnoissa. ADAPT-ohjelmistolla saatu suunnitteluratkaisu tarkastettiin soveltamalla normipohjaisia suunnittelukaavoja.

Laatan vedenpitävyys varmistettiin halkeilun rajoittamisella ADAPT-ohjelmistolla. Täydennykseksi halkeamaleveydet laskettiin manuaalisesti. Lasketut halkeamaleveydet eivät ylittäneet Eurokoodin mukaista raja-arvoa, joka tarkastetussa tapauksessa oli 0,178 mm.

Harvinainen suunnitteluratkaisu paljasti kolme ohjelmavirhettä ADAPT-ohjelmistossa. Näitä virheitä ei olisi ehkä löydetty tavallisilla suunnitteluratkaisuilla. Kaikki ohjelmavirheet ilmoitettiin ADAPT-ohjelmiston kehitysryhmälle. Virheet korjataan ohjelmiston tuleviin versioihin.

Tässä tutkimuksessa löydettyä suunnitteluratkaisua voidaan käyttää yleisratkaisuna mille tahansa vaihtelevalle pystykuormitukselle alttiille jälkijännitetulle betonilaatalle. Suorat jännepunokset laatan pinnoissa helpottavat myös halkeilun hallintaa.

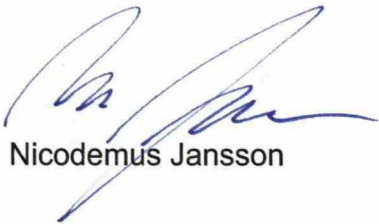
FOREWORD

I have conducted this Master's thesis at Aaro Kohonen Oy, Espoo, Finland, as part of the degree of Master of Science (Technology) at the Helsinki University of Technology (TKK).

I would like to express my warmest gratitude for the guidance and support to my instructor M.Sc. (Tech.) Teuvo Meriläinen, Aaro Kohonen Oy, and to my supervisor Professor Jari Puttonen, Helsinki University of Technology. I would also like to thank M.Sc. (Tech.) Jyrki Jauhiainen, Finnmap Consulting Oy, for his assistance.

Finally, I would like to thank all my friends and my family who have supported me during my studies.

Espoo, March 26, 2008



Nicodemus Jansson

LIST OF CONTENTS

1	INTRODUCTION	11
1.1	Background	11
1.2	Study problem	12
1.3	Restrictions of the study	12
2	THEORETICAL BACKGROUND.....	14
2.1	General.....	14
2.2	The basics of post-tensioning	14
2.2.1	Unbonded post-tensioning system	14
2.2.2	Bonded post-tensioning system	15
2.2.3	Choice of post-tensioning system.....	16
2.3	Post-tensioning analysis	17
2.3.1	Load balancing	17
2.3.2	Prestressing force.....	18
2.3.3	Losses of prestress for post-tensioning	18
2.3.4	Hyperstatic actions	18
2.4	Equivalent Frame Method.....	19
2.5	Finite Element Method.....	21
2.6	Principal merits of the two methods	24
3	ADAPT SOFTWARE	25
3.1	General.....	25
3.2	ADAPT-Floor Pro.....	25
3.3	ADAPT-PT.....	25
3.4	The general design process using ADAPT software	25
3.4.1	The three-dimensional model	26
3.4.2	The material properties.....	26
3.4.3	The criteria	26
3.4.4	The loads and load combinations	26
3.4.5	The support lines and design strips	27
3.4.6	The determination of post-tensioning	27
3.4.7	The Finite Element Analysis	27
3.4.8	The design sections.....	27
3.4.9	The final design solution.....	28
4	STRUCTURE DESCRIPTION	29
4.1	General.....	29
4.2	Structure geometry	29
4.3	Material properties.....	29
4.3.1	Concrete.....	29
4.3.2	Non-prestressed reinforcement	30
4.3.3	Post-tensioning.....	30
5	DESIGN CRITERIA	31
5.1	The Eurocodes	31
5.2	General design criteria.....	31
5.3	Post-tensioning criteria	31
5.4	Watertightness and crack control	32
5.5	Stress limitation	32
5.6	Deflection control.....	33
5.7	Temperature and shrinkage.....	33

5.8	Stress losses	33
6	LOADS AND LOAD COMBINATIONS.....	35
6.1	Loads during Phase 1 and Phase 2.....	35
6.1.1	Dead load	35
6.1.2	Live load	35
6.1.3	Hydraulic pressure.....	36
6.1.4	Prestressing	36
6.1.5	Load summary.....	36
6.2	Load combinations	36
6.2.1	Combination of actions according to the Eurocodes.....	37
6.2.2	The load combinations used in this study.....	38
7	PRELIMINARY CALCULATIONS	40
7.1	General.....	40
7.2	Preliminary calculation data.....	40
7.2.1	The selected section of the slab	40
7.2.2	Design criteria and loading	41
7.3	Obtaining the design solution	42
7.4	Design solutions	43
7.4.1	Design solution 1	43
7.4.2	Design solution 2	45
7.4.3	Design solution 3	46
7.4.4	Design solution 4	47
7.5	Choice of design solution.....	48
8	VERIFICATION BY CODE-BASED METHODS	49
8.1	General.....	49
8.2	The basics of the calculations.....	49
8.2.1	Post-tensioning and mild steel reinforcement.....	49
8.2.2	Stress losses	50
8.3	Preliminary section – midspan – top.....	50
8.4	Preliminary section – midspan – bottom.....	51
8.5	Stress losses	51
8.6	Comparison and conclusions.....	51
8.6.1	Post-tensioning and mild steel reinforcement.....	51
8.6.2	Stress losses	52
9	APPLYING THE DESIGN SOLUTION.....	54
9.1	General.....	54
9.2	Beams	54
9.2.1	Separate beam analysis	54
9.3	Slab	55
10	CRACK CONTROL	58
10.1	General.....	58
10.2	Calculation of crack widths	59
10.2.1	The height of the compressed section.....	60
10.3	Calculation of the minimum reinforcement areas.....	61
10.4	Results.....	62
10.5	Crack width conclusions	62
11	JOINT REINFORCEMENT	63
11.1	General.....	63
11.2	Frame analysis	63
11.2.1	Lateral loads.....	63

11.2.2	Frame analysis results.....	63
11.3	Reinforcement calculations.....	64
12	ANCHORAGE ZONE DESIGN	66
12.1	General.....	66
13	FINITE ELEMENT ANALYSIS	69
13.1	General.....	69
13.2	The analysis and results	70
13.2.1	Slab deflection.....	71
13.2.2	Slab moments.....	73
13.3	FEM-analysis conclusions	79
14	SUMMARY AND CONCLUSIONS	80
APPENDIX A – THE PRELIMINARY CALCULATIONS.....		86
	Design solution 1	86
	Design solution 2.....	88
	Design solution 3.....	90
	Design solution 4.....	92
APPENDIX B – VERIFICATION BY CODE-BASED METHODS		94
	Preliminary section – midspan – top.....	94
	The National Building Code of Finland	94
	The Eurocodes	96
	Preliminary section – midspan – bottom.....	97
	The National Building Code of Finland	97
	Stress losses	98
	Initial data	98
	Losses due to friction.....	98
	Losses at anchorage	99
	Final losses due to friction including losses at anchorage	99
	Losses due to instantaneous deformation of concrete.....	100
	Losses due to creep and shrinkage	100
	Losses due to steel relaxation	101
	Total time dependent loss.....	101
APPENDIX C – SEPARATE BEAM AND SLAB ANALYSIS.....		103
	Separate beam analysis	103
	Slab	105
APPENDIX D – CRACK WIDTH CALCULATIONS.....		107
	Preliminary section- midspan- bottom.....	107
	Preliminary section – midspan – top	111
	Beam including the point load – midspan – bottom	111
	Beam including the point load – midspan – top	112
	Slab section – midspan – bottom.....	113
	Slab section – midspan – top.....	114
	Slab section – support – bottom	114
	Slab section – support – top	115
APPENDIX E – JOINT REINFORCEMENT CALCULATIONS.....		117
	Lateral loads.....	117
	Reinforcement calculations	117
	Strength analysis	117
	Crack control.....	119
APPENDIX F – PRELIMINARY DRAWING		120

NOTATION

In this Master's thesis, the following major symbols apply. The notation used is based on the Eurocodes and the National Building Code of Finland.

Latin upper case letters

A	Cross sectional area
A_c	Cross sectional area of concrete
$A_{c,eff}$	Effective area of concrete in tension surrounding the reinforcement or prestressing tendons
A_{ct}	Area of concrete in the tensile zone
A_p	Area of a prestressing tendon or tendons
A_s	Cross sectional area of reinforcement
$A_{s,min}$	Minimum cross sectional area of reinforcement
$A_{s,req}$	Required cross sectional area of reinforcement
C	Concrete strength
E_c	Tangent modulus of elasticity of concrete
E_{cj}	Tangent modulus of elasticity of concrete at stressing
E_{cm}	Secant modulus of elasticity of concrete
E_p	Design value of modulus of elasticity of prestressing steel
E_s	Design value of modulus of elasticity of reinforcing steel
F	Action
F_d	Design value of an action
G	Permanent action
H	Lateral action
K	Concrete cube strength or factor
K_j	Concrete cube strength at stressing
L	Length
M	Bending moment
M_d	Design value of a bending moment
M_k	Characteristic value of a bending moment
M_u	Moment resistance capacity
N	Axial force
P	Prestressing force or action
P_0	Initial force at the active end of the tendon immediately after stressing
P_d	Design value of a prestressing force or action
Q	Variable action
W_b	Upward and downward forces due to tendon drape

Latin lower case letters

a	Coefficient or ratio
b	Width
b_0	Width of the flange of a T-section
b_w	Width of the web of a T-section
c	Concrete cover
c_p	Concrete cover to prestressing tendons
d	Effective height of a cross-section
d_p	Effective height to prestressing tendons
d_s	Effective height to reinforcing steel
e	Eccentricity
f_{cd}	Design value of concrete compressive strength
f_{ck}	Characteristic compressive cylinder strength of concrete at 28 days
$f_{ct,eff}$	Mean value of the tensile strength of the concrete
f_{ctk}	Characteristic axial tensile strength of concrete
f_{ctm}	Mean value of axial tensile strength of concrete
f_{puk}	Characteristic tensile strength of prestressing steel
$f_{p0,2k}$	Characteristic 0,2% proof-stress of reinforcement
f_y	Yield strength of reinforcement
f_{yd}	Design yield strength of reinforcement
f_{yk}	Characteristic yield strength of reinforcement
h	Height
h_e	Modified height
h_f	Height of the flange of a T-section
h_w	Height of the web of a T-section or height of the hydrostatic pressure
k	Coefficient
n_p	Number of prestressing tendons
n_s	Number of reinforcing bars
q	Variable action
$s_{r,max}$	Maximum crack spacing
u, v, w	Components of the displacement of a point
w_k	Crack width
x	Distance
x, y, z	Coordinates
y	Height of the compression part
z	Lever arm of internal forces

Greek upper case letters

Δ Deviation

Greek lower case letters

α	Angle or ratio
β	Wobble coefficient of friction or relative height of compression part
ε	The difference between the mean strain in the concrete and the mean strain in the reinforcement
ε_c	Compressive strain in the concrete
ε_{cm}	Mean strain in the concrete
ε_{cs}	Final shrinkage
ε_{cs0}	Final shrinkage reference value
ε_{sm}	Mean strain in the reinforcement
ϕ	Creep coefficient or angle of friction
ϕ_0	Creep coefficient reference value
ϕ_p	Diameter of a prestressing tendon
ϕ_s	Diameter of a reinforcement bar
γ	Density or partial factor
γ_c	Partial factor for concrete
γ_G	Partial factor for permanent actions, G
γ_p	Partial factor for actions associated with prestressing, P
γ_Q	Partial factor for variable actions, Q
γ_s	Partial factor for reinforcing steel
μ	Angular coefficient of friction or relative moment
θ_x	Rotation about the X-axis
θ_y	Rotation about the Y-axis
ρ	Reinforcement ratio
σ_c	Stress in the concrete
σ_p	Stress in a prestressing tendon
$\sigma_{p,0}$	Stress in a prestressing tendon after immediate stress losses
$\sigma_{p,inf}$	Stress in a prestressing tendon after immediate and time dependent stress losses
σ_s	Stress in the reinforcing steel
ξ	Reduction factor for unfavorable permanent actions or ratio
ψ	Factors defining representative values of variable actions
	ψ_0 for combination values
	ψ_1 for frequent values
	ψ_2 for quasi-permanent values

1 INTRODUCTION

1.1 Background

In 2002 an architectural design contest for the city centre of Kauniainen was arranged. The winning suggestion was presented by B&M Architects (Figure 1) and involves the rebuilding of a major part of the city centre (Figure 2). In 2007 selected structures in the city centre were demolished and now the structural design of the new structures is in progress. The design and build contractor is NCC Oy. Aaro Kohonen Oy is responsible for the structural design.

The structural design of the new city centre includes some very challenging engineering problems, such as vibrations caused by the nearby railway and hydraulic pressure due to high groundwater level. The construction works are estimated to be completed in 2012.



Figure 1. The design suggestion by B&M Architects [1].

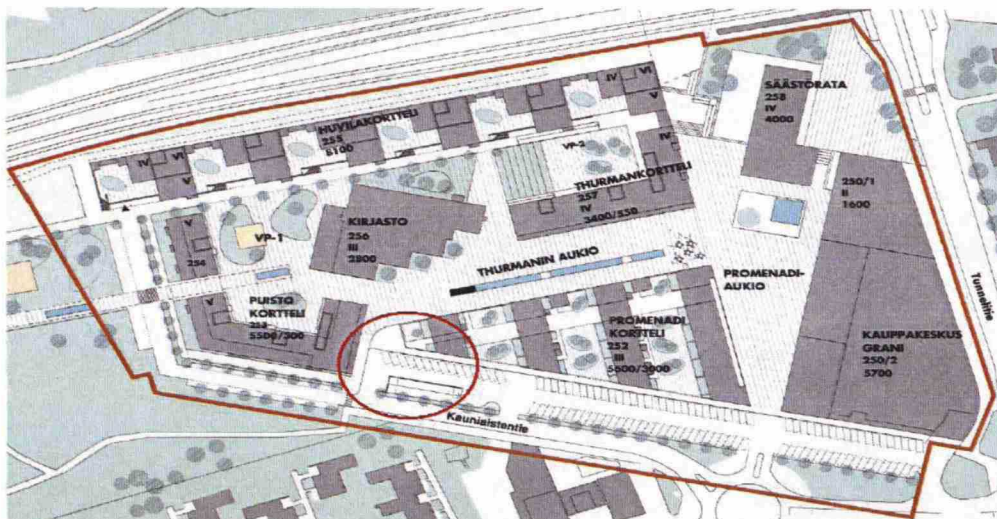


Figure 2. The design plan for the new city centre of Kauniainen [1].

1.2 Study problem

In spite of high groundwater level and weakly supporting soil, consisting mainly of clay, a major part of the parking space in the city centre will be situated underground. This implies that underground parking structures will be constructed partly under the groundwater level. The parking structures must therefore be made watertight. The slabs will be founded on steel piles supported on the rock below.

The watertightness will be achieved by mitigating the cracks in concrete, so that all crack widths are below limitation values. However, the structural design of the concrete slabs involves an unusual challenge, as the slabs will be exposed to two-phased bidirectional loading. During the first phase (henceforward referred to as Phase 1), the construction site will be kept dry using water pumps and pile planking. The slabs are then only exposed to the dead and live load, not to any hydraulic pressure. The second phase (henceforward referred to as Phase 2), will be reached after approximately two years, when the water pumps are removed and the slabs exposed to the hydraulic pressure of the groundwater from below. In order to resist this hydraulic pressure, the slabs will be prestressed. In addition, the slabs will be anchored to the rock below, through the steel piles, using non-prestressed mild reinforcement.

This Master's thesis challenges this engineering problem of how to design a post-tensioned waterproof concrete slab exposed to this variable hydraulic pressure. The slab will be analyzed in the two different phases and a solution involving an optimal combination of prestressed and non-prestressed reinforcement will be sought. The main part of the analysis will be done using ADAPT software, presented in Chapter 3. An additional challenge is that this study will be done using the recently implemented Eurocodes.

1.3 Restrictions of the study

This study focuses on the bottom slab of the parking structure entrance tunnel, shown in Figure 3, with the main focus on how to resist the variable hydraulic pressure and ensure the watertightness of the slab. A section of the entrance tunnel is shown in Figure 4, where the bottom slab is encircled. The maximum groundwater level +19.650 is also shown. The slab is shown in greater scale in the initial drawing (Appendix F), and the location of the entrance tunnel is encircled in Figure 2. Neither the design of the other slabs of the underground parking structures in the city centre, nor the design of the structures above the slab in focus, are included in the study. The piles supporting the slab and anchoring the slab to the rock will be included as supports. Any drawings included in this study are preliminary drawings. No fabrication drawings are included.

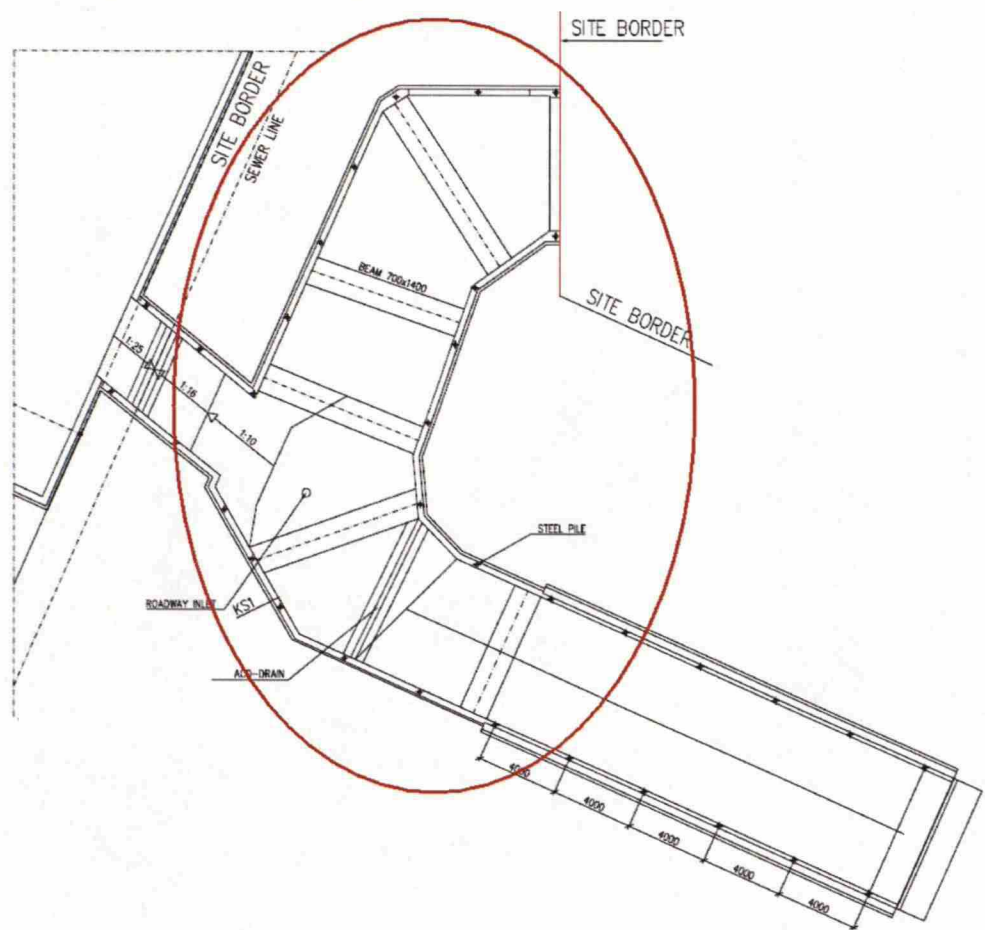


Figure 3. The slab in focus.

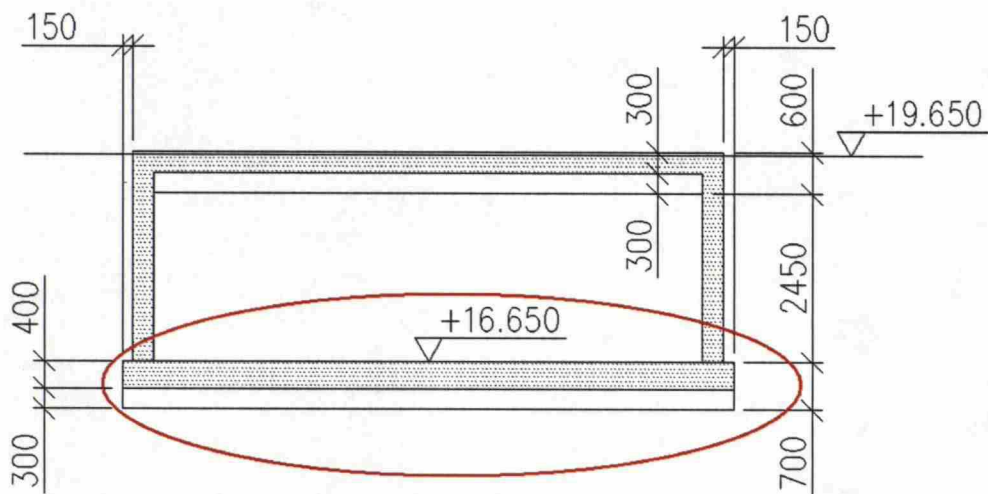


Figure 4. Section view of the entrance tunnel.

2 THEORETICAL BACKGROUND

2.1 General

In this chapter, the basics of post-tensioning and the theoretical background of post-tensioning analysis will be presented. The basics of the Equivalent Frame Method and the Finite Element Method will also be discussed, as the software used for this study is based on these two analysis methods.

2.2 The basics of post-tensioning

Post-tensioning is one of the two commonly used methods of prestressing concrete. The other method is called pre-tensioning. The basic idea of both methods is to prestress the concrete of a structure to counteract the internal stresses caused by external loads. The difference between these two methods is the time of stressing. Pre-tensioning means that the prestressing steel is stressed before the concrete is cast, while in a post-tensioned structure, the prestressing steel is stressed after the cast of the concrete. This study will focus on post-tensioning.

There are two main types of post-tensioning systems, each with its own advantages and disadvantages. These are the unbonded post-tensioning system and the bonded post-tensioning system. Other post-tensioning systems exist, like the external post-tensioning system where the tendons are installed outside the concrete member. This is, however, mainly used in repair applications and will not be further discussed in this study.

[2]

2.2.1 Unbonded post-tensioning system

The characteristic feature of unbonded tendons is that the forces in the stressed tendons are transferred to the concrete member primarily through the anchors at its ends, as the tendons do not form a bond with the concrete. This makes the long-term durability and reliability of the anchors, and the anchorage zone design for unbonded tendons, essential.

Unbonded tendons are usually monostrand tendons coated with a plastic sheathing. The sheathing acts as a bond breaker, but it also protects the tendon from mechanical handling and prevents the ingress of moisture and chemicals. Inside the plastic sheathing, the tendons are also coated with a corrosion-inhibiting coating, or grease, that provides additional protection against corrosion and reduces the friction between the strand and the plastic sheathing. The tendon can move freely inside the plastic sheathing, but variations in force along the tendon exist due to friction between the strand and sheathing. The components and the construction sequence of an unbonded post-tensioning system are illustrated in Figure 5.

[2][3]

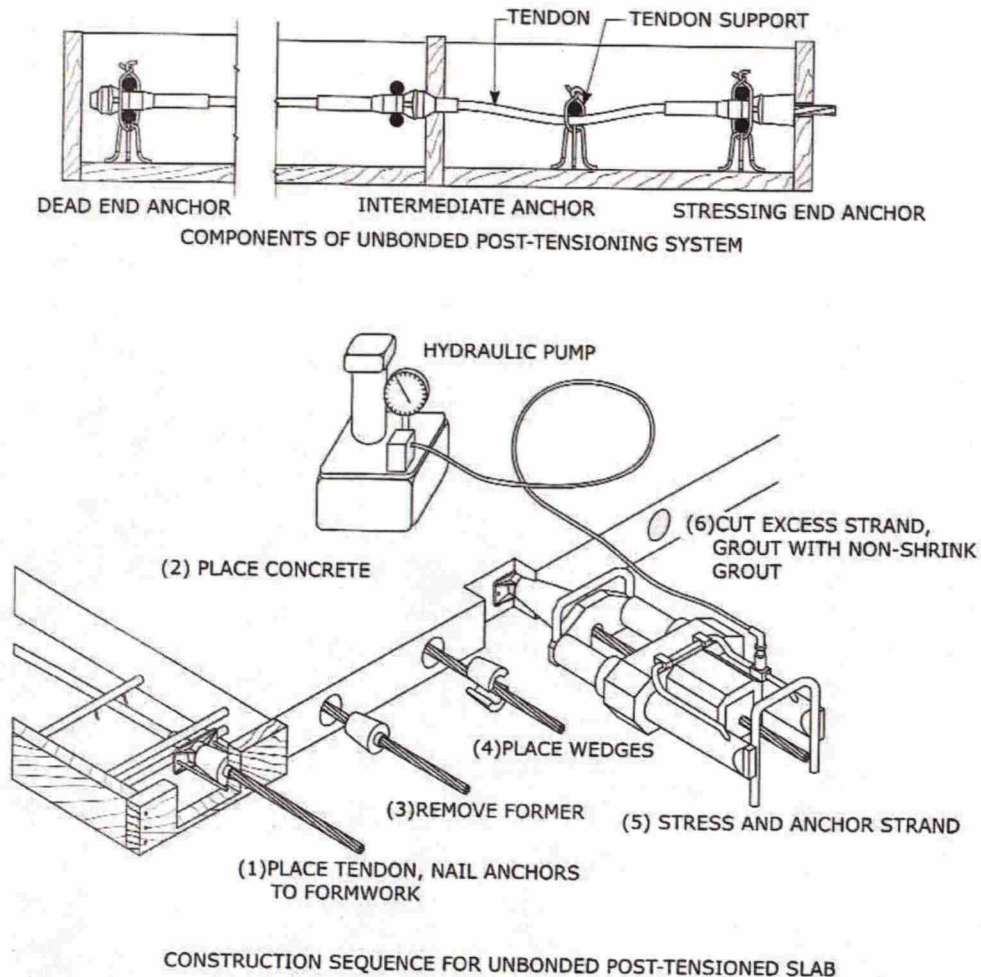


Figure 5. The components and the construction sequence of an unbonded post-tensioning system [2].

2.2.2 Bonded post-tensioning system

The characteristic feature of bonded tendons is the bond formed between the tendon and the concrete, transferring the prestressing force to the concrete along the whole length of the tendon. The bond is obtained by injecting a cementitious matrix, or grout, into the duct surrounding the strand. The duct, typically of corrugated galvanized steel, high density polyethylene or polypropylene, is encased in the concrete member. The duct is installed before the cast of concrete, either with or without the strands. After the cast of concrete, the tendon is stressed and the void of the duct is filled with the grout. Once the grout is hardened, it locks the movement of the strand within the duct and provides protection against corrosion. This way a bond is achieved.

Bonded tendons are typically multistrand tendons. Bonded post-tensioning systems also require anchors at both ends of the tendon, but their primary objective is to hold the prestressing forces until the grout is hardened. The long-term durability of bonded post-tensioning system anchors is therefore not as crucial as it is for unbonded post-tensioning

system anchors. The components of a multistrand bonded post-tensioning system are illustrated in Figure 6. [2][3]

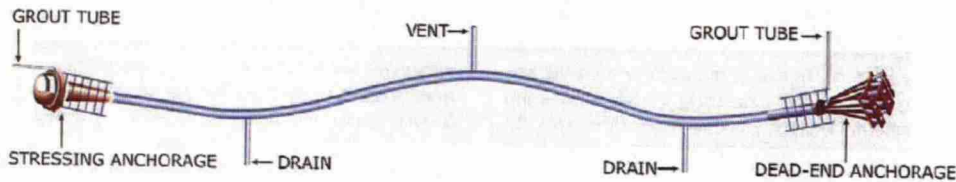


Figure 6. The components of a bonded post-tensioning system [2].

2.2.3 Choice of post-tensioning system

Both unbonded and bonded post-tensioning systems have their certain advantages and disadvantages. Unbonded tendons are usually used in building construction, while bonded tendons are more common in bridge construction. The choice of post-tensioning system is based on the technical characteristics of the two systems, as well as on economical aspects. The three main technical considerations are strength, protection against corrosion, and safety.

A bonded tendon will develop more force at design loads than an unbonded tendon due to strain compatibility. Because of the bond between the concrete and the tendon, a change in strain in the concrete near the bonded tendon will result in the same change in strain in the tendon. However, non-prestressed reinforcement is usually added in unbonded systems, supplementing the lower force, and a minimum amount of non-prestressed reinforcement is required in any case.

The grout surrounding bonded tendons provides a powerful protection against corrosion. Unbonded tendons can also be effectively protected against corrosion, using corrosion-inhibiting coating, when needed.

A bonded tendon is in a way more fail-safe than an unbonded tendon, as a failure in an unbonded tendon will cause a loss of the entire prestressing force in the tendon. A failure in a bonded tendon will only cause a loss of prestressing force in a certain area, as the force is transferred to the concrete along the whole length of the tendon. This safety problem with unbonded tendons is mitigated by adding at least one additional tendon, and this way succeed the required amount of post-tensioning, and by including non-prestressed reinforcement.

The duct size of bonded tendons is normally larger than the duct size of unbonded tendons. This causes a smaller drape, if bonded tendons are used in a member instead of unbonded tendons and the member thickness is remains the same. The drape is the distance between the tendons highest and lowest point in a span and affects the uplift of the tendon. A higher drape provides a larger uplift. This is especially essential in two-way slab construction, where shallow slab depths are common.

The economical aspects depend much on the design, but the exclusion of grout in unbonded post-tensioning systems might prove to be economical. The unbonded post-tensioning system was chosen for this study.

[2]

2.3 Post-tensioning analysis

Herein the basic theory of post-tensioning analysis is described. The analysis is based on Eurocode 2 [4]. The theory described here is applied by ADAPT software.

2.3.1 Load balancing

Balanced loading is one of the most common methods for the analysis of post-tensioned structures. The basic idea of the load balancing approach is to remove the tendon from its duct and replace it with the forces the tendon exerts on the concrete member. The forces are divided into upward and downward forces (W_b), due to the tendon drape, and a uniform compression force (P) along the longitudinal axis. The balanced loading method applies for both strength and serviceability checks. The method is presented in Figure 7. [5][6]

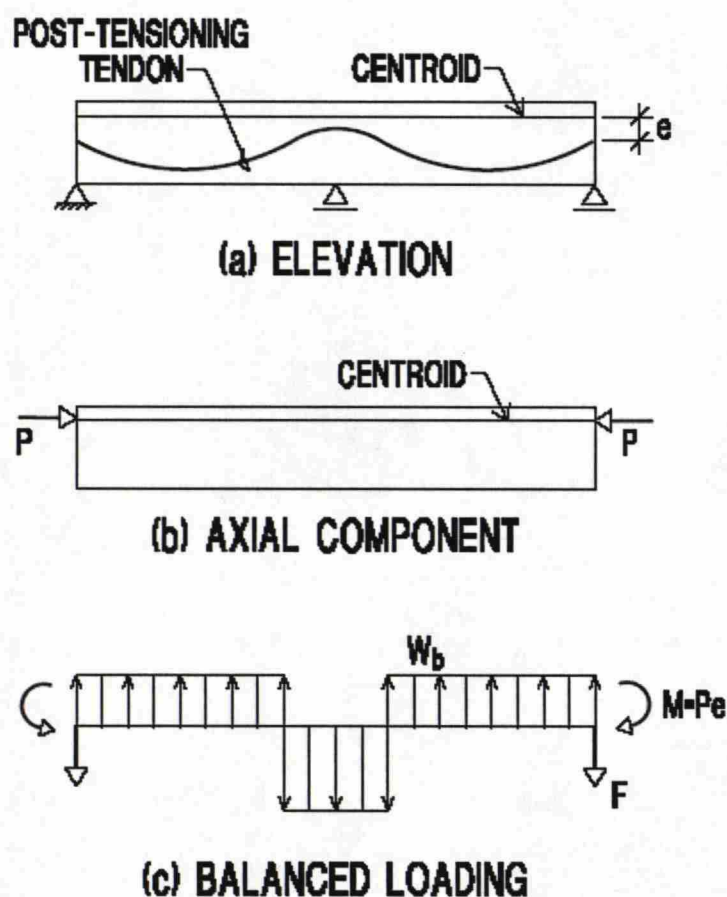


Figure 7. Load balancing [5].

2.3.2 Prestressing force

The prestressing force applied to a tendon, or the force at the active end during tensioning, shall, according to Eurocode 2 [4], not exceed the following value:

$$P_{\max} = A_p \times \sigma_{p,\max} \quad (1)$$

Where, A_p is the cross sectional area of the tendon and $\sigma_{p,\max}$ is the maximum stress applied to the tendon.

The value of the initial prestressing force is obtained by subtracting the immediate losses of prestress from the prestressing force at tensioning (P_{\max}). The value of the prestressing force at any given time is obtained by subtracting the immediate losses and the time dependent losses of prestress from the prestressing force at tensioning (P_{\max}).

2.3.3 Losses of prestress for post-tensioning

The prestress losses are divided into immediate losses and time dependent losses. These are also known as short-term and long-term losses. Immediate losses occur between the time the stressing process begins and the time the initial prestress force is transferred to the concrete. Time dependent losses occur after the prestress force has been transferred to the concrete. The estimation of prestress losses is covered in Eurocode 2 [4].

There are three types of immediate losses of prestress for post-tensioning. These are losses due to instantaneous deformation of concrete, losses due to friction, and losses at anchorage. Losses due to instantaneous deformation of concrete occur when the prestressing force shortens the concrete elastically, which leads to a reduction of stress in the previously stressed tendons. Losses due to friction are caused by friction between the tendon and the tendon sheathing. Losses at anchorage are due to wedge draw-in of the anchorage devices after tensioning and due to deformation of the anchorage itself. This reduces the stress in a certain length of the tendon.

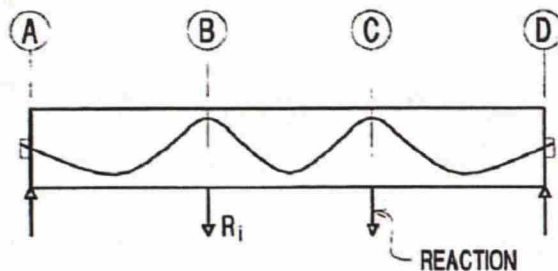
The time dependent losses of prestress for post-tensioning include losses due to concrete shortening, caused by shrinkage and creep, and losses due to the relaxation of prestressing steel.

[2][4]

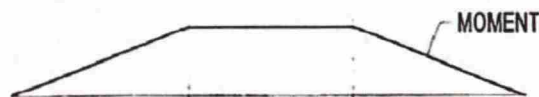
2.3.4 Hyperstatic actions

Hyperstatic actions, also known as secondary actions, develop due to prestressing forces if supports constraint the movement of a prestressed concrete member. If a structure is allowed to move freely, no hyperstatic actions will develop, but in most cast-in-situ cases, free movement of the concrete member is limited and the hyperstatic actions can be significant. They must therefore be included in the analysis.

An illustrative example of hyperstatic actions would be to cast and stress a beam prior to installation. When the stressed beam, now curved due to the prestressing force, would be installed it would have to be forced down at the centre in order to be attached to supports. The forces necessary at the supports to keep the beam straight are indicative of the hyperstatic actions that will develop, if the beam is stressed after installation (Figure 8).



(a) REACTIONS AT SUPPORTS DUE TO PRESTRESSING (HYPERSTATIC REACTIONS)



(b) MOMENTS DUE TO PRESTRESSING SUPPORT REACTIONS (HYPERSTATIC MOMENTS)

Figure 8. Hyperstatic actions [7].

The hyperstatic actions are commonly calculated using a method called the direct method. An indirect method also exists, but is less common. The direct method involves first replacing the prestressing force with the balanced loading and then solving the frame for balanced loading due to prestressing.

[7]

2.4 Equivalent Frame Method

The Equivalent Frame Method (EFM) is an improved modification of the Simple Frame Method. Both methods involve modeling three-dimensional slabs as a series of two-dimensional frames. However, in the EFM the relative slab and column stiffness are adjusted to account for biaxial bending. This does not apply for the Simple Frame Method. Both methods are approximate and the degree of approximation depends on the irregularity of the slab.

The EFM is currently the most common method for the analysis of post-tensioned floor systems in the United States. The EFM is originally based on theoretical plate behavior studies, but the validity of the EFM is

nowadays resting more on the satisfactory performance of the huge amount of structures designed using the EFM.

The basic idea of the EFM is to divide the slab into a series of equivalent frames, in two directions, along the supports (Figure 9). Each frame consists of a row of supports and an associated (tributary) area of the slab. The slab and columns are modeled as non-prismatic members, allowing variations in slab thickness as well as drops and openings.

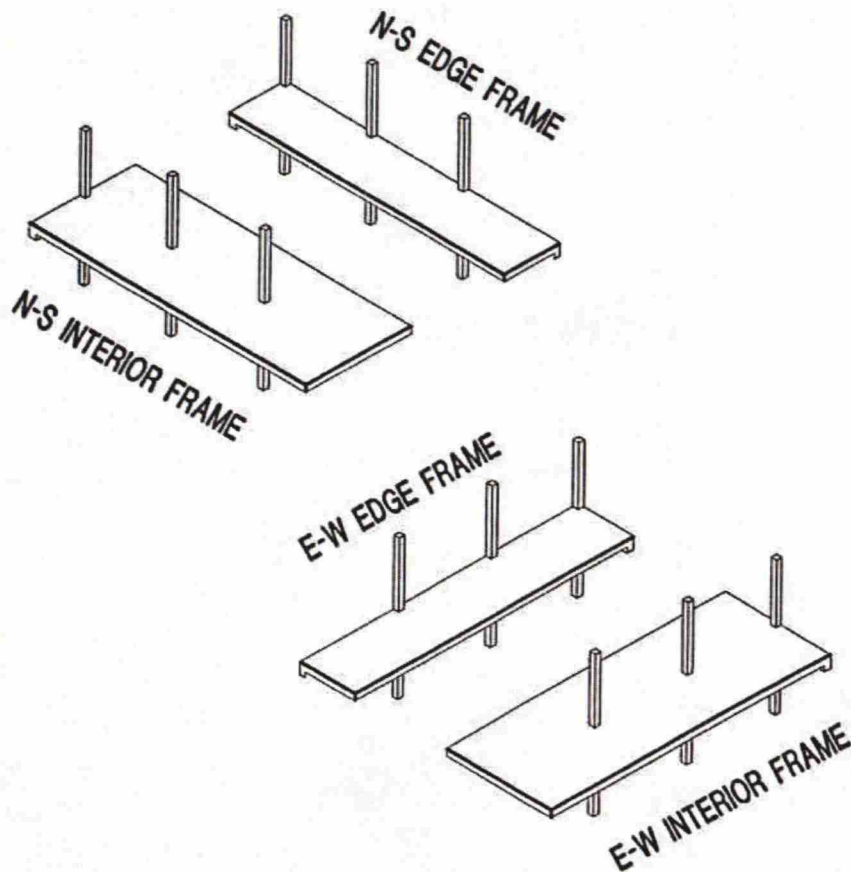


Figure 9. Breakdown of slab into equivalent frames in two directions [8].

Each frame is analyzed separately for loads assumed to act in the plane of the frame and modified to approximate the effect of possible torsional rotations in actual three-dimensional systems. The critical sections of the frame are then designed using the cross sectional resultant forces and moments obtained.

To allow torsion in the slab, the supports are assumed to be attached to the slab by torsional members, perpendicular to the span (Figure 10). The moments are transferred between the slab and columns only through the torsional members, so there is no moment transfer through the slab-column connection at the face of the support.

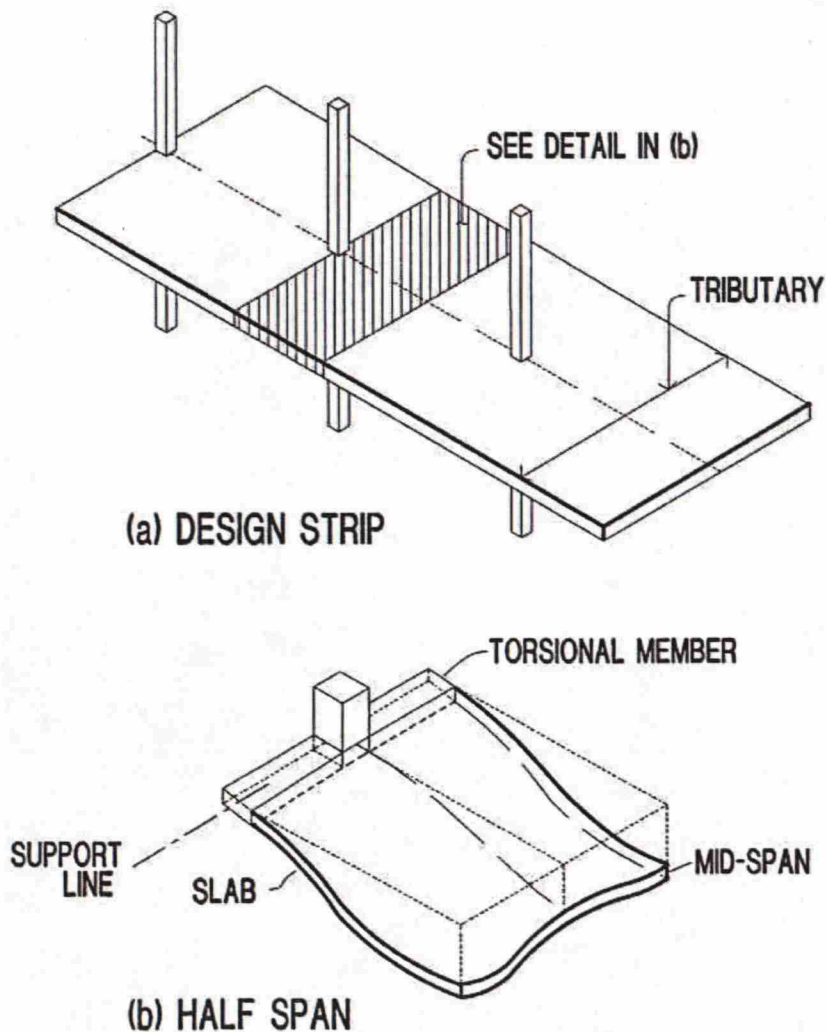


Figure 10. The torsional member envisaged for the design strip [8].

The columns and their attached torsional members are then substituted with equivalent columns, so that the stiffness of each equivalent column represents the stiffness of the column and torsional member combined. The equivalent column stiffness is used for the calculations and this way the column moments obtained are lower than those obtained using the Simple Frame Method, resulting in a more efficient design. [8][9][10]

2.5 Finite Element Method

The basic idea of the Finite Element Method (FEM) is to divide the slab or structure into small pieces or finite elements (Figure 11). The elements are defined based on their geometry, location in the slab, material properties, and relationship with surrounding elements. Their behavior is formulated to capture the local behavior of the slab. The elements are usually formulated either through displacement-based formulations or through hybrid formulations. Both formulation methods are based on relating the energy inside the element to the energy of the forces applied on each element, in other words, stresses through strains are related to

forces through displacement. Different types of elements, such as shell elements, frame elements (beam or column), and spring elements can be used. Several different element types, for example shell elements for the slab regions and frame elements for the beams and columns, can be used simultaneously in a structure. The number and size of the elements directly affect the accuracy of the solution.

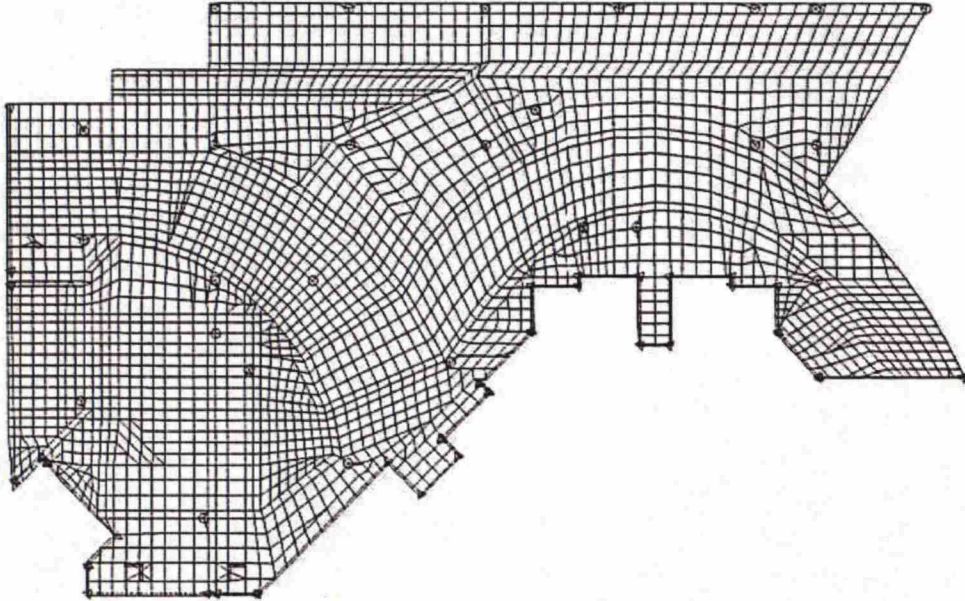


Figure 11. The discretization of a building floor [8].

Using the FEM, the entire slab can be analyzed at one time even though the slab is complex or irregular. However, the processing of the results for the code check must be done using design sections. But these design sections can be selected after the analysis, and the analysis results may prove helpful when selecting the design sections.

The elements are connected at reference points, or nodes, through which all forces from one element to another are transferred. When analyzing the flexural response of the slab, forces assumed at each node are usually M_x , M_y , and F_z . When membrane actions (stretching) are included, the additional forces F_x and F_y are assumed at each node (Figure 12).

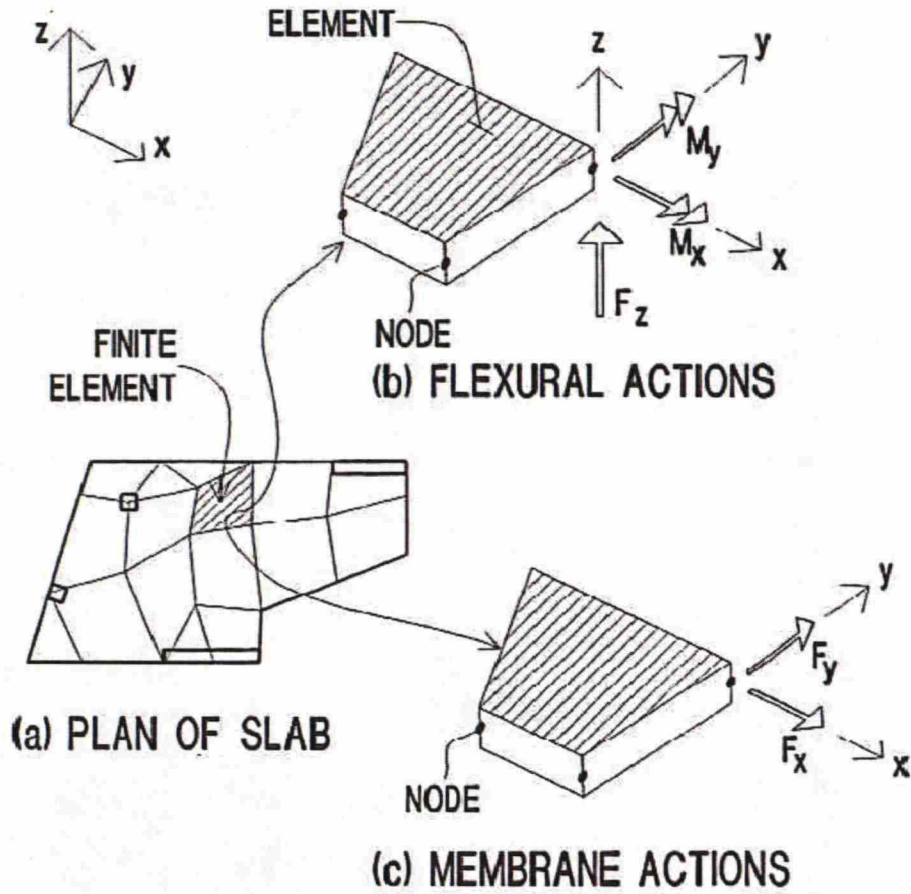


Figure 12. Flexural and membrane actions assumed at each node [8].

For each element, the forces and element deflections are related by the equation:

$$\{f\} = [k]\{u\} \quad (2)$$

Where, $\{f\}$ is the force vector for the element's nodes, $[k]$ is the element stiffness matrix and $\{u\}$ is the displacement vector for the element's nodes. The displacement vector has three degrees of freedom for flexural behavior. These are the displacement normal to the plane w and rotations about the X and Y-axes θ_x and θ_y .

The equilibrium at each node requires that the forces from elements sharing a node must be equal to the external forces at the node and the displacement of a node common to several elements must be the same for all elements. Using these two criteria, a system of simultaneous linear equations for the whole plate can be created. The equation takes the form:

$$\{F\} = [K]\{U\} \quad (3)$$

Where, $\{F\}$ is the applied force, $[K]$ is the system stiffness matrix and $\{U\}$ is the displacement relative to the global coordinate system of the plate.

Based on the system of equations and the boundary conditions of the slab, the displacements of the nodes are obtained. Using this information and the properties of the elements, the internal deflections and stresses for each element can be specified.

[8][9][10][11]

2.6 Principal merits of the two methods

The EFM and the FEM are both powerful analysis methods and their design processes are similar for the engineer, although the methods are theoretically totally different. Both methods help the engineer to reach safe designs, but case studies show that the required amount of reinforcement in a slab can vary between the two methods. Which method requires more reinforcement for a design, usually depends on the complexity of the slab.

The EFM is a general and simple procedure and is generally suitable for more simple designs. The information obtained with the EFM is usually enough for the code check. The principal merit of the FEM is that irregular and complex structures can be analyzed with the same ease as simple structures. However, the accuracy of the results might decrease somewhat when analyzing more complex structures. The FEM also provides the engineer with a realistic picture of the structure's behavior. [8]

In this study both methods will be used. The EFM will be used to find the optimal amount of post-tensioning and the FEM will be used to analyze the whole complex and irregular slab.

3 ADAPT SOFTWARE

3.1 General

A major part of the calculations in this study is done using ADAPT software. ADAPT is a USA-based corporation, which provides a wide range of structural analysis software solutions for the design of building and bridge structures. In this study two ADAPT programs are used. ADAPT-PT is used for the post-tensioning design and ADAPT-Floor Pro for the Finite Element analysis. These two programs, and the general design process using them, are described herein.

3.2 ADAPT-Floor Pro

ADAPT-Floor Pro is three-dimensional Finite Element software for the modeling, analysis, and design of concrete and post-tensioned floor systems. The modeling is based on Building Information Model (BIM) technology, which is a standard digital information repository of building design, while the analysis and design is performed using the Finite Element Method.

A model is created using different structural components and then the model is analyzed using the Finite Element Method, based on an either automatically or manually created Finite Element mesh. The program provides the engineer with results including deflection, moments, shears, prestressing, and hyperstatic moments due to prestressing.

Profiled tendons can be modeled in a slab or beam, if post-tensioning is desired, and the prestressing can be considered in the Finite Element analysis. The post-tensioning design can also be imported from ADAPT-PT.

[12]

3.3 ADAPT-PT

ADAPT-PT is post-tensioning software for the design of post-tensioned beams, slabs, and floor systems. The analysis is based on the Equivalent Frame Method and both bonded and unbonded tendons can be used. The design can be optimized to use the least amount of post-tensioning demanded by the building code and other design criteria. The amount of post-tensioning needed is also based on the percentage of dead load to be balanced and the average precompression, specified by the engineer. ADAPT-PT also calculates stress losses and hyperstatic actions. ADAPT-PT can be used together with ADAPT-Floor Pro. The model generated using ADAPT-Floor Pro can be imported into ADAPT-PT for the optimized post-tensioning design and the tendons created can then be exported back to ADAPT-Floor Pro for additional analysis. [12]

3.4 The general design process using ADAPT software

The general design process of a post-tensioned concrete slab using ADAPT software involves a series of steps presented herein. The order in

which the steps are done can vary somewhat and some of the steps may overlap one another. Naturally, many of the steps need to be adjusted during the design process, in order to obtain an optimal design. All the steps are done using ADAPT-Floor Pro, unless mentioned otherwise. The design process is illustrated in Figure 13.

3.4.1 The three-dimensional model

The first objective in the general design process of a post-tensioned concrete slab using ADAPT software is to generate a three-dimensional model, which represents all the structural parts intended to resist the loads. The model can be generated either by directly creating the different structural members, such as beams, columns, and slab regions, in ADAPT-Floor Pro or by importing an AutoCAD-drawing into ADAPT-Floor Pro and then transforming the entities into structural members. The model can also be generated by importing geometry from software such as REVIT, ETABS, and STAAD.Pro.

3.4.2 The material properties

The materials used in ADAPT are concrete, mild steel, and prestressed steel. The material properties, such as strength and modulus of elasticity, all have default values, but can be modified by the engineer. Several different types of concrete, mild steel, and prestressing steel can be used simultaneously.

3.4.3 The criteria

The next step is to setup the design criteria. The engineer chooses the design code from eight available codes and then the program automatically specifies the design criteria, such as safety factors and stress limitations, associated with the chosen code. The engineer then has the option to adjust these factors and modify the design criteria as desired.

3.4.4 The loads and load combinations

The dead load of the model, or self weight, is calculated automatically by the program, using the density of the material and geometry of the model. The other loads need to be manually applied by the engineer. An essentially unlimited number of loads can be applied on the structure. The load types are point loads, line loads, and area loads, also known as patch loads. The point load can be a concentrated load or a moment, the line load can be a linearly varying force or moment, and the patch load can be of uniform intensity or varying in magnitude.

All the loads belong to load combinations. There are a number of predefined load combinations, based on the chosen design code, for both strength and serviceability checks. These can be modified by the engineer and additional load combinations can be defined.

3.4.5 The support lines and design strips

The support lines define how the applied loads are distributed to the different supports. Support lines can be generated using ADAPT-Floor Pro's support line wizard or created manually. Once the support lines are created in both the x-direction and the y-direction, ADAPT-Floor Pro automatically calculates the tributary for each support line. This way the model is broken into design strips, which will be used for the design of the structure.

3.4.6 The determination of post-tensioning

This step is done using ADAPT-PT and is based on the Equivalent Frame Method. The generated design strips are idealized and individually exported, along with the information of the design strips, such as geometry and loading, from ADAPT-Floor Pro to ADAPT-PT for the post-tensioning design.

This is basically an optional step, as the tendons can be created directly with ADAPT-Floor Pro, if the engineer knows how he wants to prestress his structure. However, ADAPT-PT has the ability to calculate the minimum amount of post-tensioning demanded by the chosen code, and this way, optimize the design.

Based on the requirements of the chosen code and other restrictions defined by the engineer, ADAPT-PT calculates the required post-tensioning and presents a solution, including the tendon profile and force, as well as other essential information. The solution can then be modified by the engineer. Next, the tendons are exported from ADAPT-PT into ADAPT-Floor Pro and the design process continues in ADAPT-Floor Pro.

3.4.7 The Finite Element Analysis

When all the design strips have been analyzed with ADAPT-PT and the tendons imported into ADAPT-Floor Pro, it is time for the Finite Element analysis of the structure. First a Finite Element mesh is generated either automatically or manually. The engineer can also manually modify an automatically generated mesh. ADAPT-Floor Pro uses flat quadrilateral or triangular shell elements for slab regions and walls, frame elements for beams and columns, as well as point spring elements and soil support elements, if required. The tendons are also divided into finite elements. A solution for every load combination is then obtained using the Finite Element Method.

3.4.8 The design sections

In order to perform the code check, a number of design sections need to be created for each design strip. Again, this can be done either automatically or manually. A design section is a cut, normal to the support line, through the entire width of a design strip. When the design sections have been generated, the program expresses the Finite Element results as three moments and three forces at the centroid of each design section. The program then performs a stress check and calculates the demanded

supplemental reinforcement based on these six actions and the chosen building code.

3.4.9 The final design solution

If the design does not meet the requirements of the code in the Finite Element analysis, the engineer needs to modify the design. Eventually a final solution, meeting all the requirements of the code, is obtained. Last, the program generates a design report. The scope of the design report can be defined by the engineer.

[13][14]

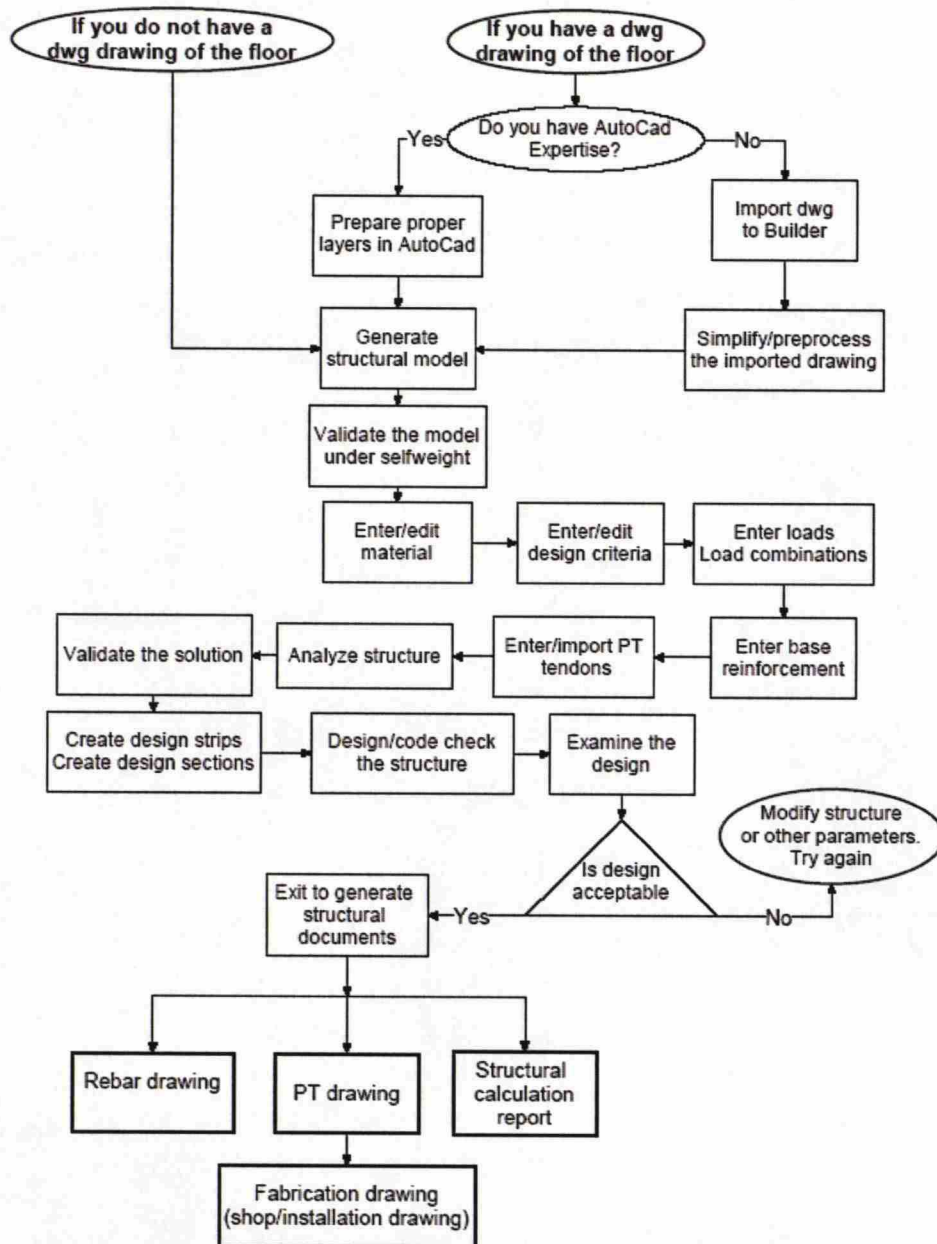


Figure 13. Flowchart of the design process using ADAPT software [14].

4 STRUCTURE DESCRIPTION

4.1 General

The structure in focus in this study is a curved post-tensioned concrete slab. It is the bottom slab of an entrance tunnel of a parking structure. The entrance tunnel leads to two underground parking structures and has a connection to the outside through a driving ramp. The tunnel is not heated. The slab is exposed to dead and live load from above, but as well to hydraulic pressure from beneath, as the structure is partly situated under the groundwater level. The structure is supported on steel piles but also anchored to the rock through the steel piles, in order to resist the hydraulic pressure from beneath. The geometry of the slab and the material properties are presented in the following chapters.

4.2 Structure geometry

The structure consists of a concrete slab, with a thickness of 400 mm and six beams, five beams with a 700x1400 mm² cross-section and one beam with an 865x1050 mm² cross-section. The geometry of the slab and the locations of the beams and piles can be seen in the preliminary drawing (Appendix F). A three-dimensional model of the slab is presented in Figure 14.

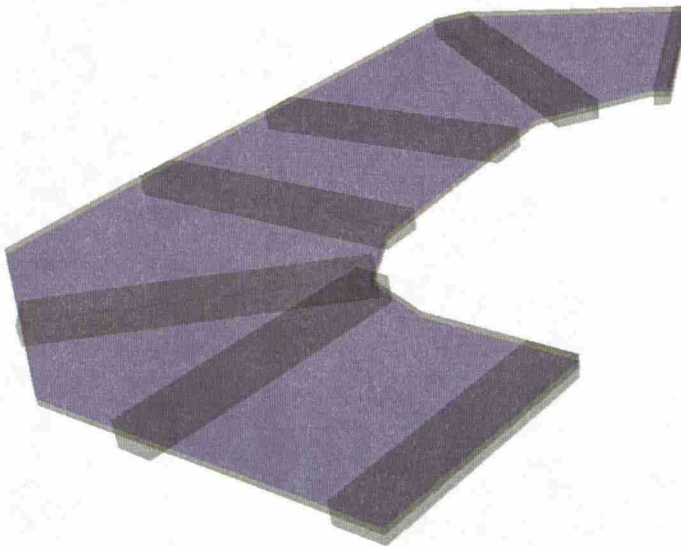


Figure 14. Three-dimensional model of the slab.

4.3 Material properties

4.3.1 Concrete

The concrete strength chosen for the slab and the beams is C35/45. This means that the concrete, at 28 days, has the cylinder strength 35 N/mm² and the cube strength 45 N/mm². The modulus of elasticity at 28 days, calculated by ADAPT-PT based on the Eurocodes and the concrete strength, is 34313 N/mm². The concrete cube strength at stressing is

defined as 27 N/mm^2 , 60% of the cube strength at 28 days. The ultimate creep coefficient of the concrete, based on the Eurocodes, is 1,25.

4.3.2 Non-prestressed reinforcement

The non-prestressed reinforcement of the slab and beams has a yield strength of 500 N/mm^2 and a modulus of elasticity of $200\,000 \text{ N/mm}^2$. The reinforcement type is A500HW, which is a common type in Finland.

4.3.3 Post-tensioning

An unbonded post-tensioning system will be used, including a monostrand tendon type St 1570/1770, with a diameter of 15,7 mm and a cross sectional area of 150 mm^2 . The characteristic 0,2% proof-stress of the prestressing steel is 1570 N/mm^2 and the characteristic tensile strength is 1770 N/mm^2 .

5 DESIGN CRITERIA

5.1 The Eurocodes

The design of the slab will be done using the Eurocodes, along with the Finnish National annex. The Eurocodes can be used for structural design in Finland from November 10, 2007. When using the Eurocodes, it is important not to use any other design codes simultaneously. The design criteria of the ultimate limit states (ULS) and the serviceability limit states (SLS) are covered in Eurocode 2 [4]. Selected design criteria are also discussed in the following chapters.

5.2 General design criteria

The design working life of the parking structure is 50 years. The exposure classes related to environmental conditions, based on Eurocode 2 [4], are XD1, XC3 and XF1 for the top of the slab and XC2 and XF1 for the bottom. The top surface of the slab is exposed to moderate humidity, while the bottom surface of the slab is wet, rarely dry. The top surface is exposed to corrosion induced by carbonation (XC3) as well as corrosion induced by chlorides (XD1). The bottom surface is only exposed to corrosion induced by carbonation (XC2). Both surfaces are exposed to moderate water saturation (XF1).

The minimum concrete cover, defined as the distance between the surface of the reinforcement closest to the nearest concrete surface and the nearest concrete surface, is based on the exposure classes. According to the Finnish National annex of Eurocode 2 [4], exposure class XD1 requires a minimum concrete cover of 30 mm to the non-prestressed reinforcement and 40 mm to the prestressing steel. To be on the safe side, the minimum cover chosen for this study is 35 mm to the non-prestressed reinforcement and 50 mm to the prestressing steel.

5.3 Post-tensioning criteria

In addition to the material properties of the prestressed steel, post-tensioning criteria such as tendon profile, including shape and drape, average precompression, and percentage of dead load to balance, must be specified and the post-tensioning system selected.

The tendons are usually banded in one direction and distributed in the other. The tendon shape is commonly a reversed parabola with the lowest point of the tendon at midspan, but many different tendon shapes, such as straight, partial parabola, and harped parabola, may be used.

The average precompression is defined as the total post-tensioning force divided by the gross cross sectional area normal to the post-tensioning force. In general, a minimum average precompression of 0,85 N/mm² and a maximum of 2,0 N/mm² should be used. However, if watertightness is a concern, a minimum average precompression of 1,0 - 1,4 N/mm² should be used for parking structures. The minimum average precompression of

1,0 N/mm² was chosen for the slab in focus. It is important to understand, though, that an increase in precompression does not guarantee watertightness or cracking elimination. Additional non-prestressed reinforcement is usually required for crack mitigation and the crack widths should be checked in order to ensure the watertightness of a construction. The maximum precompression limit is not connected with any code limit of maximum compressive stress of concrete. The reason for the upper limit of precompression is that, in most cases, values higher than this lead to a less economical design. [5]

The percentage of dead load to balance, or the uplift due to the tendon drape, is usually between 60 and 80% for the critical span of a slab. However, a straight tendon profile might be a suitable option in this case, as the loading is bidirectional. If only straight tendons are used, the percentage of balanced dead load will be 0%.

5.4 Watertightness and crack control

The greatest challenge of this study is to ensure the watertightness of the slab. The slab itself must be made watertight by crack mitigation. The crack widths will be separately analyzed. In addition, the joints of the slab, where the slab is connected to the walls, must be made watertight. These joints will also be separately analyzed and the necessary reinforcement calculated.

5.5 Stress limitation

According to the Eurocodes, the compressive stress in the concrete shall be limited in order to avoid longitudinal- and micro-cracks and the tensile stress in the reinforcement shall be limited in order to avoid inelastic strain, unacceptable cracking, or deformation. The stress limitation is therefore important to ensure the watertightness of the slab. The compressive stress of the concrete shall be limited to a value kf_{ck} . The tension stress limits are based on the mean value of the axial tensile strength of concrete, which is obtained through the expression:

$$f_{ctm} = 0,3 * f_{ck}^{(2/3)} \quad (4)$$

The tension and compressive stress limitation values are specified in Eurocode 2 [4] and presented in Figure 15, obtained from ADAPT-PT. In ADAPT-PT, the limitation values for the initial, frequent, and quasi-permanent load conditions are entered as multiples of f_{ck} .

Tension stresses			
	Initial Stress / $f_{ck}^{1/2}$	Quasi Stress / $f_{ck}^{2/3}$	Freq. Stress / $f_{ck}^{2/3}$
Top Fiber :	<input type="text" value="0.25"/>	<input type="text" value="0.3"/>	<input type="text" value="0.3"/>
Bottom Fiber :	<input type="text" value="0.25"/>	<input type="text" value="0.3"/>	<input type="text" value="0.3"/>

Compression Stresses		
Initial Stress / f_{ck}	Quasi Stress / f_{ck}	Freq. Stress / f_{ck}
<input type="text" value="0.6"/>	<input type="text" value="0.45"/>	<input type="text" value="0.6"/>

Figure 15. The tension and compressive stress limits entered in ADAPT-PT.

5.6 Deflection control

The deflection of a structure shall not affect its proper functioning or appearance. The span deflection of the slab in focus will be downwards during Phase 1, but during Phase 2, the span deflection will be upwards due to the hydraulic pressure from beneath. According to the Eurocodes, the deflection of a structure shall be limited to span/500 for quasi-permanent loads. [4]

5.7 Temperature and shrinkage

The temperature alternation in the entrance tunnel is estimated to -10°C - +20°C. Temperature and shrinkage reinforcement can be used to minimize crack widths caused by thermal contraction or expansion. Generally, temperature and shrinkage reinforcement is required if the average precompression is below 0,70 N/mm². But since the minimum average precompression is 1,0 N/mm² in this study, temperature and shrinkage reinforcement is not required. [15]

5.8 Stress losses

ADAPT-PT has the ability to automatically calculate both immediate and time dependent losses of prestress for post-tensioning. Based on stress loss parameters, ADAPT-PT determines the stress in the tendon at both ends and at the center of each span, and calculates the initial stress, total long-term losses, anchor set influence distance, and elongations for both one- and two-ended pulls. The values given as defaults for the stress loss calculations are fairly typical and should be used unless more precise information is available. The values are presented in Figure 16.

Friction stress losses		
Ratio of jacking stress to ultimate strength :	<input type="text" value="0.8"/>	
Strand's Modulus of Elasticity :	<input type="text" value="200000"/>	N/mm ²
Angular Coefficient of Friction (Mu) :	<input type="text" value="0.07"/>	
Wobble Coefficient of Friction (K) :	<input type="text" value="0.00459"/>	rad/m
Anchor set (Draw-in of wedges) :	<input type="text" value="6"/>	mm

Long - term stress losses		
Perform Long-term Loss Calculations :	<input type="radio"/> No <input checked="" type="radio"/> Yes	
Long - Term stress loss estimate	<input type="text" value="0"/>	N/mm ²

Long - term stress loss parameters		
Type of Strand :	<input checked="" type="radio"/> Low-Lax <input type="radio"/> Stress-Relieved	
Age of Concrete at Stressing :	<input type="text" value="5"/>	days
Concrete's Modulus of Elasticity at Stressing :	<input type="text" value="10509.5"/>	N/mm ²
Relative Ambient Humidity (RH) :	<input type="text" value="80"/>	%
Volume to Surface Ratio (V/S) :	<input type="text" value="100"/>	mm
Are all tendons stressed at one time:	<input checked="" type="radio"/> Yes <input type="radio"/> No	

Figure 16. The default stress loss parameters in ADAPT-PT.

When checking the stress loss parameters in Figure 16, one may notice that the concrete's modulus of elasticity at stressing is too small. This turned out to be a bug in the program. This bug and its consequences are explained in Chapter 8.6.2.

6 LOADS AND LOAD COMBINATIONS

6.1 Loads during Phase 1 and Phase 2

6.1.1 Dead load

The dead load includes the dead load, or self weight, of the slab and beams. ADAPT software calculates the self weight of the bottom slab and beams automatically, based on the geometry and density.

Most of the dead load from the upper slab will go directly to the steel piles, and will therefore not affect the slab. However, a section of the dead load of the upper slab, beam, and the surface structure is transferred to the lower slab through a composite column. This load will act as a point load on one of the beams. The composite column carries the load of an area of approximately 40 m². The surface structure has a weight of 8 kN/m² and the concrete weight is 25 kN/m³. The upper slab has a thickness of 300 mm and the beam above the column has the cross-section 1400x600 mm² and the length 8 m. This results in a point load on the lower slab:

$$F_{dead} = 40m^2 * 0,3m * 25kN / m^3 + 8m * 0,3m * 1,4m * 25kN / m^3 + 40m^2 * 8kN / m^2 = 704kN \quad (5)$$

6.1.2 Live load

The parking structure belongs to category F of traffic areas, presented in Eurocode 1 [16]. In category F, live load due to vehicle traffic consists of either a uniform load of 2,5 kN/m² or a single axle with two 10 kN point loads, depending on which load model will produce the most adverse effect. The load models are compared below on a part of the slab with a length of 8,5 m a width of 6,0 m. The same slab section will be used later on for preliminary calculations.

$$M_{q,max} = \frac{ql^2}{8} = \frac{(2,5 \frac{kN}{m^2} \times 6m) \times (8,5m)^2}{8} = 135,47kNm \quad (6)$$

$$M_{Q,max} = \frac{ql}{4} = \frac{20kN \times 8,5m}{4} = 42,50kNm \quad (7)$$

A uniformly distributed load of 2,5 kN/m² results in a maximum moment of 135,47 kNm, while a single point load of 20 kN at midspan gives a maximum moment of 42,50 kNm. The uniformly distributed load model will be used.

The live load transferred to the lower slab through the column is 10 kN/m², including a snow load of 2,5 kN/ m². This results in a point load of:

$$F_{live} = 40m^2 * 10kN / m^2 = 400kN \quad (8)$$

6.1.3 Hydraulic pressure

The maximum groundwater level is approximately +19.650 and the minimum ground water level approximately +18.650. The lowest point of the slab is 3,7 m below the maximum groundwater level, at +15.950. This result in a maximum hydraulic pressure of 37 kN/m². The hydraulic pressure is a dead load and the direction of the load is upwards. The hydraulic pressure is only present during Phase 2. The lateral hydraulic pressure, as well as the lateral earth load, is calculated in Chapter 11, for the analysis of the joints.

6.1.4 Prestressing

The prestressing is normally viewed as an applied loading divided into two groups. One group includes the components that cause bending and the other group the components that cause precompression. The effects of these groups are viewed as independent. The bending determines the moments and shears, while the precompression is superimposed on the stresses from the flexural analysis. [8] The required prestressing force will be calculated by ADAPT-PT, based on the tensile stresses, the minimum precompression, and the percentage of dead load to balance.

6.1.5 Load summary

The vertical loads are summarized in Table 1. The self weight is not included, as it is calculated later by ADAPT automatically. No wind load is included in this study.

Table 1. The vertical loads acting on the slabs.

Load	
	[kN/m ²]
Upper slab	
Surface structures	8
Live load (including snow load)	10
Bottom slab	
Live load	2,5
Hydraulic pressure	-37

6.2 Load combinations

ADAPT provides the engineer with default load combinations based on the Eurocodes. But the Eurocodes contain a number of parameters left open for national choice, known as the Nationally Determined Parameters, including the load combination safety factors. These parameters are specified in the national annexes. Therefore, it is important to understand that the default values provided by computer programs, such as ADAPT, need to be checked by the engineer and corrected according to the national annex, if necessary. The combination of actions using Eurocode: Basis of structural design [17], applied with the Finnish National annex is described herein.

6.2.1 Combination of actions according to the Eurocodes

The combination of actions for persistent or transient design situations in the ultimate (strength) limit state is based on the following two expressions:

$$\left\{ \begin{array}{l} \sum_{j \geq 1} \gamma_{G,j} G_{k,j} + \gamma_P P + \gamma_{Q,1} \psi_{0,1} Q_{k,1} + \sum_{i > 1} \gamma_{Q,i} \psi_{0,i} Q_{k,i} \\ \sum_{j \geq 1} \xi_j \gamma_{G,j} G_{k,j} + \gamma_P P + \gamma_{Q,1} Q_{k,1} + \sum_{i > 1} \gamma_{Q,i} \psi_{0,i} Q_{k,i} \end{array} \right. \quad (9)$$

Where,

G	is permanent actions
Q	is variable actions
P	is prestressing actions
γ	is a partial factor
ψ	is a factor for imposed loads
ξ	is a reduction factor for unfavorable permanent actions

In the Finnish National annex these two expressions are presented as following:

$$\left\{ \begin{array}{l} 1,15 K_{FI} G_{kj,sup} + 0,9 G_{kj,inf} + 1,5 K_{FI} Q_{k,1} + 1,5 K_{FI} \sum_{i > 1} \psi_{0,i} Q_{k,i} \\ 1,35 K_{FI} G_{kj,sup} + 0,9 G_{kj,inf} \end{array} \right. \quad (10)$$

Where,

$G_{kj,sup}$	is unfavorable permanent actions
$G_{kj,inf}$	is favorable permanent actions
$Q_{k,1}$	is main variable actions
$Q_{k,i}$	is other variable actions
K_{FI}	is a multiplication factor depending on the reliability class
γ	is a partial factor

The combination of actions in the serviceability limit state is based on the following expressions:

$$\sum_{j \geq 1} G_{k,j} + P + \psi_{1,1} Q_{k,1} + \sum_{i > 1} \psi_{2,i} Q_{k,i} \quad (11)$$

$$\sum_{j \geq 1} G_{k,j} + P + \sum_{i > 1} \psi_{2,i} Q_{k,i} \quad (12)$$

The first expression is called the frequent combination and is normally used for reversible limit states. The second expression is called the

quasi-permanent combination and this combination is normally used for long-term effects and the appearance of the structure.

6.2.2 The load combinations used in this study

The partial factor of the self weight and dead load for the strength load combinations is 1,35 or 1,15 if the load is unfavorable and 0,9 if the load is favorable. The self weight and dead load are unfavorable in Phase 1, but in Phase 2 the self weight and other dead load from above is favorable as the hydraulic pressure from beneath is the unfavorable dead load. The partial factor of the live load for the strength load combinations is 1,5.

The hyperstatic moment is not factored. The reasons to this is that the parameters governing the hyperstatic actions are usually more accurately known than those governing the dead and live loads. In addition, the hyperstatic actions counteract the dead and live loads in most cases, so an increase of the hyperstatic actions is not justified.

The reliability class, associated with the consequence class, for this structure is RC2. This class is for structures where the consequences of failure or malfunction of the structure would include medium consequences for loss of human life and considerable economical, social, or environmental consequences. The reliability class RC2 gives the value of 1,0 for the multiplication factor K_{FI} .

For the service load combinations, the partial factors of the permanent loads, including prestressing, should be taken as 1,0. The factors for imposed loads for the service load combinations are obtained from the national annex. The structure in focus belongs to Category F: traffic area, vehicle weight $\leq 30\text{kN}$. Category F has the following values:

$$\psi_0 = 0,7$$

$$\psi_1 = 0,7$$

$$\psi_2 = 0,6$$

The two different load phases will be simulated using load combinations excluding or including the hydraulic pressure. Load combinations excluding the hydraulic pressure simulate Phase 1 and load combinations including the hydraulic pressure simulate Phase 2. The load combinations used can be seen in Figure 17 and Figure 18, obtained from ADAPT-PT.

Strength load combination factors									
1:	1.15	SW +	1.5	LL +	0	SDL +	0	X +	1 HYP
2:	1.35	SW +	0	LL +	0	SDL +	0	X +	1 HYP
3:	0.9	SW +	0	LL +	1.35	SDL +	0	X +	1 HYP
4:	0.9	SW +	1.5	LL +	1.15	SDL +	0	X +	1 HYP

Figure 17. The strength load combinations.

Service load combination factors											
1:	1	SW +	0.6	LL +	0	SDL +	0	X +	1	PT	Quasi Permanent Load
2:	1	SW +	0	LL +	1	SDL +	0	X +	1	PT	
3:	1	SW +	0.7	LL +	0	SDL +	0	X +	1	PT	Frequent Load
4:	1	SW +	0	LL +	1	SDL +	0	X +	1	PT	
Initial load combination factors											
1:	1	SW +	0	LL +	0	SDL +	0	X +	1.15	PT	

Figure 18. The service and initial load combinations.

Legend: SW = self weight, LL = live load, SDL = superimposed dead load, X = other loading, HYP = hyperstatic actions, PT = prestressing.

The hydraulic pressure is entered as a superimposed dead load. As only two different service load combinations for the two service load types, quasi-permanent load and frequent load, can be entered in ADAPT-PT, the live load is excluded from Phase 2. The live load in Phase 2 is favorable, so in order to analyze the worst case the live load is excluded. The factors of the initial (transfer) load combination are default values of ADAPT-PT and are based upon the common practice of engineers in the USA.

7 PRELIMINARY CALCULATIONS

7.1 General

The design process of the concrete slab in this study will be slightly different from the general design process using ADAPT software, described in Chapter 3.4. This is due to the complexity of the slab and the exceptional two-phased bidirectional loading. The objective is to find a design solution for the slab exposed to the variable hydraulic pressure and in order to do this, many different post-tensioning solutions must be examined. Therefore, a solution will first be sought for a smaller section of the slab, through preliminary calculations, and afterwards the solution found will be applied on the whole slab. The preliminary calculations will be done using only ADAPT-PT and the Equivalent Frame Method. Later on, the whole slab will be analyzed with ADAPT-Floor Pro using the Finite Element Method.

7.2 Preliminary calculation data

7.2.1 The selected section of the slab

The section of the slab chosen for the preliminary calculations has a span length of 8,5 m and a width of 6 m. The section is encircled in Figure 19 and the model created by ADAPT-PT is shown in Figure 20. The section also includes a beam with a cross-section of 700x1400 mm. This section was chosen for the preliminary calculations, because the structure geometry in this section is quite simple. It should therefore not be too difficult to find a solution to the engineering problem for this section, and then later apply the solution on the whole complex slab.

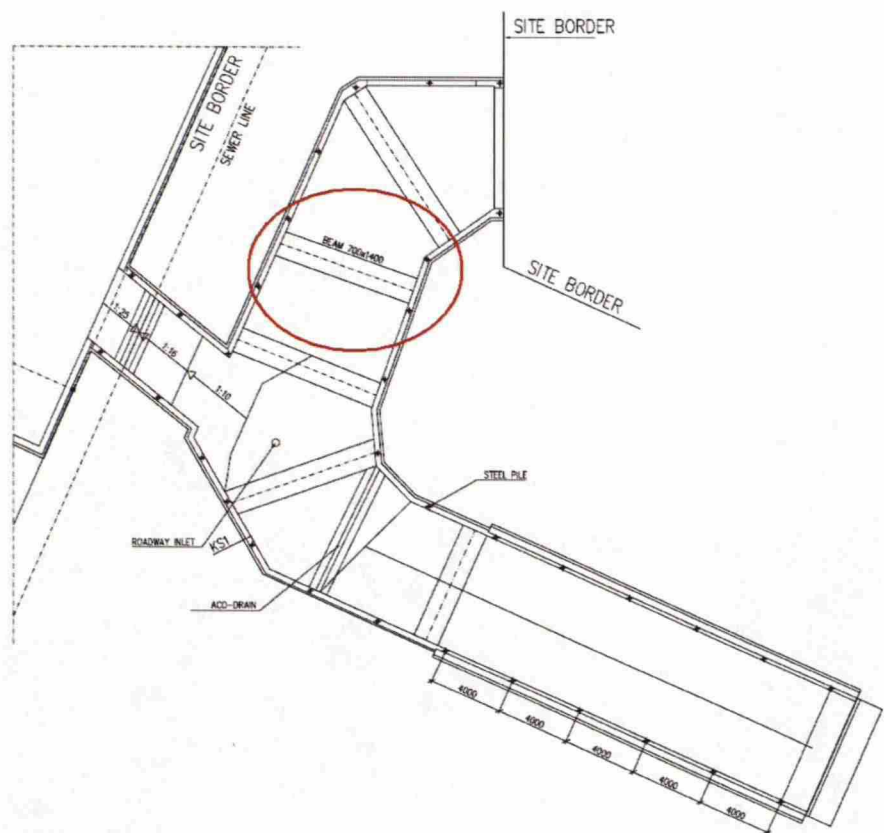


Figure 19. The section chosen for the preliminary calculations.

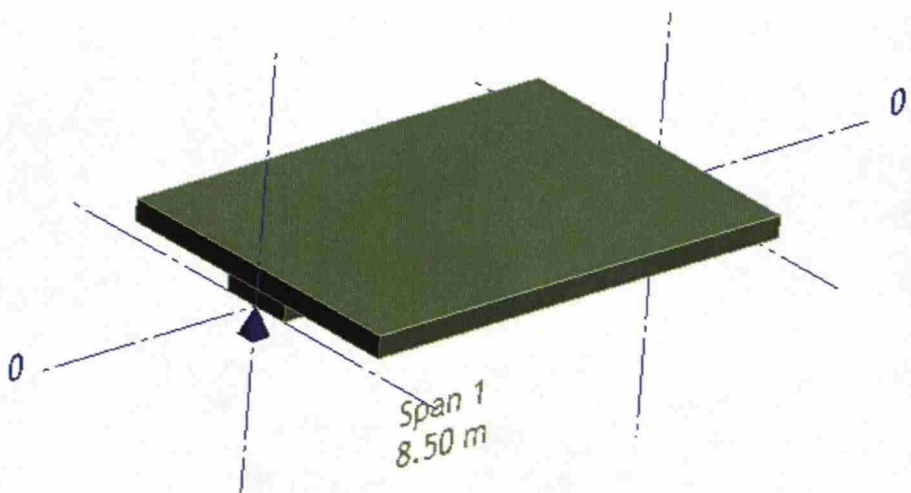


Figure 20. The model for the preliminary calculations.

7.2.2 Design criteria and loading

The design criteria presented in Chapter 5 and the loads and load combinations presented in Chapter 6 also apply for the preliminary calculations. The boundary conditions selected for the preliminary calculations are two hinged point supports at both ends of the span. In reality, the slab is the bottom slab of the tunnel, which acts as a frame. This means that there naturally exists a moment at the joints at both ends of the slab. Including these moments in the post-tensioning analysis

would, however, only reduce the span moment. For that reason, the hinged point supports can be used in the post-tensioning analysis, but the moments at the joints and the necessary joint reinforcement has to be checked separately later on. Using hinged supports also mean that no hyperstatic moments will develop in this preliminary section. But the hyperstatic actions are taken into consideration in the FEM-analysis later on.

7.3 Obtaining the design solution

The slab exposed to two-phased bidirectional loading requires a post-tensioning design solution able to resist both the loads from above during Phase 1, as well as the hydraulic pressure from beneath, involved in Phase 2. In addition the solution must mitigate the cracks in order to ensure the watertightness of the slab. A general post-tensioning solution, involving a reversed parabola tendon profile, would not be applicable. A reversed parabola tendon profile would not be able to resist the hydraulic pressure from beneath, as the reversed parabola profile is suitable for vertical loads from above only. A non-reversed (normal) parabola profile is not an option either, as a normal parabola profile would be able to resist the hydraulic pressure from beneath, but not the loads from above during Phase 1, when the hydraulic pressure is not present.

The post-tensioning solution could involve for example straight tendons, either somewhere in the center of the slab or both at the top and bottom of the slab. Another solution could be to use both normal and reversed parabola tendon shapes, either with a large drape or a smaller drape, and this way resist the bidirectional loading. These four design solutions will be examined. It is also possible to stress the tendons at different times. First, selected tendons could be stressed in Phase 1, and then other tendons could be stressed in Phase 2. This might, however, be quite a complicated solution and therefore, a solution involving stressing all tendons in Phase 1 will first be sought, and used if found.

ADAPT-PT provides the engineer with a design solution involving the minimum amount of post-tensioning demanded by the code and other design criteria. However, if multiple tendon paths are desired, some manual optimization is required, and finding an optimal solution for this unusual design problem requires a rather large amount of manual optimization.

In ADAPT-PT, the engineer has the option to choose between 5 different tendon profile types. All profile types can then be manually adjusted. The profile types are shown in Figure 21. Tendon profile types 1 and 4, in other words the reversed (or normal) parabola and straight tendon, will be used for the preliminary calculations. For the reversed parabola, a profile with the low point at mid-span and inflection points at span length/10 is the default.

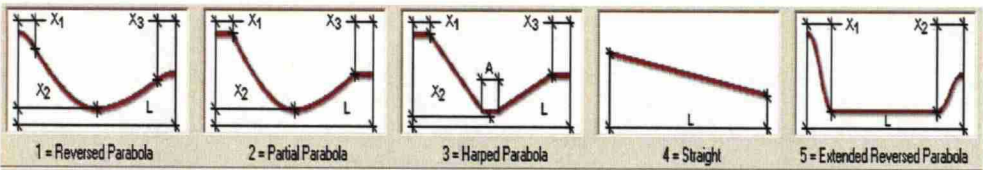


Figure 21. The tendon profile types available for ADAPT-PT.

The crack widths are not presented by ADAPT-PT, although the cracking is checked in the serviceability design. As crack mitigation is a central issue in this study, the crack widths for the design solution obtained using ADAPT software, will be manually analyzed at a later stage.

7.4 Design solutions

A distinguishing feature of post-tensioning design is that there is not only one solution to a design problem. Instead, several equally acceptable design solutions usually exist and it is up to the engineer to choose the solution most appropriate for his design.

Herein, four different design solutions are presented and compared. Each design solution is shortly described and a moment and a deflection diagram for each solution, are also presented. The deflection limit is $\text{span}/500$, in other words 17 mm. The design solutions are presented in more detail, through summary reports created by ADAPT-PT and selected tables from more detailed reports created by ADAPT-PT, in Appendix A. Finally, the design solutions are compared and the most appropriate solution will be selected and adapted on the rest of the slab.

7.4.1 Design solution 1

Design solution 1 involves straight tendons in the centre of the slab (Figure 22). The optimal height of the tendons, resulting in the smallest amount of non-prestressed reinforcement, is at the centre of gravity, which is at approximately 445 mm from the bottom of the beam.

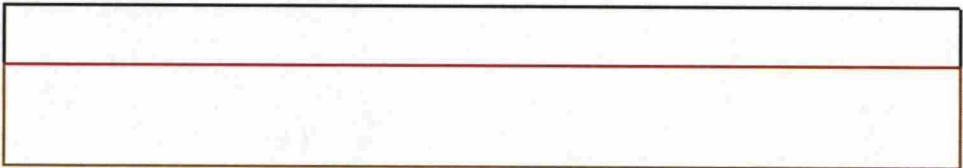


Figure 22. Tendon profile of design solution 1.

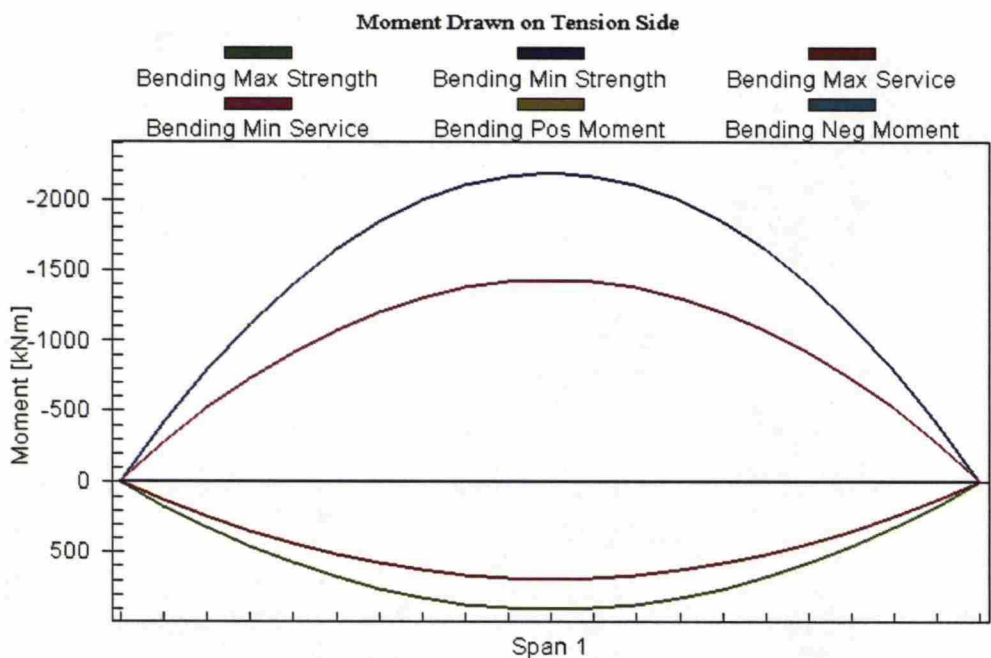


Figure 23. Moment diagram for design solution 1.

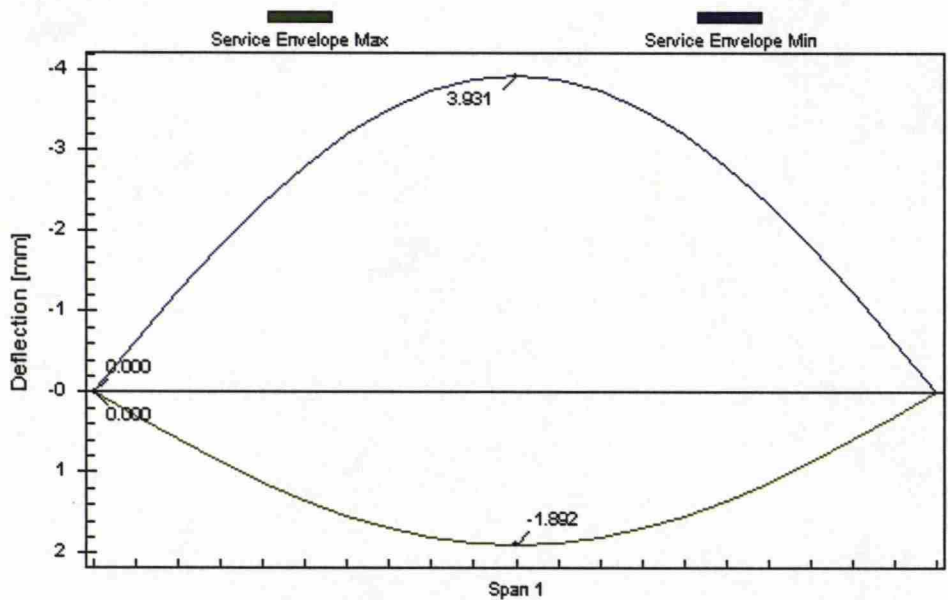


Figure 24. Deflection diagram for design solution 1.

7.4.2 Design solution 2

Design solution 2 also involves straight tendons, but both at the top and bottom of the slab, 100 mm from the slab surface (Figure 25).

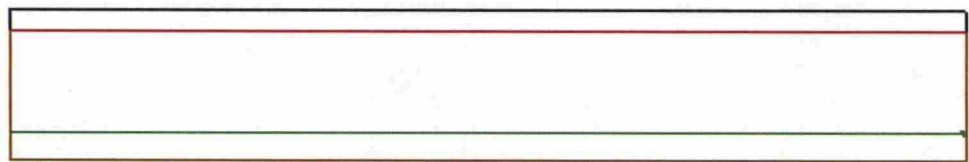


Figure 25. Tendon profile of design solution 2.

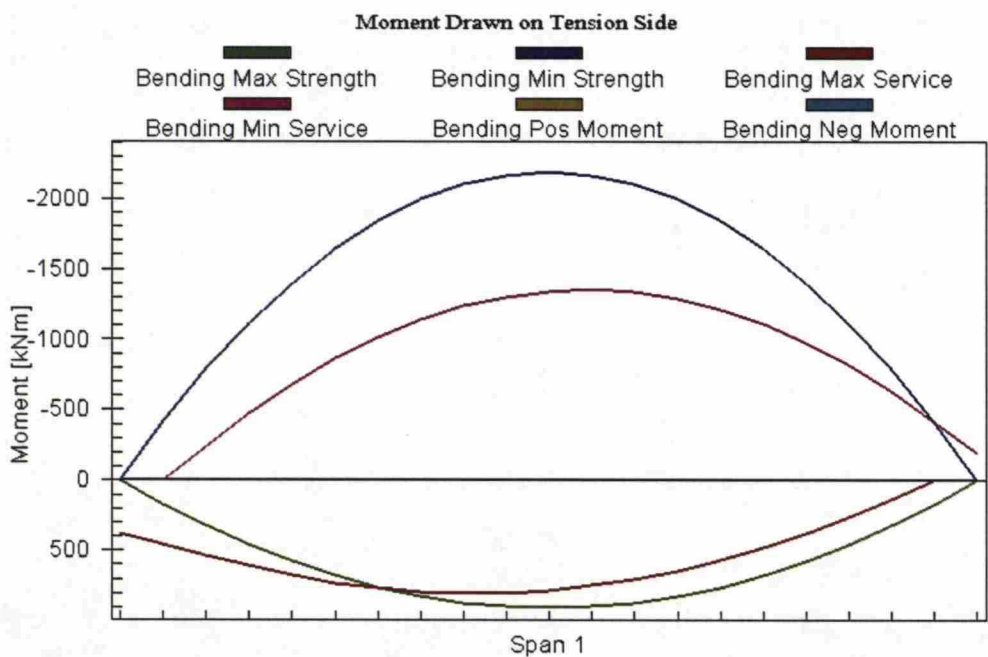


Figure 26. Moment diagram for design solution 2.

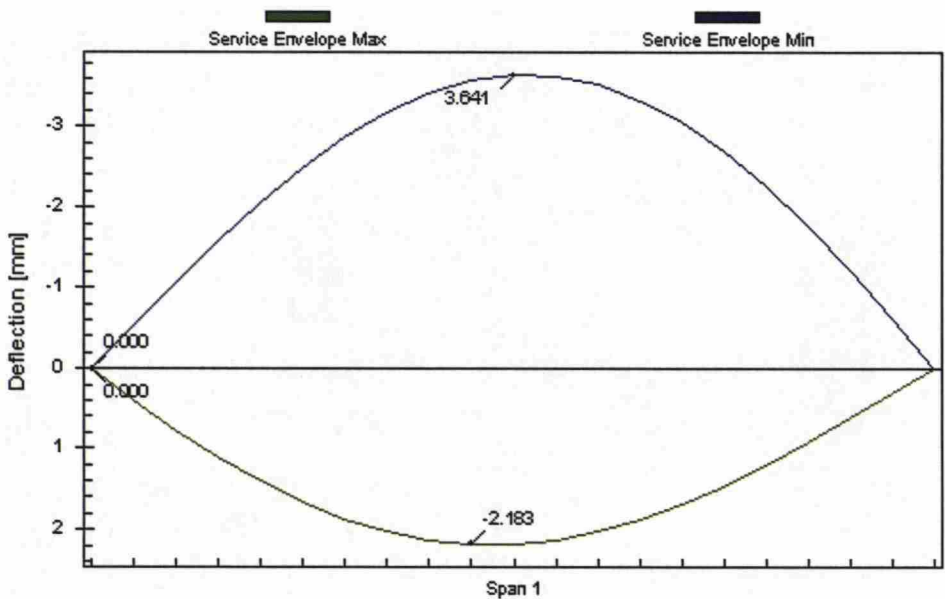


Figure 27. Deflection diagram for design solution 2.

7.4.3 Design solution 3

Design solution 3 involves both normal and reversed parabola tendon shapes with a large drape of 500 mm (Figure 28).

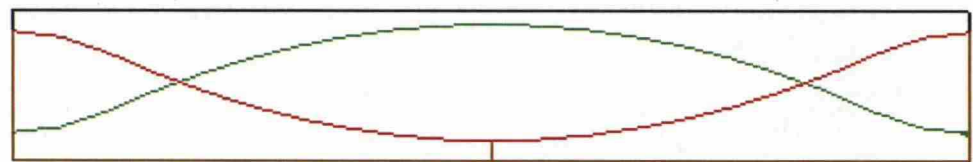


Figure 28. Tendon profile of design solution 3.

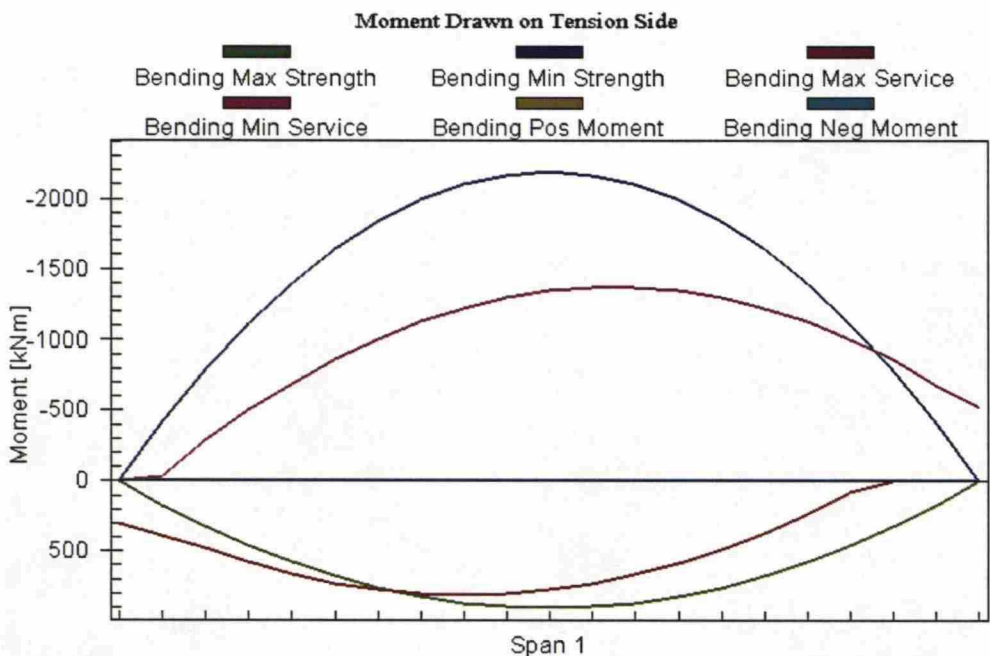


Figure 29. Moment diagram for design solution 3.

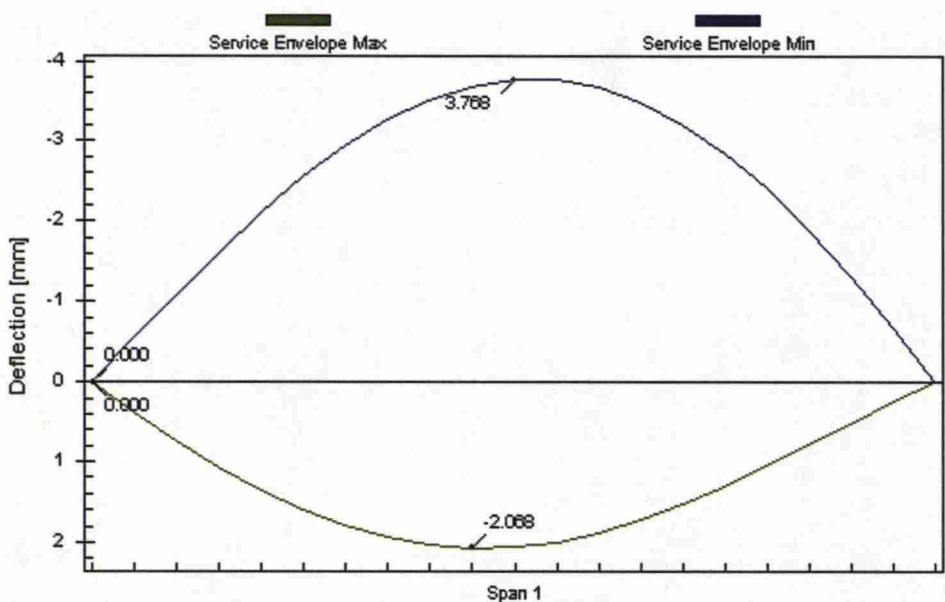


Figure 30. Deflection diagram for design solution 3.

7.4.4 Design solution 4

Design solution 4 involves both normal and reversed parabola tendon shapes with a smaller drape of 250 mm (Figure 31).

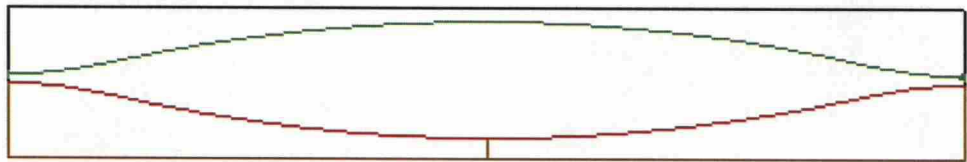


Figure 31. Tendon profile of design solution 4.

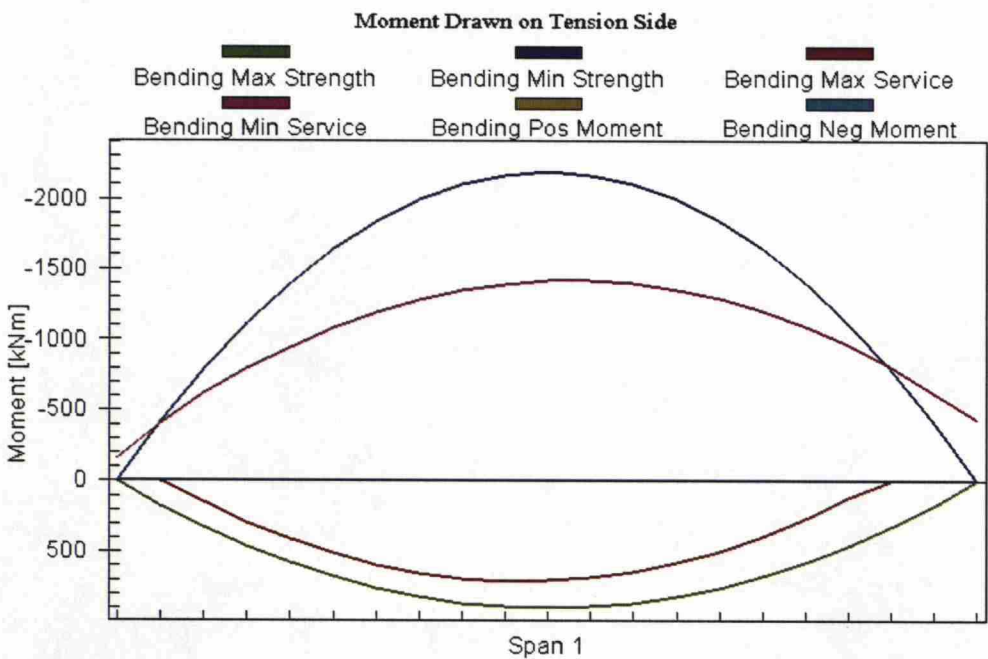


Figure 32. Moment diagram for design solution 4.

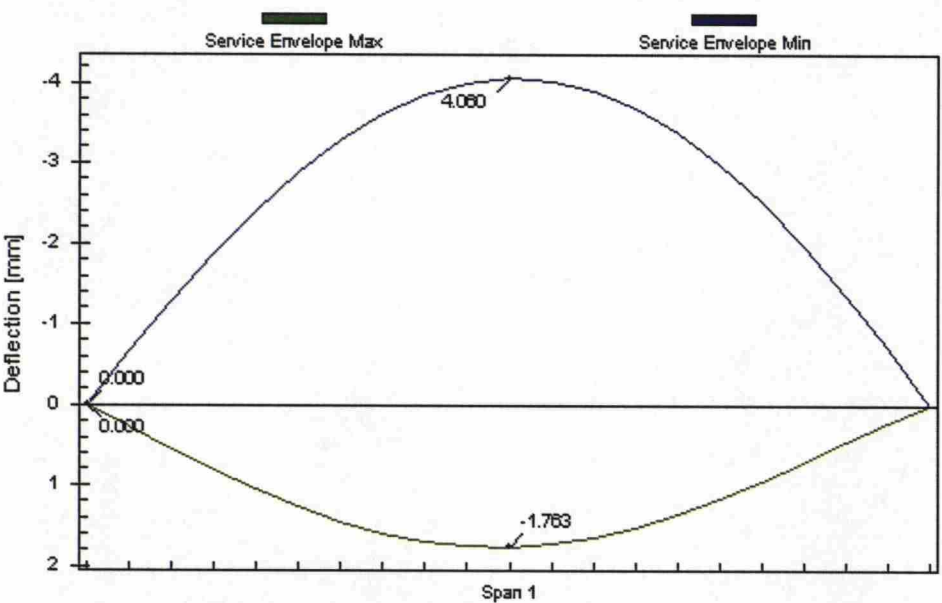


Figure 33. Deflection diagram for design solution 4.

7.5 Choice of design solution

The four design solutions presented above are all acceptable solutions, but they have certain advantages and disadvantages. The easiest way to compare the designs is by the necessary material quantities, presented in Table 2, but other factors should be considered as well. Other factors considered are installation easiness, space for anchors, and contribution to crack mitigation. Tendon A is the red tendon and tendon B the green tendon in the tendon profile figures.

Table 2. The material quantities of the design solutions.

Solution	Tendons	Tendons	Top rebar	Bottom rebar	Prestressing steel	Mild steel
	A	B	(25mm)	(25mm)	[kg/m³]	[kg/m³]
1	20		8	4	9,34	10,1
2	12	8	10	6	9,34	14,32
3	10	12	10	6	10,27	14,51
4	8	14	9	4	10,27	10,59

The ease of installation at the construction site is important. More complex post-tensioning designs require more effort at installation and it is therefore a disadvantage. The straight tendon type is easier to install than the parabola, and two different parabola tendon types used in the same construction requires even more effort. The available space at the anchorage zone can be relevant if a large number of tendons have the same height at the ends. Design solutions 1 and 4 have this disadvantage. Crack mitigation is extremely important in this study in order to ensure the watertightness of the slab. Tendons closer to the slab surface contribute more to crack mitigation than tendons in the centre of the slab. Design solution 1 has tendons only in the centre of the slab.

Many other factors could be considered in the choice of design solution, but these considered factors already bring forth design solution 2. Design solution 2 involves straight tendons, which are easy to install. It has the same amount of prestressing material as design solution 1, however, placing the tendons at two different locations in the slab, the top and bottom, reduces the problem of insufficient space for anchors and contributes to the mitigation of cracks. Therefore, straight tendons at the top and bottom of the slab, is the chosen design solution for this study. This design solution will be adopted on the whole slab. The design solution found could act as a general solution for any post-tensioned slab exposed to bidirectional vertical loading, where the reversed parabola tendon profile is not suitable.

The ADAPT-PT summary report shows the tendon force, the number of strands, and the stress for some reason only for tendon A, when using multiple tendon paths, not for tendon B. This turned out to be a bug in the reporting feature and was reported to the ADAPT development team.

8 VERIFICATION BY CODE-BASED METHODS

8.1 General

When using advanced post-tensioning software like ADAPT-PT, it is extremely important that the engineer understands the concepts of post-tensioning, and that the results are verified. Therefore, the solution found for the smaller section of the slab will be verified through manual calculation using code-based methods and Mathcad software. The verification will be done using the National Building Code of Finland [18], although the design of the concrete slab is done using the Eurocodes. Different design codes should not be used simultaneously, however, as these manual calculations are only a verification of results already obtained using the Eurocodes, the National Building Code of Finland may be used. This way, not only the results obtained with ADAPT-PT are verified, but also the results of the Eurocodes. As manual calculation using multiple tendon paths is very complicated, design solution 2 will be somewhat simplified for the manual verification. Design solution 2 involved twelve tendons at 600 mm from the bottom of the beam and eight tendons at 100 mm from the bottom of the beam. In the manual verification, all tendons will be placed in the middle, at the height 400 mm, instead. The stress losses calculated with ADAPT-PT will also be manually verified.

8.2 The basics of the calculations

8.2.1 Post-tensioning and mild steel reinforcement

The manual verification calculations are based on BY27 Tartunnattomat jänteet betonirakenteissa [19] and presented in Appendix B. The principle of the calculations is to determine the ultimate moment resistance of the tendons and the tension reinforcement, and then compare this moment resistance to the external design moment. The ultimate moment resistance is determined through the total prestress design force P_d and the non-prestressed reinforcement design force F_{sd} , both shown in Figure 34. The height of the compression part in the ultimate limit state is calculated through the expression:

$$y = \frac{P_d + F_{sd}}{f_{cd}b} \quad (13)$$

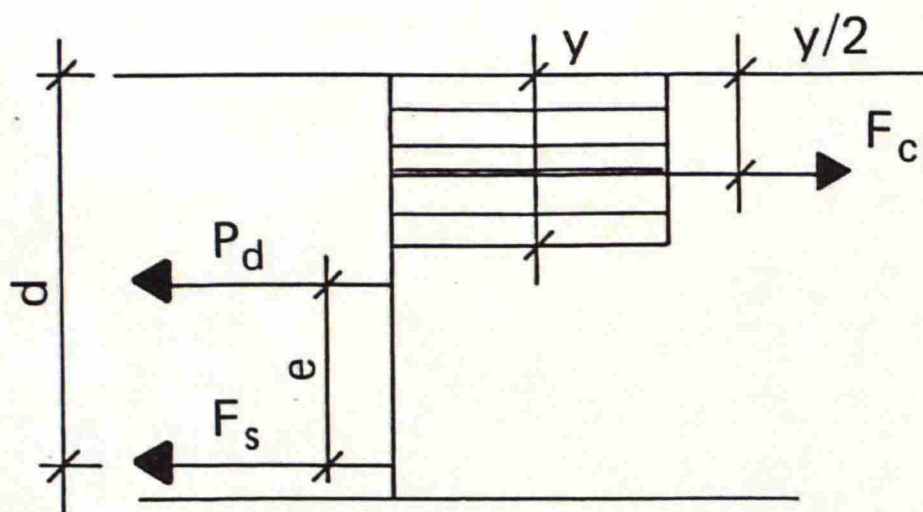


Figure 34. The principle of the manual verification calculations.

The material factors for concrete, mild steel, and prestressing steel used for the ADAPT calculations are the following, although, according to the Eurocodes a reduction of the factors based on quality control and reduced deviations would be allowed:

$$\gamma_c = 1,5$$

$$\gamma_s = 1,15$$

$$\gamma_p = 1,15$$

Therefore, the material factors of structure class 2 (Rakenneluokka 2) of the National Building Code of Finland [18] will be used. The material factors of structure class 2 correspond to the factors of the Eurocodes, without the allowed reduction.

8.2.2 Stress losses

The manual verification of stress losses is also based on BY27 Tartunnattomat jänteet betonirakenteissa [19] and presented in Appendix B. The basics of stress loss calculations are described in Chapter 2.3.3.

8.3 Preliminary section – midspan – top

The required reinforcement area for the top, calculated by ADAPT-PT, is 4553 mm² (see Table 21, Appendix A) and is based on the ultimate limit state. ADAPT-PT suggests ten mild steel bars with a diameter of 25 mm. This gives a reinforcement area of 4909 mm².

The manual verification of the results, using the National Building Code of Finland, indicates that only seven bars would be needed at the top, while ADAPT-PT suggests ten bars. The results vary quite notably. The variation in the results could be either due to the different calculation methods or due to the inequality of the partial safety factors for loads of the Eurocodes and the National Building Code of Finland. In order to

determine the reason for the variation in the results, the same manual calculations are done using the partial safety factors of the Eurocodes (Appendix B).

The manual verification using the Eurocodes suggests ten mild steel bars at the top. The same amount is suggested by ADAPT-PT. This proves that the variation in the results is due to the inequality of the partial safety factors for loads of the Eurocodes and the National Building Code of Finland.

8.4 Preliminary section – midspan – bottom

The required reinforcement area for the bottom, calculated by ADAPT-PT, is 2639 mm² (see Table 21, Appendix A). This is based on the minimum reinforcement area. ADAPT-PT suggests six mild steel bars with a diameter of 25 mm. This gives a reinforcement area of 2945 mm². The minimum amount of mild steel bars, calculated with the National Building Code of Finland, is six bars with the diameter 25 mm. This is the same amount as calculated with ADAPT-PT.

8.5 Stress losses

The immediate and time dependent losses of prestress for post-tensioning are manually calculated using the National Building Code of Finland and BY27 Tartunnattomat jänteet betonirakenteissa [19]. The calculations are presented in detail in Appendix B. In Chapter 8.6.2, the manually obtained results are compared to the results obtained using the default stress loss parameters of ADAPT-PT.

8.6 Comparison and conclusions

8.6.1 Post-tensioning and mild steel reinforcement

The required amount of non-prestressed reinforcement bars at the bottom is the same manually calculated using the National Building Code of Finland as it is calculated with ADAPT-PT.

The required amount of non-prestressed reinforcement bars at the top is the same manually calculated using the Eurocodes as it is calculated with ADAPT-PT. However, the required amount non-prestressed reinforcement bars at the top manually calculated using the National Building Code of Finland is only seven mild steel bars with the diameter 25 mm, while the Eurocodes requires ten bars. The reason for the difference in the results turned out to be the inequality of the partial safety factors of the Eurocodes and the National Building Code of Finland. The partial safety factors of the Eurocodes are 1,35 for unfavorable permanent actions when no variable actions are present, and 0,9 for favorable permanent actions. This results in the design moment:

$$M_d = (1,35 * 2004,97 - 0,9 * 599,63)kNm = 2167kNm \quad (14)$$

But the partial safety factors of the National Building Code of Finland are

1,2 for unfavorable permanent actions and 0,9 for favorable permanent actions. This results in a difference of 14% in design moment:

$$M_d = (1,2 * 2004,97 - 0,9 * 599,63)kNm = 1866kNm \quad (15)$$

A comparison of the design moments and moment resistance capacities manually calculated using the National Building Code of Finland and using the Eurocodes is shown in Table 3. In addition, a comparison of the minimum reinforcement area at the top manually calculated, using the National Building Code of Finland and the Eurocodes, and the minimum reinforcement area obtained from ADAPT-PT is shown in Table 4.

Table 3. Comparison of design moments and moment resistance capacities.

	Design moment	Moment resistance (10 25mm)
	[kNm]	[kNm]
National Building Code of Finland	1866	2227
Eurocodes	2167	2272

Table 4. Comparison of the required rebar area at the top.

	Required rebar area	Number of 25 mm bars
	[mm ²]	
National Building Code of Finland	3436	7
Eurocodes	4497	10
ADAPT-PT	4553	10

This study is based on the Eurocodes and therefore the amount of reinforcement required by the Eurocodes will be used. The larger amount of reinforcement might also be necessary for the mitigation of cracks. This manual verification confirms that the results obtained with ADAPT-PT could be considered as accurate enough for design purposes.

8.6.2 Stress losses

The stresses after immediate losses and time dependent losses calculated with ADAPT-PT are shown in Table 5. The values manually calculated are shown in Table 6. The results obtained with ADAPT-PT and the manually calculated results are in the same order of magnitude. This confirms that the stress losses calculated with ADAPT-PT are accurate.

Table 5. Stresses after immediate and time dependent losses calculated with ADAPT-PT.

Tendon	Span	Stress Left FL Only	Stress Center Only	Stress Right FL	Stress Left FL+LTL	Stress Center FL+LTL	Stress Right FL+LTL
		MPa	MPa	MPa	MPa	MPa	MPa
TENDON_A1	1	1275.00	1248.00	1220.00	1207.00	1183.00	1159.00
TENDON_B1	1	1275.00	1248.00	1220.00	1207.00	1183.00	1159.00

Table 6. Stresses after immediate and time dependent losses manually calculated.

Stress after immediate losses	Stress after immediate and time dependent losses
[N/mm ²]	[N/mm ²]
1235	1125

When manually verifying the stress losses a bug in ADAPT-PT was found. The program is supposed to calculate the concrete's modulus of elasticity at stressing using the equation of the Eurocodes and the cube strength of the concrete at stressing. However, for some reason the program does not use the concrete strength at stressing when calculating the modulus of elasticity. The cube strength of the concrete at stressing is 27 N/mm² (cylinder strength 21,6 N/mm²) and the concrete's modulus of elasticity according to the Eurocodes should then be:

$$E_{cm} = 22 \left[\frac{21,6 + 8}{10} \right]^{0,3} \frac{N}{mm^2} = 30465 \frac{N}{mm^2} \quad (16)$$

However, the default value provided by ADAPT-PT, shown earlier in Figure 16, is only 10509,6 N/mm². This bug was reported to the ADAPT development team. The effect of this bug was inspected by calculating the stress losses with ADAPT-PT again and manually change the concrete's modulus of elasticity at stressing to 30465 N/mm². The stresses after immediate and time dependent losses obtained with this value are shown in Table 7.

Table 7. Stresses using the corrected concrete's modulus of elasticity.

Tendon	Span	Stress Left FL Only	Stress Center FL Only	Stress Right FL Only	Stress Left FL+LTL	Stress Center FL+LTL	Stress Right FL+LTL
		MPa	MPa	MPa	MPa	MPa	MPa
TENDON_A	1	1275.00	1248.00	1220.00	1214.00	1191.00	1166.00
TENDON_B	1	1275.00	1248.00	1220.00	1214.00	1191.00	1166.00

Comparison of the corrected results with the results using the default value for the concrete's modulus of elasticity shows that the default value results in smaller final stresses. However, the difference is less than a percent, and as the results obtained, using the default value, are on the safe side, these values may be used.

9 APPLYING THE DESIGN SOLUTION

9.1 General

Design solution 2 was chosen as the most appropriate solution for the slab in focus, as tendons at both slab surfaces reduce the problem of insufficient space for anchors and contribute to the mitigation of cracks (see Chapter 7.5), and will now be applied on the whole slab and the other beams. A FEM-analysis of the whole slab is presented in Chapter 13.

9.2 Beams

Design solution 2 will be directly applied on the beams. However, the beam carrying the point load from the composite column will be separately analyzed to confirm that the design solution is appropriate for this beam as well and to determine the required non-prestressed reinforcement for the point load.

9.2.1 Separate beam analysis

The beam carrying the point load from the composite column is separately analyzed with ADAPT-PT and the results are presented in Appendix C. Design solution 2 is applied on this beam as well and the solution is appropriate. The same amount of prestressing tendons is used, however, due to the point load, the necessary amount of non-prestressed reinforcement changes both in the top and bottom of the beam. Twelve mild steel bars with the diameter 25 mm are required at the bottom, but only seven bars at the top. The material quantities are shown in Table 8, a moment diagram in Figure 35, and a deflection diagram in Figure 36.

Table 8. The material quantities of the separate beam analysis.

Solution	Tendons	Top rebar (25mm)	Bottom rebar (25mm)	Prestressing material	Mild steel
				[kg/m ³]	[kg/m ³]
Beam	20	7	12	9,34	18,43

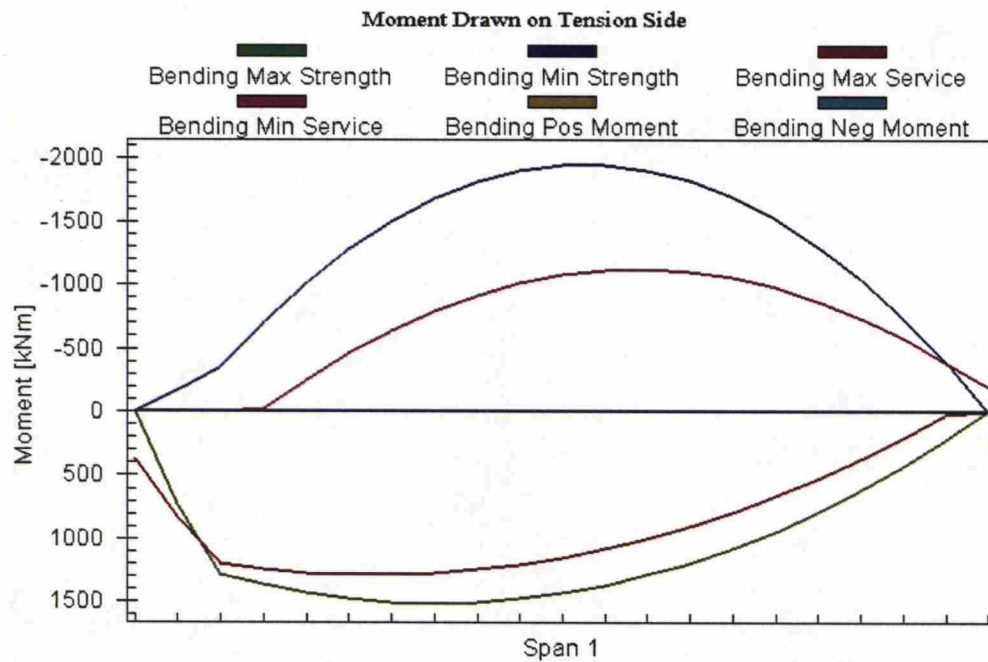


Figure 35. Moment diagram for the beam carrying the point load.

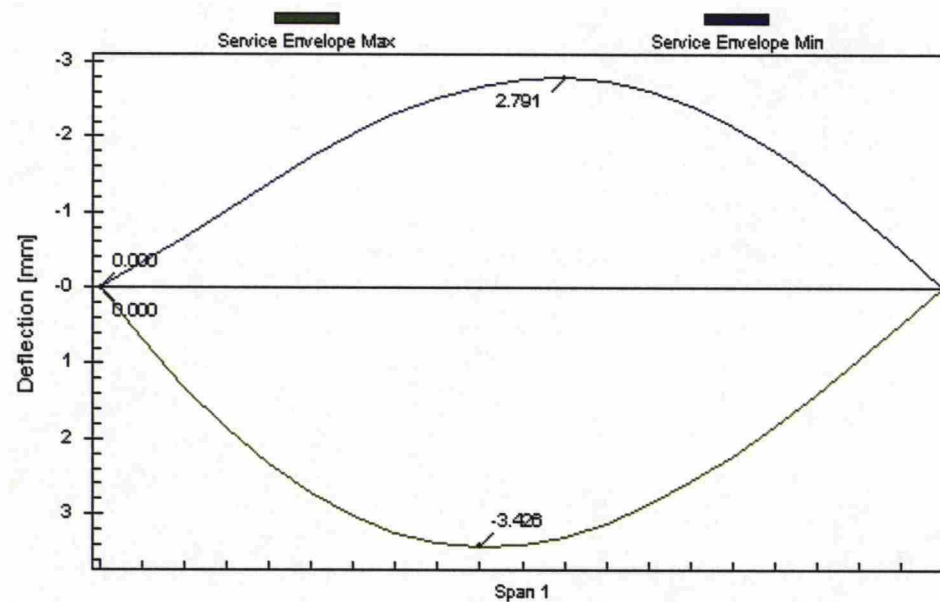


Figure 36. Deflection diagram for the beam carrying the point load.

9.3 Slab

A separate analysis with ADAPT-PT for a one meter wide section of the slab, including the transverse beams acting as supports for the slab, is done using the concept of the design solution 2. The location of the most critical section of the slab is estimated in Figure 37. This section has a long span length of 7,5 m, but is still not very close to the supporting walls. A model created by ADAPT-PT, including the transverse beams, is shown in Figure 38. The slab area encircled in Figure 37 will not be post-tensioned due to the short span length.

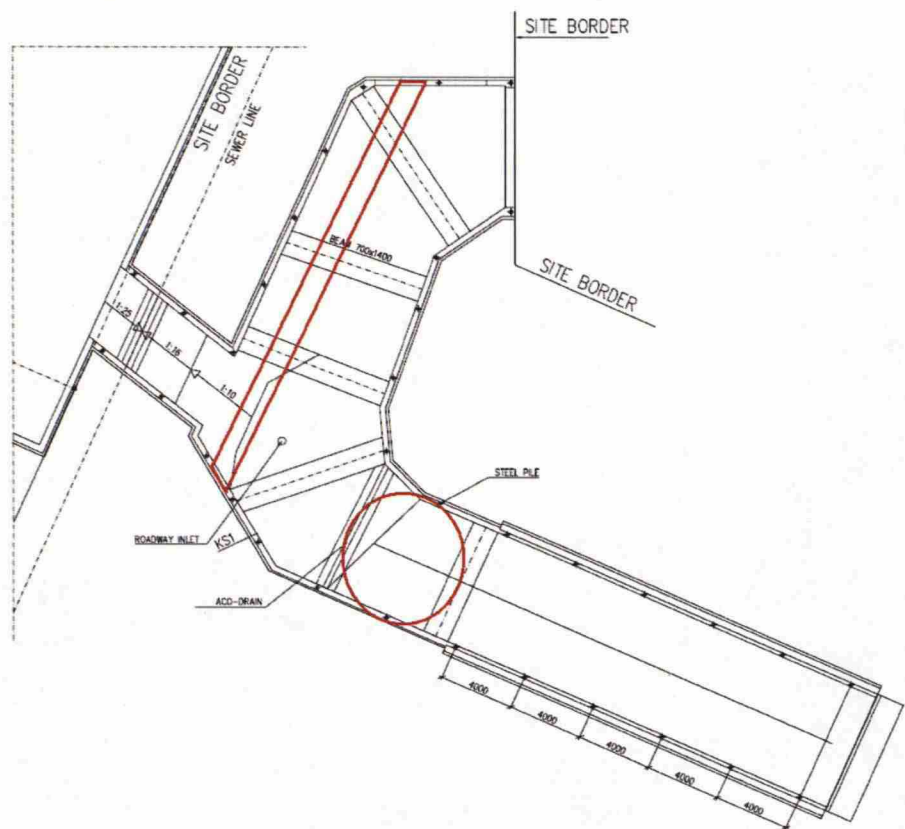


Figure 37. The slab section.

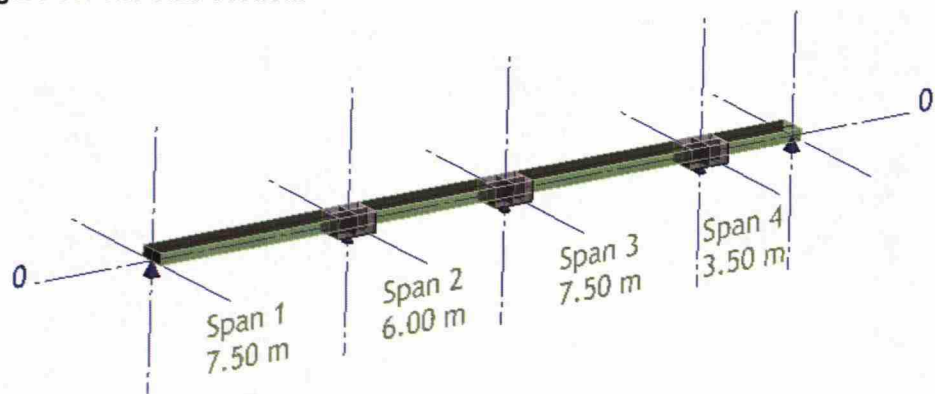


Figure 38. The model created with ADAPT-PT.

The design is again presented through a summary report created by ADAPT-PT and selected tables (Appendix C). The tendon profile, which is the same as in design solution 2 with straight tendons at the top and bottom of the slab, is shown in Figure 39. The material quantities are shown in Table 9, a moment diagram in Figure 40, and a deflection diagram in Figure 41.

Figure 39. The tendon profile of the slab section.

Table 9. The material quantities of the slab section.

Solution	Tendons	Tendons	Prestressing steel	Mild steel
	A	B	[kg/m³]	[kg/m³]
Slab	2/m	1/m	9,15	2,86

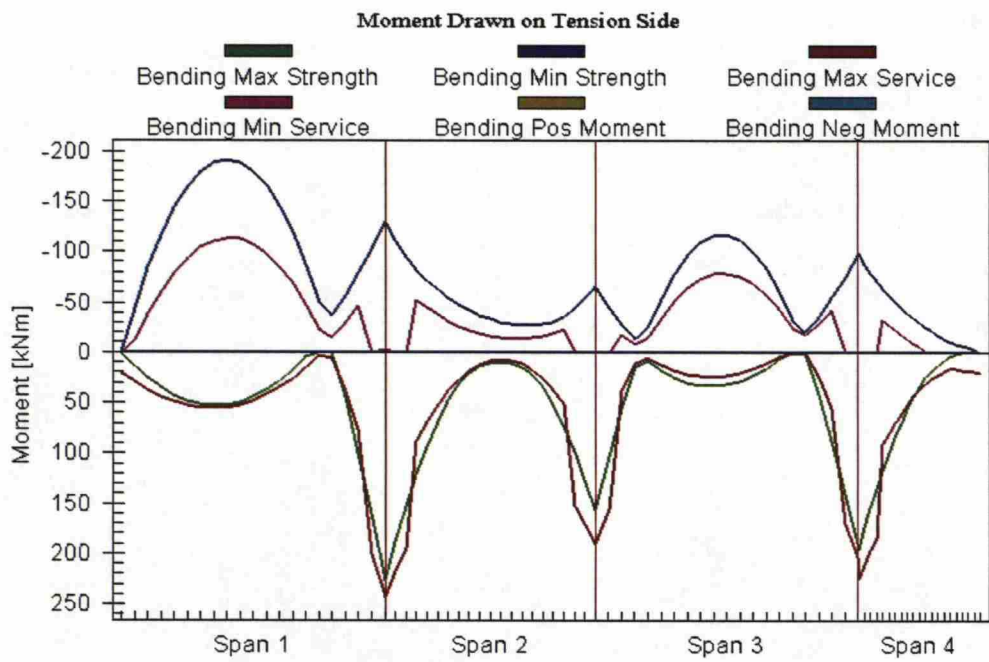


Figure 40. Moment diagram for the slab section.

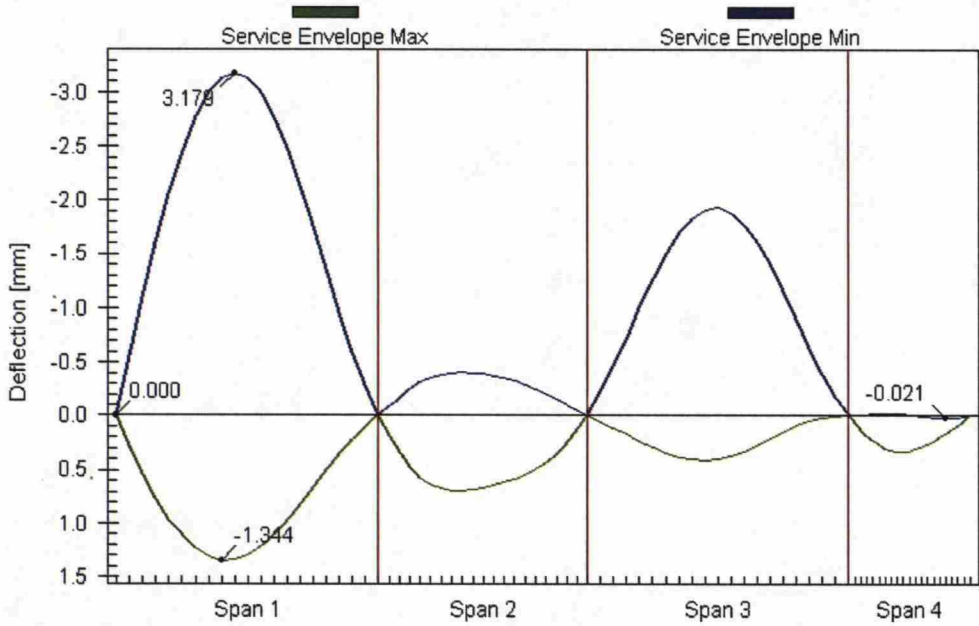


Figure 41. Deflection diagram for the slab section.

10 CRACK CONTROL

10.1 General

According to Eurocode 2 [4], cracking shall be limited to an extent that will not impair the proper functioning or durability of the structure or cause its appearance to be unacceptable. Crack control was done in the serviceability check of ADAPT-PT, but as ADAPT-PT does not present the crack widths, the cracking is double-checked by manually calculating the crack widths herein. Cracking can be controlled either without direct calculation or by calculating the crack widths. A minimum amount of bonded reinforcement is also required in areas where tension is expected.

Comparison of crack widths calculated using the Eurocodes and using the National Building Code of Finland shows that the crack widths calculated using the Eurocodes tend to be smaller than the crack widths calculated using the National Building Code of Finland. Hence, the Eurocodes give too optimistic values for cracking from a Finnish point of view. [20] Therefore, the Finnish National annex of Eurocode 2 Part 1-1 refers to Eurocode 2 Part 3: Liquid retaining and containment structures [21], when determining the limiting crack width for structures where tightness is required. It is as well recommended in Finland not to control cracking without direct calculation, but instead always calculate the crack widths.

Cracking control in this study is a very important issue, as watertightness is a concern. The crack widths are calculated and compared to the limitation values. The recommended values for the limiting crack width are dependent on the exposure class and are shown in Table 10.

Table 10. Recommended values for the limiting crack width [mm] [4].

Exposure Class	Reinforced members and prestressed members with unbonded tendons	Prestressed members with bonded tendons
	Quasi-permanent load combination	Frequent load combination
X0, XC1	0,4 ¹	0,2
XC2, XC3, XC4	0,3	0,2 ²
XD1, XD2, XS1, XS2, XS3		Decompression
Note 1: For X0, XC1 exposure classes, crack width has no influence on durability and this limit is set to guarantee acceptable appearance. In the absence of appearance conditions this limit may be relaxed.		
Note 2: For these exposure classes, in addition, decompression should be checked under the quasi-permanent combination of loads.		

However, Eurocode 2 Part 3 gives the recommended values for structures retaining water. The values are defined as a function of the ratio of the hydrostatic pressure h_w to the wall thickness h :

$$\frac{h_w}{h} \leq 5, w_{k,\max} = 0,2mm \quad (17)$$

$$\frac{h_w}{h} \geq 35mm, w_{k,\max} = 0,05mm. \quad (18)$$

For intermediate values of $\frac{h_w}{h}$ linear interpolation should be used. The ratio for the slab in focus is

$$\frac{h_w}{h} = \frac{3,7m}{0,4m} = 9,25 \quad (19)$$

Interpolation gives the limiting crack width

$$w_{k,\max} = 0,2mm - \frac{(9,25 - 5)}{(35 - 5)} * (0,2mm - 0,05mm) = 0,178mm \quad (20)$$

[21]

10.2 Calculation of crack widths

Using the Eurocodes, the crack width w_k may be calculated as the product of the maximum crack spacing and the mean strain using the expression:

$$w_k = s_{r,\max} (\varepsilon_{sm} - \varepsilon_{cm}) \quad (21)$$

Where,

$s_{r,\max}$	is the maximum crack spacing
ε_{sm}	is the mean strain in the reinforcement
ε_{cm}	is the mean strain in the concrete between cracks

The difference between the mean strain in the reinforcement and the mean strain in the concrete $\varepsilon_{sm} - \varepsilon_{cm}$ may be calculated from the expression:

$$\varepsilon_{sm} - \varepsilon_{cm} = \frac{\sigma_s - k_t \frac{f_{ct,eff}}{\rho_{p,eff}} (1 + \alpha_e \rho_{p,eff})}{E_s} \geq 0,6 \frac{\sigma_s}{E_s} \quad (22)$$

Where,

σ_s	is the stress in the tension reinforcement assuming a cracked section
k_t	is a factor dependent on the duration of the load
$f_{ct,eff}$	is the mean value of the tensile strength of the concrete

α_e is the ratio $\frac{E_{cm}}{E_s}$

$\rho_{p,eff}$ is $\frac{(A_s + \xi_1^2 A_p')}{A_{c,eff}}$

Where,

E_{cm} is the modulus of elasticity of concrete

E_s is the modulus of elasticity of reinforcement steel

A_s is the area of reinforcing steel

A_p' is the area of post-tensioned tendons within $A_{c,eff}$

$A_{c,eff}$ is the effective area of concrete in tension surrounding the reinforcement

ξ_1 is the adjusted ratio of bond strength taking into account the different diameters of prestressing and reinforcing steel

The maximum crack spacing may be calculated from the expression:

$$s_{r,max} = k_3 c + k_1 k_2 k_4 \frac{\phi}{\rho_{p,eff}} \quad (23)$$

Where,

ϕ is the bar diameter

c is the cover to the longitudinal reinforcement

k_1, k_2, k_3, k_4 are coefficients taking into account the bond properties of the reinforcement and the distribution of strain

10.2.1 The height of the compressed section

For the mean strain calculations, the tension in the reinforcement is needed. It is obtained by first determining the height of the compressed section x of the cross-section for the prestressed member and then the ratio of the height of the compressed section and the effective height:

$$\zeta = \frac{x}{d_s} \quad (24)$$

This is done with the help of BY16 Suunnittelun sovellusohjeet [22]. The parameters for a T-section are presented in Figure 42 and the parameters for a rectangular cross-section in Figure 43.

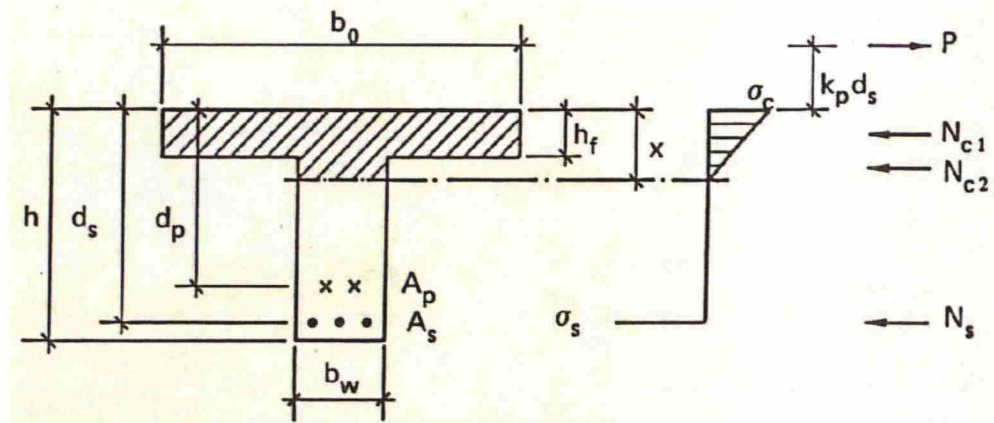


Figure 42. The T-section [22].

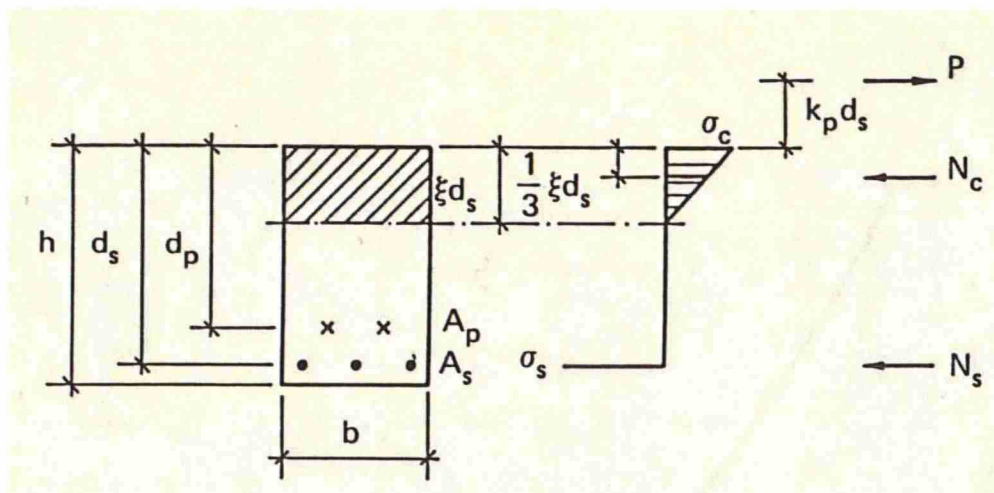


Figure 43. The rectangular cross-section [22].

If the height of the compressed section x is equal to the height of the cross-section, the cross-section is totally compressed and no tension exists. In this case, the crack width is equal to zero.

10.3 Calculation of the minimum reinforcement areas

According to the Eurocodes, the minimum amount of reinforcement in tension areas may be calculated from the expression:

$$A_{s,min} \sigma_s = k_c k f_{ct,eff} A_{ct} \quad (25)$$

Where,

- $A_{s,min}$ is the minimum area of reinforcement in the tensile zone
- σ_s is the maximum stress permitted in the reinforcement immediately after the formation of the crack
- k_c is a coefficient taking into account the stress distribution within the section
- k is a coefficient which allows for the effect of non-uniform self-equilibrating stresses

$f_{ct,eff}$ is the mean value of the tensile strength of the concrete
 A_{ct} is the area of concrete in the tensile zone

10.4 Results

The crack widths and the minimum reinforcement areas are calculated using Mathcad software. The beam is analyzed as a T-section, while the slab is analyzed as a rectangular section. The calculations are presented in Appendix D and the results in Table 11. The calculation of crack widths for the bottom of the preliminary section is shown as a whole in Appendix D, while only concise calculations are shown for the other areas. The moments and prestressing forces are obtained from ADAPT-PT as well as the number and size of mild steel bars.

Table 11. The manually calculated crack widths and minimum rebar areas.

Section	Crack width	Minimum rebar area
	[mm]	[mm ²]
Preliminary section		
Midspan - bottom	0,049	289
Midspan - top	0,099	2074/m
Beam with point load		
Midspan - bottom	0,095	289
Midspan - top	0,051	2074/m
Slab section		
Midspan - bottom	9,18E-05	82
Midspan - top	0	0
Support - bottom	0,099	553
Support - top	0	0
Limiting crack width	0,178	

10.5 Crack width conclusions

The crack width calculations show that all crack widths are below the limitation value $w_{k,max} = 0,178mm$. According to Eurocode 2 Part 3 "Limitation of the crack widths to these values should result in the effective sealing of the cracks within a relatively short time" [21], but the crack width limitation value may seem quite large from a Finnish point of view. However, the largest calculated crack width is only 0,099 mm. This value should ensure the watertightness of the structure even from a Finnish point of view. The variation in hydraulic pressure during Phase 2 will not have any significant effect on the crack widths or watertightness, as the maximum change in ground water level is only approximately one meter. The minimum reinforcement areas are to be taken into account in the final design, if the amount of provided non-prestressed reinforcement is less than the minimum amount.

11 JOINT REINFORCEMENT

11.1 General

In the previous calculations, the slab has been analyzed as supported by hinge supports. However, the slab is actually the bottom slab of a tunnel acting as a frame. Therefore, the joints will be separately analyzed herein and the necessary joint reinforcement calculated. The moments of the joints will be calculated using WIN-Statik Frame Analysis software. The moments obtained will then be used to calculate the necessary non-prestressed reinforcement at the joints, also considering crack widths.

11.2 Frame analysis

11.2.1 Lateral loads

The lateral loads caused by the earth pressure H_g , hydraulic pressure H_w , and live load H_q are calculated in Appendix E, using Mathcad software. The lateral loads are shown in Figure 44.

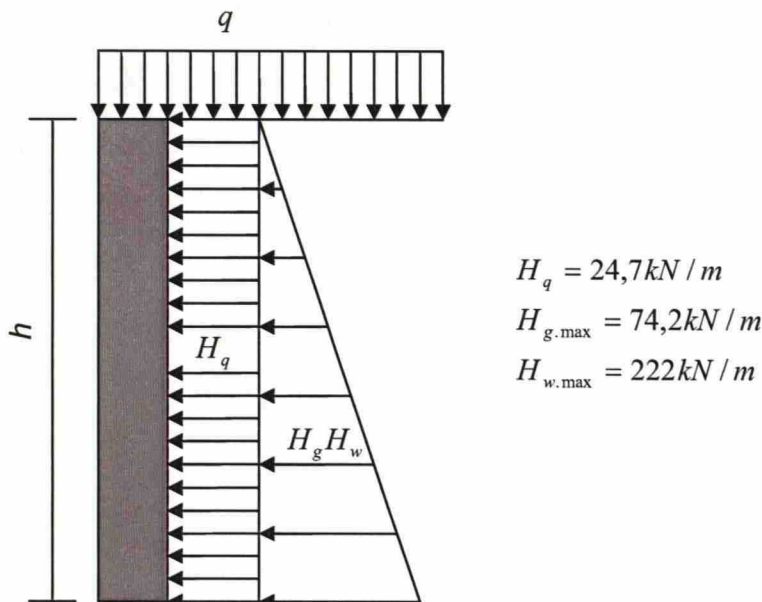


Figure 44. The lateral loads.

11.2.2 Frame analysis results

The lateral loads and the loads described in Chapter 6 are entered in the WIN-Statik Frame Analysis software and two separate analyses are done, one excluding the hydraulic pressure and one including it. The geometry of the frame is presented earlier as a section view of the entrance tunnel in Figure 4. The Frame Analysis results excluding the hydraulic pressure are presented in Figure 45 and the results including the hydraulic pressure in Figure 46.

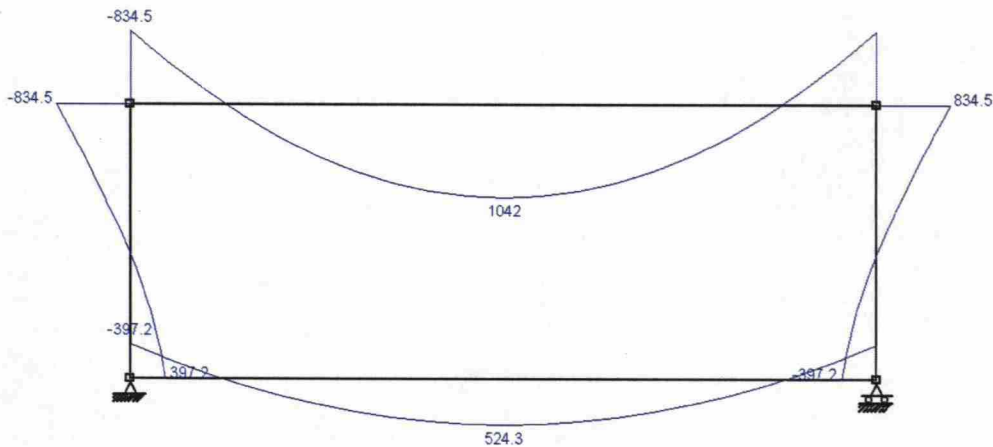


Figure 45. The moments excluding the hydraulic pressure [kNm].

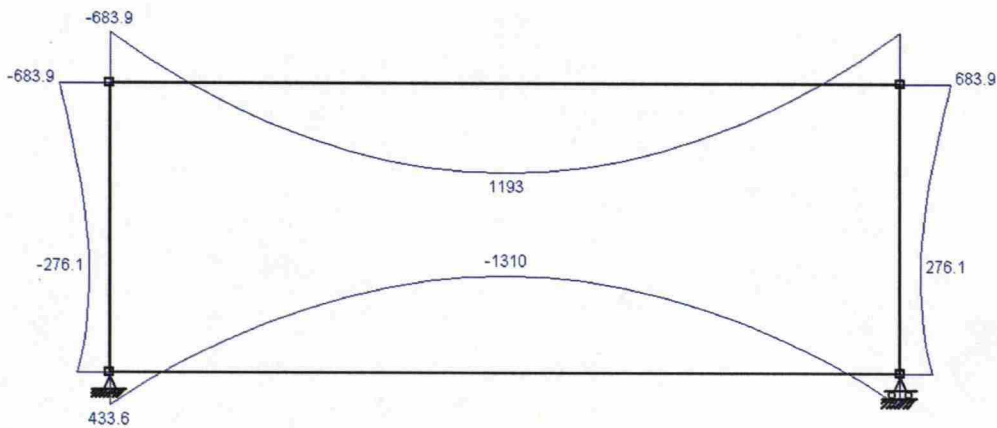


Figure 46. The moments including the hydraulic pressure [kNm].

The lateral loads also cause axial compression in the slabs. Even though this compression causes a minor loss of prestress in the bottom slab, it mitigates cracking at the same time. It is therefore not an aggravating action and will not be further analyzed in this study.

11.3 Reinforcement calculations

The reinforcement calculations are done for a one meter wide section using the largest joint moment 433,6 kNm and the thickness of the wall 300 mm, as this is the most severe combination. The calculations are presented in Appendix E.

Four reinforcement bars per meter, at the top and bottom, with a diameter of 16 mm is enough according to the strength analysis of the joints. However, the crack width limit is 0,178 mm. The optimal amount of reinforcement bars, keeping the crack widths below the limitation value, is seven reinforcement bars per meter, at the top and bottom.

The Frame Analysis results also confirm that the decision to use hinged supports in the preliminary calculations was justified, as the maximum span moments of the frame are smaller than the maximum span

moments using the hinged supports. A comparison of the span moments is shown in Table 12.

Table 12. Comparison of maximum span moments.

	Maximum span moment excluding hydraulic pressure	Maximum span moment including hydraulic pressure
	[kNm]	[kNm]
Hinged supports	735	2004
Frame	524,3	1310

12 ANCHORAGE ZONE DESIGN

12.1 General

According to the Eurocodes, the strength of the anchorage zone shall be sufficient for the transfer of the tendon force to the concrete. In addition the formation of cracks shall not impair the function of the anchorage. The anchorage zone is the area where the stresses caused by the prestressing force P spread out from the anchor towards a uniform stress distribution. The stress trajectories in a rectangular beam are shown in Figure 47.

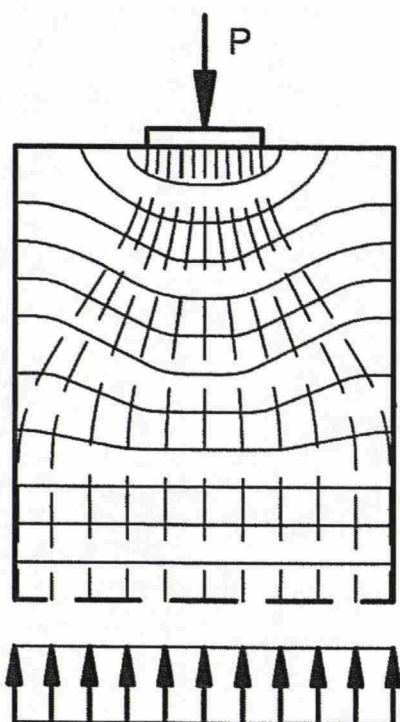


Figure 47. Stress trajectories in the anchorage zone [23].

The dispersion of the compression stresses in the anchorage zone also causes lateral stresses. A lateral compressive stress C develops close to the anchor and a lateral tensile stress T , usually referred to as the bursting force, further off. The lateral stresses of the anchorage zone are shown in Figure 48 and an idealized load path of the resultant forces in Figure 49. In order to resist the stresses in the anchorage zone, additional non-prestressed reinforcement is usually required. [23]

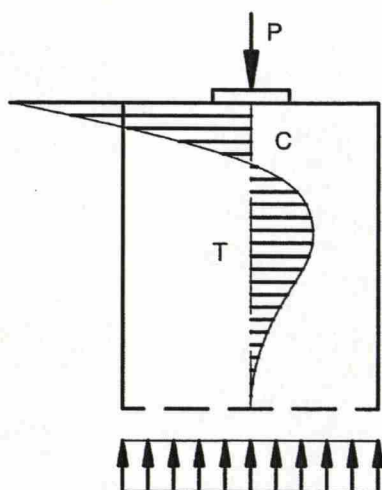


Figure 48. The lateral stresses of the anchorage zone [23].

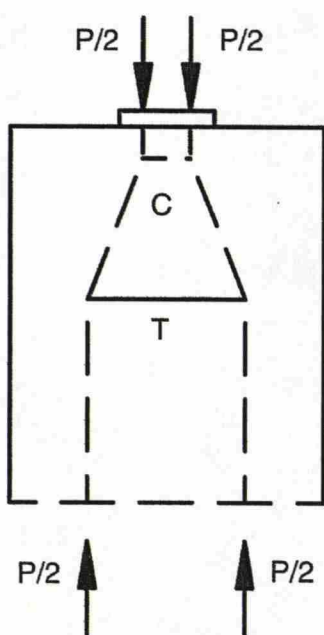


Figure 49. Idealized load path of the resultant forces [23].

Earlier, the tendon type St 1570/1770 was chosen for the calculations of this study. At this point, at the latest, it is necessary to choose a post-tensioning system in order to design the anchorage zone. In Finland the post-tensioning system must be approved by the Ministry of the Environment or have a CE marking. DYWIDAG-unbonded tendons post-tensioning system is approved by the Ministry of the Environment and has been creditable on previous post-tensioning designs by Aaro Kohonen Oy. This post-tensioning system was therefore chosen for this project. The DYWIDAG post-tensioning system manual [24] provides the engineer with the information necessary to design the anchorage zone, such as anchor dimensions, minimum anchor spaces, and necessary anchorage zone reinforcement. The DYWIDAG anchor dimensions and anchorage zone reinforcement are presented in Figure 50. The stresses

in the anchorage zone are resisted by adding a stirrup with a diameter of 8 mm around each anchor and two additional mild steel bars, also with a diameter of 8 mm, going through all the anchors.

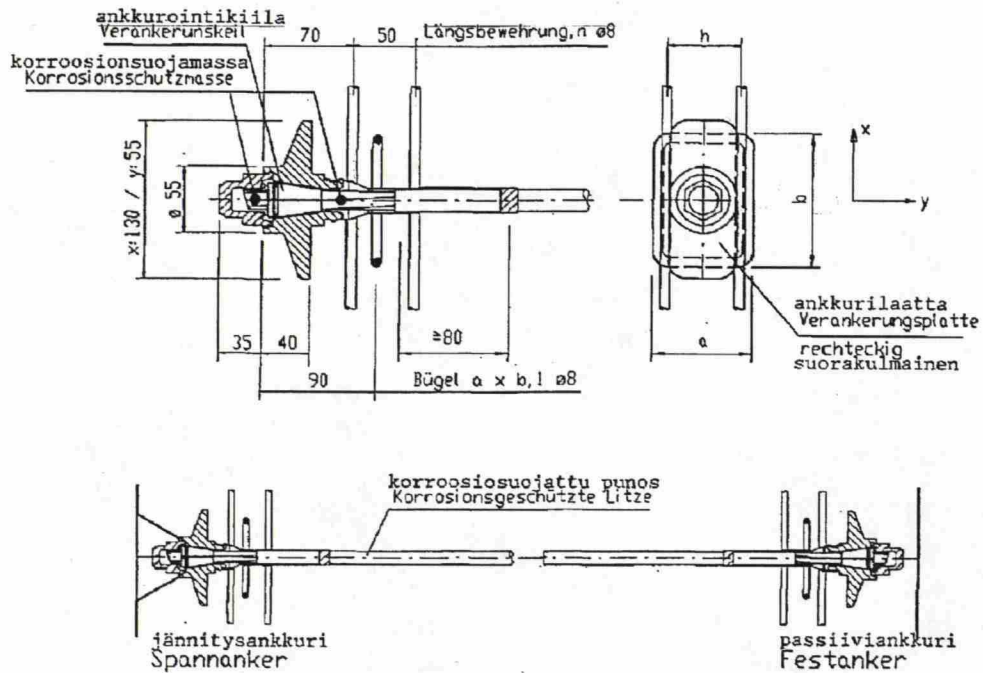


Figure 50. The anchor dimensions and anchorage zone reinforcement [24].

13 FINITE ELEMENT ANALYSIS

13.1 General

After determining the required post-tensioning, the general design process would continue in ADAPT-Floor Pro towards the final fabrication drawings. As mentioned earlier, the design process in this study differs from the general design process using ADAPT software, due the complexity of the slab and loading. In this study, the necessary non-prestressed reinforcement has already been determined using ADAPT-PT, so it is not necessary to design the slab again with ADAPT-Floor Pro. However, a finite element analysis of the whole slab will be done in order to understand how the whole slab behaves and to check that no critical section has eluded observation. This will be done by examining the deflections and the moments of the whole slab, obtained through the Finite Element analysis.

First a three-dimensional model of the slab is created by importing the AutoCAD-drawing (Appendix F) into ADAPT-Floor Pro and transforming the entities into the slab and beams. The walls, with a thickness of 300 mm, are also added. However, the upper slab can not be added in ADAPT-Floor Pro, so it is excluded from the FEM-analysis. But this will not considerably affect the behavior of the bottom slab, which is the focus for the FEM-analysis. Next, the material properties and load cases used in ADAPT-PT are entered in ADAPT-Floor Pro. Then, the tendons are added manually according to the design obtained with ADAPT-PT. The distributed tendons of the slab are all entered individually, but the banded tendons of the beams are modeled as a single tendon in the top and bottom of each beam. The single tendon at the top includes all twelve top tendons and the tendon at the bottom includes all eight bottom tendons. The results will be the same, this is only a simplification used in modeling. No non-prestressed reinforcement is added as the aim here is to see the behavior of the structure exposed to the external loading and the prestressing force. The three-dimensional model of the slab and the manually added tendons are shown in Figure 51.



Figure 51. Three-dimensional model of the slab including walls and tendons.

13.2 The analysis and results

A Finite Element mesh, shown in Figure 52, is created automatically and then the slab is analyzed using the previously entered load combinations. The slab is supported on steel piles, added as hinged point supports, shown in Figure 52. Figure 52 also shows the system of coordinates.

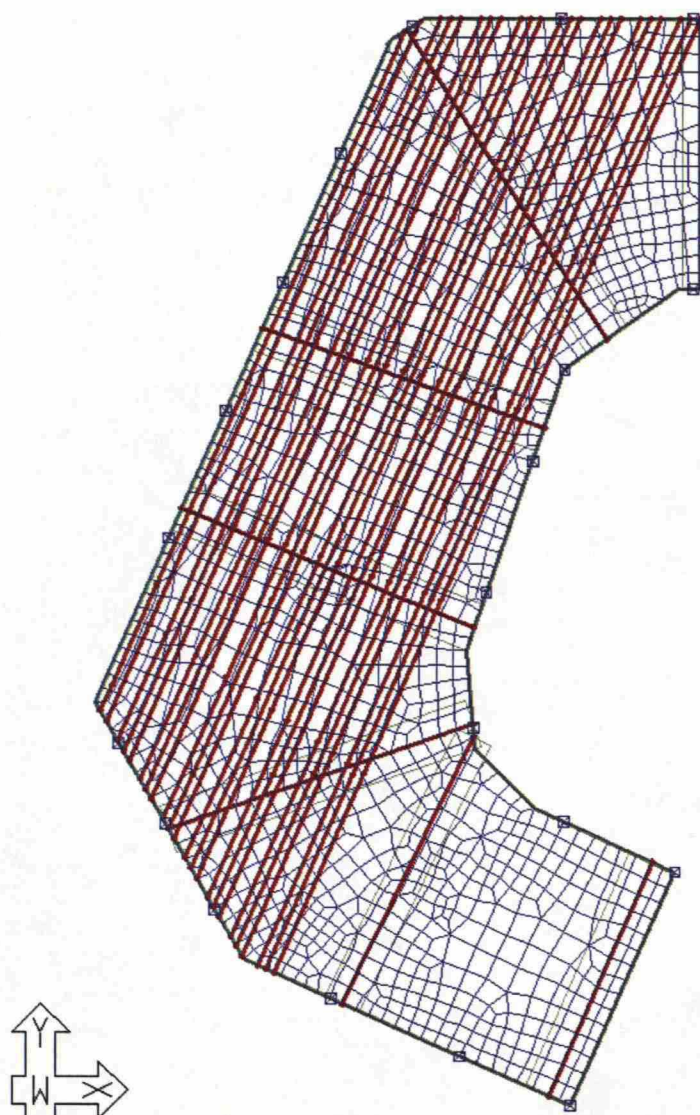


Figure 52. The automatically created Finite Element mesh.

13.2.1 Slab deflection

The deflections of the slab for the quasi-permanent loads, including and excluding the hydraulic pressure, are shown in Figure 53 and Figure 54. The behavior of the slab is as expected, with the largest deflections at the longest spans. The largest deflection is 1,94 mm for the quasi-permanent loads excluding the hydraulic pressure and -2,41 mm for the quasi-permanent loads including the hydraulic pressure. According to the Eurocodes the deflection shall be limited to span/500 for quasi-permanent loads. The span lengths at the largest deflections are approximately 8,5 meters resulting in the deflection limit:

$$\frac{8500mm}{500} = 17mm$$

(26)

Service[quasi-permanent] 1: Z-Translation: [1 Contour = 0.133 mm];
Maximum Value = 1.937e+000 (mm) @ (15.448 11.089 2.800)m;
Minimum Value = -5.439e-002 (mm) @ (26.595 23.001 2.800)m;

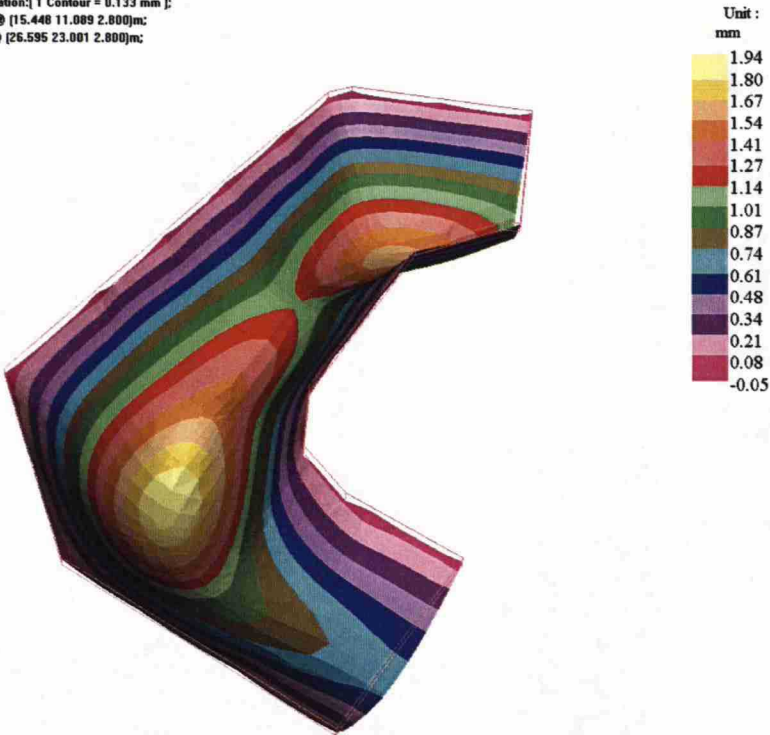


Figure 53. The deflection of the slab excluding the hydraulic pressure.

Service[quasi-permanent] 2: Z-Translation: [1 Contour = 0.166 mm];
Maximum Value = 7.405e-002 (mm) @ (15.448 11.089 2.800)m;
Minimum Value = -2.415e+000 (mm) @ (26.595 23.001 2.800)m;

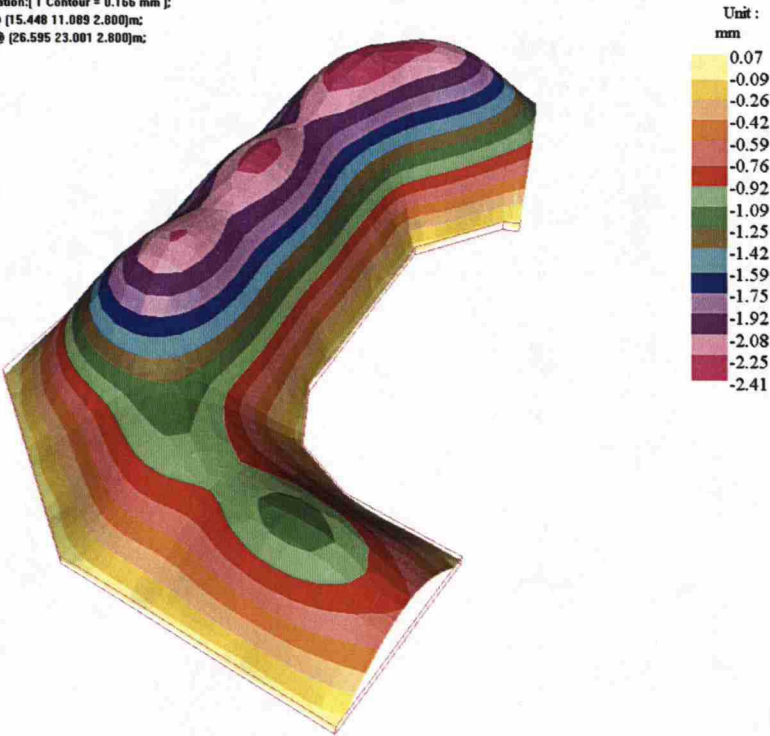


Figure 54. The deflection of the slab including the hydraulic pressure.

13.2.2 Slab moments

The largest slab moments excluding the hydraulic pressure are for load combination Strength 1, and the largest slab moments including the hydraulic pressure are for load combination Strength 3. These load combinations are presented in Chapter 6.2. The slab moments around the X- and Y-axis for load combination Strength 1 are shown in Figure 55 and Figure 56, and the slab moments for load combination Strength 3 are shown in Figure 57 and Figure 58.



Figure 55. The slab moments around the X-axis for load combination Strength 1.

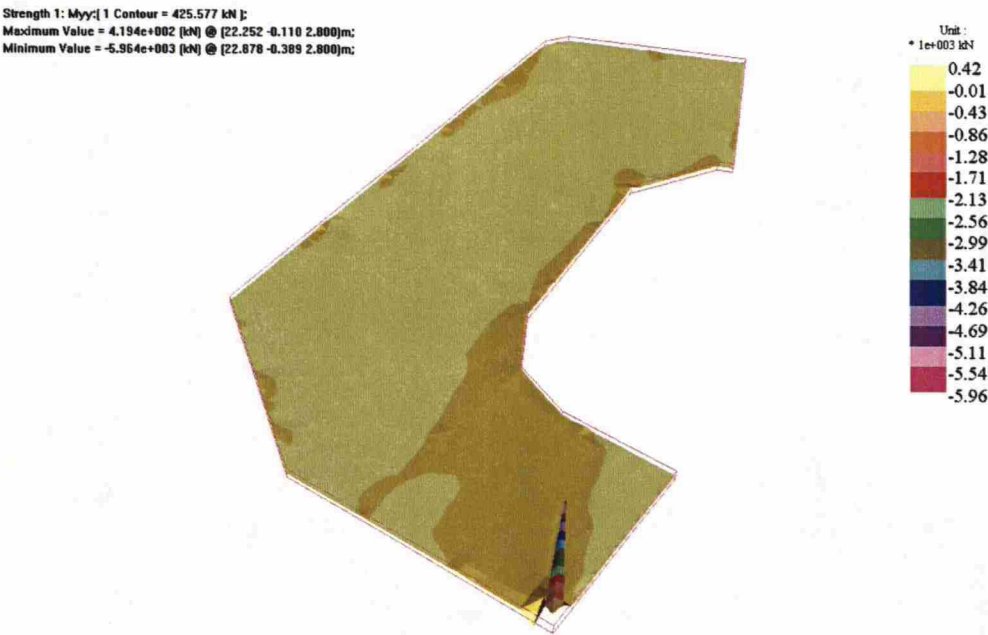


Figure 56. The slab moments around the Y-axis for load combination Strength 1.



Figure 57. The slab moments around the X-axis for load combination Strength 3.

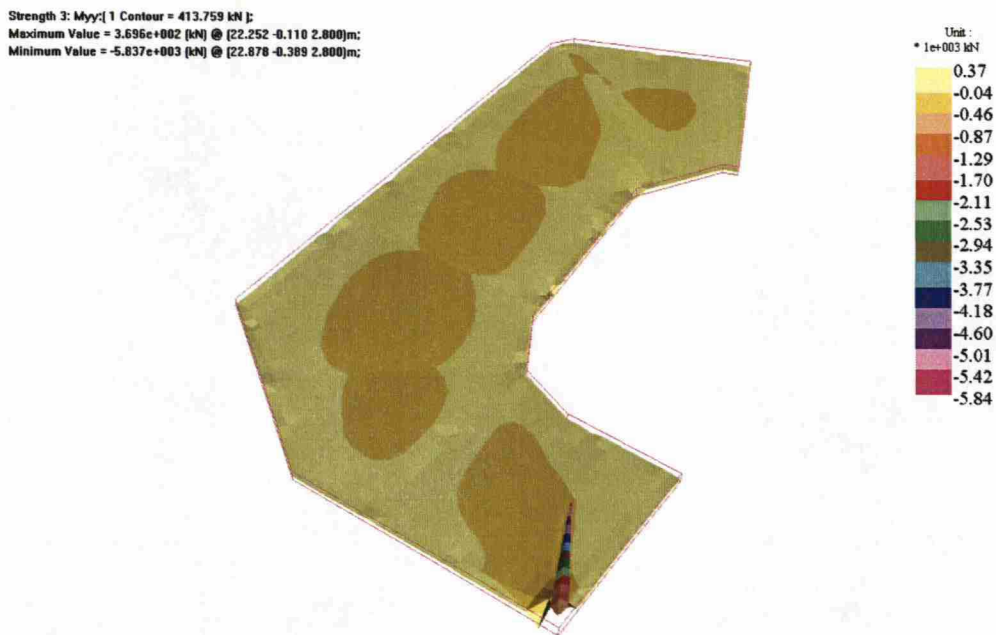


Figure 58. The slab moments around the Y-axis for load combination Strength 3.

The slab moments show a large moment peak in the bottom right corner of the slab. A moment peak of this size should not occur, so the reason for this moment peak needs to be examined. The strength load combinations consist of the self weight, dead load, live load and hyperstatic actions. By creating load combinations including only one of these loads at a time, the one causing the moment peak can be found.

The investigation reveals that the moment peak is caused by the hyperstatic actions. This can be seen in Figure 59 and Figure 60, showing the slab moment, caused only by the hyperstatic actions, around the X- and Y-axis. However, there is no reasonable explanation why a moment peak this size would occur due to hyperstatic actions. This indicates that there might be some kind of calculation problem or bug in the FEM-analysis. The model was sent to the ADAPT support team for further investigation and a bug associated with the hyperstatic moment was found. The bug is present when a tendon end and a point support share the same Finite Element cell. The bug was reported to the ADAPT development team.



Figure 59. The slab moments around the X-axis due to only hyperstatic actions.

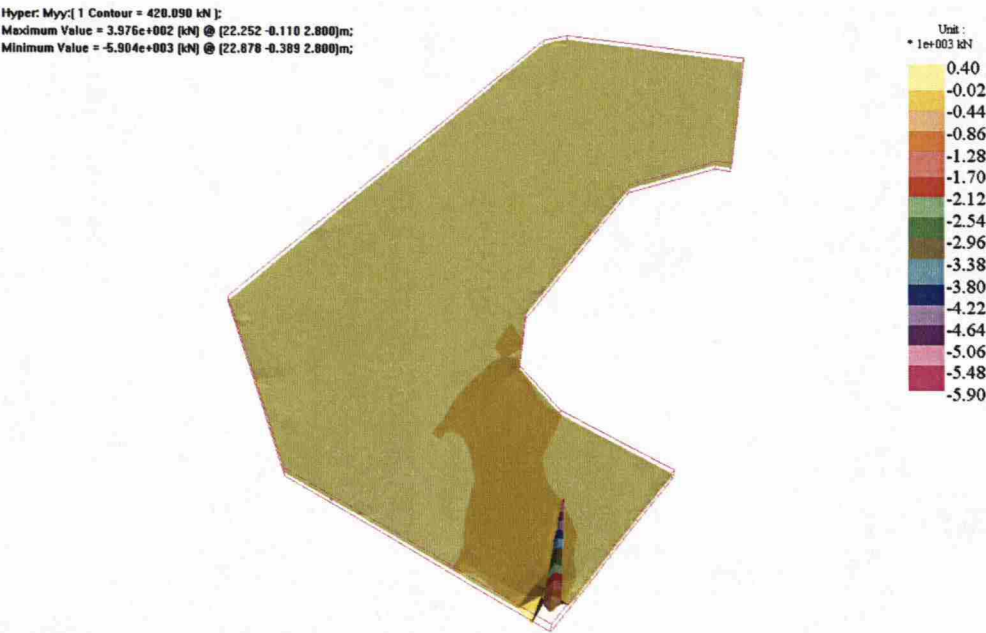


Figure 60. The slab moments around the Y-axis due to only hyperstatic actions.

As the slab moment color contours are scaled according to the moment peak, it is difficult to get a good view of the actual slab moments. The bug might also affect the slab moments and falsify the results. In order to

bypass this problem, the point supports were substituted by column supports, as the bug is present when a tendon end and a point support share the same Finite Element cell. This substitution was suggested by the ADAPT support team. Rectangular 250x250 mm concrete columns were added as hinged supports to simulate steel piles with a 250x250 mm steel plate at the top, and the structure reanalyzed. The slab moments, using column supports, for load combination Strength 1 are shown in Figure 61 and Figure 62 and for load combination Strength 3 in Figure 63 and Figure 64.

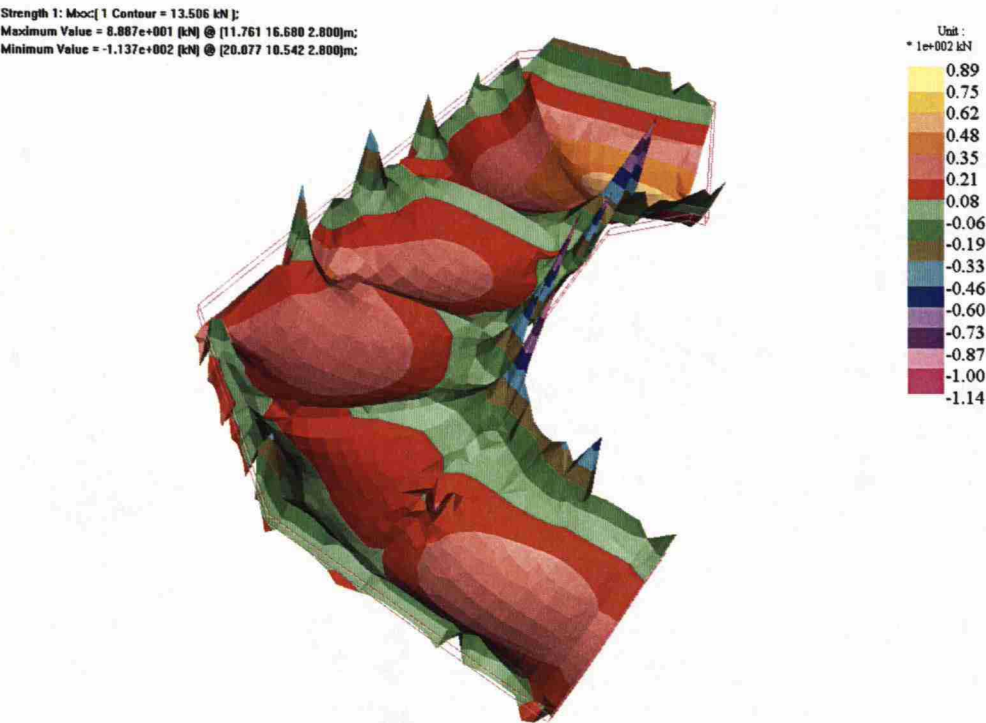


Figure 61. The recalculated slab moments around the X-axis for load combination Strength 1.

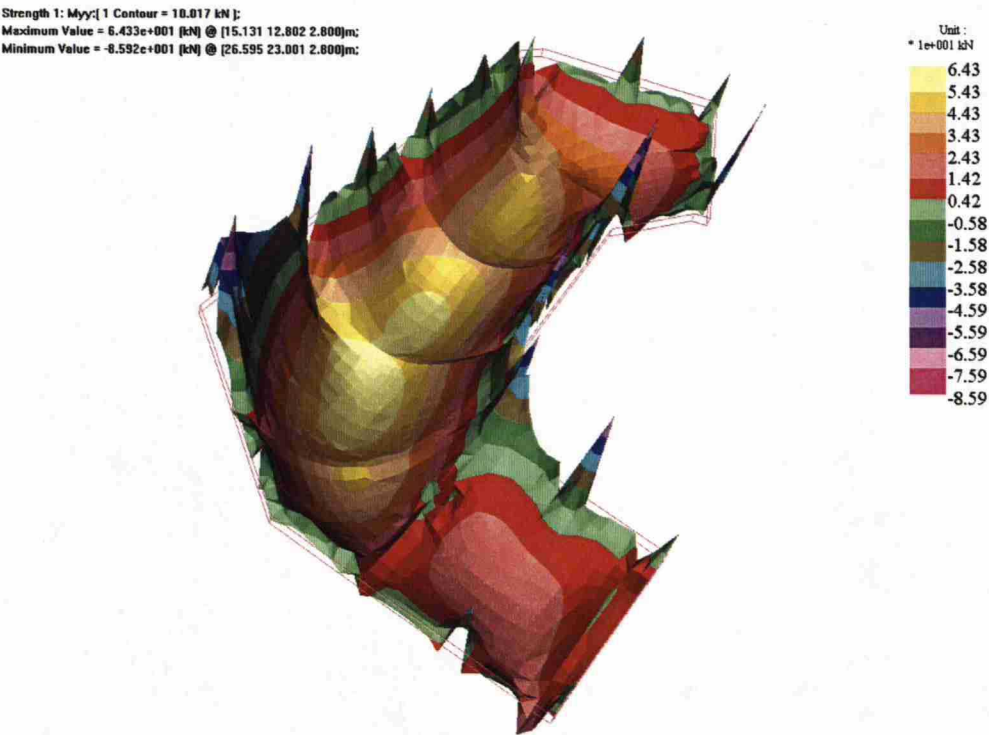


Figure 62. The recalculated slab moments around the Y-axis for load combination Strength 1.

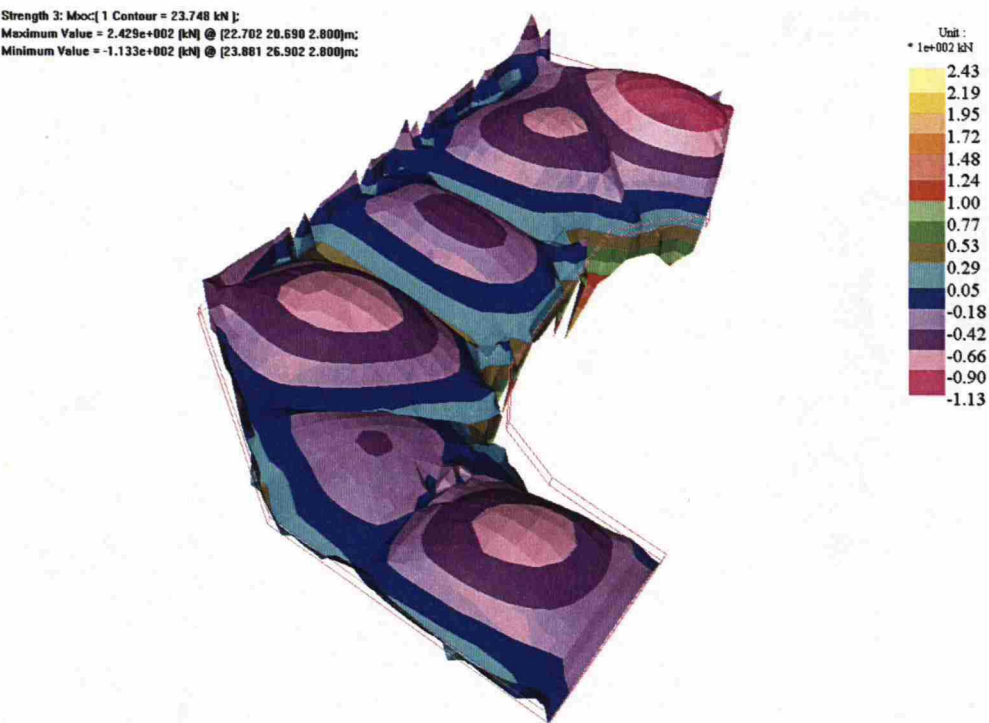


Figure 63. The recalculated slab moments around the X-axis for load combination Strength 3.

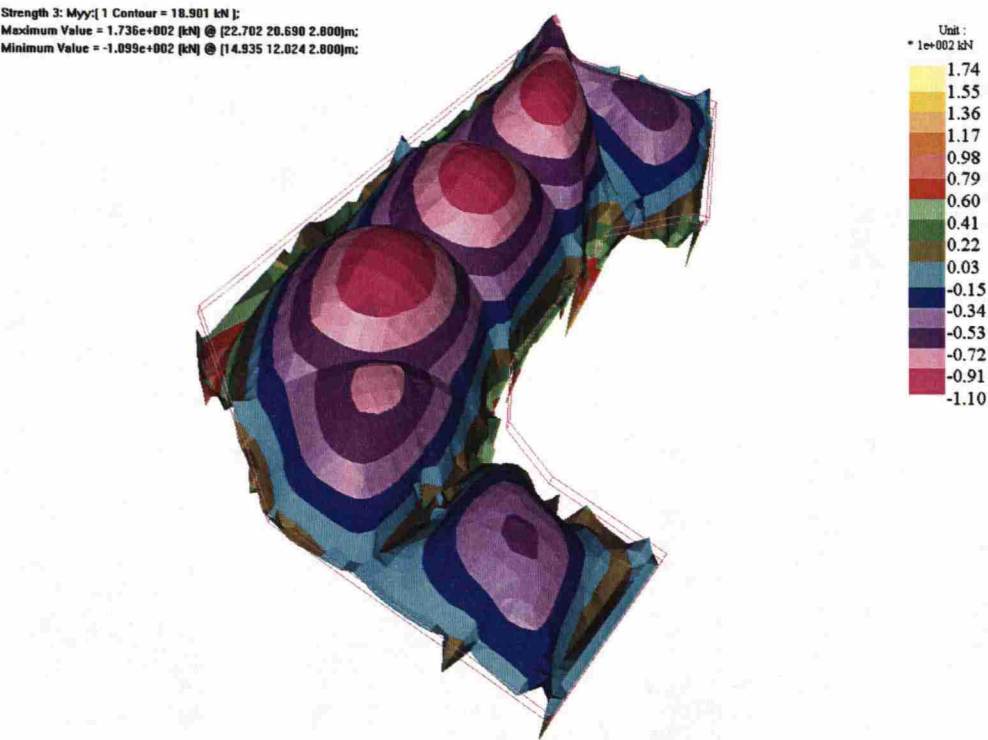


Figure 64. The recalculated slab moments around the Y-axis for load combination Strength 3.

13.3 FEM-analysis conclusions

The slab deflections and recalculated moments show that the behavior of the whole slab, post-tensioned according to the results obtained with ADAPT-PT, is as expected. This confirms that the design solution is adequate. The FEM-analysis results also confirm that the decision not to prestress the slab area in the bottom right corner was appropriate.

14 SUMMARY AND CONCLUSIONS

The aim of this Master's thesis was to seek a solution to the unusual engineering problem of how to design a post-tensioned concrete slab exposed to variable hydraulic pressure and ensure the watertightness of the slab. This engineering problem occurred when parking structures were planned to be situated partly under the groundwater level in the new city centre of Kauniainen, Finland. A suitable design solution for a bottom slab of a parking structure entrance tunnel, exposed to bidirectional two-phased loading, was sought. An additional challenge was that the recently implemented Eurocodes, along with the Finnish National annex, were used in this study.

Initially, the general design process with ADAPT-software, described in Chapter 3.4, was intended to be used in this study. However, due to the complexity of the slab and the unusual loading, it turned out to be more suitable to examine the effect of variable hydraulic pressure, and search for a design solution, first on a smaller part of the slab, using only ADAPT-PT. ADAPT-Floor Pro was then used only to verify the design obtained with ADAPT-PT.

Traditionally, post-tensioning designs involve a reversed parabola tendon profile, but due to the variable hydraulic pressure, this design was not suitable. The reversed parabola tendon profile is only suitable for post-tension slabs where the vertical loads act in only one direction. Therefore, the different design solutions examined involved either straight tendons in the middle, or at the top and bottom of the slab, or reversed and normal parabola tendon profiles used simultaneously. Four applicable solutions were presented and compared. Finally, design solution 2, involving straight tendons at the top and bottom of the slab, was chosen as the most appropriate design solution. This design solution was then applied on the whole slab.

The results obtained with ADAPT-PT, based on the Eurocodes, were manually verified using the National Building Code of Finland. The manual verification revealed that the safety factors of the Eurocodes, when no live load is present, result in a larger amount of non-prestressed reinforcement, than the safety factors of the National Building Code of Finland. However, different building codes can never be used simultaneously, and as the Eurocodes were chosen for this study, the amount of non-prestressed reinforcement demanded by the Eurocodes will be used for the fabrication drawings of the parking structure project. The losses of prestress calculated by ADAPT-PT were also manually verified using the National Building Code of Finland. The manual verifications confirmed that the results obtained with ADAPT-PT were accurate.

Ensuring the watertightness of the slab was one of the main objectives of this study. The watertightness was ensured by crack control in the

serviceability check of ADAPT-PT. However, ADAPT-PT does not present the crack widths, so the cracking was double-checked by manually calculating the crack widths. In Finland, crack control by direct calculation of crack widths is always recommended. The Finnish National annex of Eurocode 2 Part 1-1 refers to Eurocode 2 Part 3: Liquid retaining and containment structures, when determining the limiting crack widths for structures where watertightness is a concern. The limiting crack width, obtained from Eurocode 2 Part 3, was 0,178 mm. All calculated crack widths in this study were below this limitation value. In addition, the joints were separately analyzed, and their necessary non-prestressed reinforcement manually calculated.

Finally, the whole slab, including the post-tensioning tendons, was modeled in ADAPT-Floor Pro, and a Finite Element analysis conducted. No further design was done with ADAPT-Floor Pro, but the behavior of the whole slab was examined by analyzing the deflections and the slab moments obtained through the Finite Element analysis. The Finite Element analysis justified the design done with ADAPT-PT.

A very important outcome of this study is that the exceptional design solution revealed three bugs in ADAPT-software. These bugs would perhaps never have been detected when doing more traditional post-tensioning design, but the variable hydraulic pressure and the complexity of the slab brought them forward. The bugs were all reported to the ADAPT development team, and will be corrected in a future maintenance release.

The results of this study show that variable hydraulic pressure affects the post-tensioning design quite notably. The traditional design, involving the reversed parabola tendon profile, is not suitable for post-tensioned slabs exposed to variable hydraulic pressure. Instead, straight tendons should be used, preferably at both the top and bottom of the slab. The hydraulic pressure also brings forth the importance of crack mitigation, as watertightness usually is a concern for slabs exposed to hydraulic pressure. The precompression obtained through prestressing is beneficial for crack mitigation, but a separate crack analysis is still recommended.

The solution found for the slab analyzed in this study can be viewed as a general solution for any post-tensioned slab exposed to variable bidirectional vertical loading. The use of straight tendons at the top and bottom, instead of reversed parabola tendon profiles, proved efficient and appropriate, and also advantageous in the mitigation of cracks.

In general, the structural engineering objectives of this study were well fulfilled. ADAPT proved to be a very suitable software for post-tensioning design, even for more challenging design problems, and the customer support provided by ADAPT was efficient and useful. The manual crack control based on the Eurocodes gave a clear view of how cracking is calculated with the Eurocodes, and showed how the crack control of the Eurocodes differs from the traditional crack control with the National

Building Code of Finland. All the manual calculations gave a very good understanding of the problems in general, and validated the results obtained with ADAPT-software. Many of the manual calculations done in this study can be used as examples for future calculations.

LIST OF REFERENCES

1. Arkkitehtuuritoimisto B & M Oy, Kauniaisten Keskustan Rakentamistapaohje, 2006.
2. Post-tensioning Manual, Sixth Edition. Post-Tensioning Institute, Phoenix, Arizona, USA.
3. Aalami, B. O. Unbonded and bonded post-tensioning systems in building construction. A design and performance review. PTI Technical Notes, Issue 5, September 1994, Post-Tensioning Institute, Phoenix, Arizona, USA.
4. SFS-EN 1992-1-1. Eurocode 2: Design of concrete structures. Part 1-1: General rules and rules for buildings. Applied with the Finnish National annex.
5. Aalami, B. O. & Jurgens, J. D. Guidelines for the design of post-tensioned floors. Concrete International, March 2003. American Concrete Institute.
6. Aalami, B. O. Load balancing: a comprehensive solution to post-tensioning. ACI Structural Journal, V 87, No 6, November-December 1990. American Concrete Institute.
7. Aalami, B. O. Hyperstatic (secondary) actions in prestressing and their computation. PTI Technical Notes, December 1998, Post-Tensioning Institute, Phoenix, Arizona, USA.
8. Aalami, B. O. & Bommer, A. Design fundamentals of post-tensioned concrete floors. Post-Tensioning Institute, 1999, Phoenix, Arizona, USA.
9. Aalami, B. O. & Kelley, G. S. Design of concrete floors, with particular reference to post-tensioning. PTI Technical Notes, Issue 11, January 2001, Post-Tensioning Institute, Phoenix, Arizona, USA.
10. Jansson, N. P. Analysis of a post-tensioned concrete slab with insufficient concrete strength for stressing. Helsinki University of Technology, Espoo, Finland, 2007.
11. Zienkiewicz, O.C. The Finite Element Method, Third Edition. Berkshire, United Kingdom, 1977.
12. ADAPT. A brief product description. 2002, ADAPT Corporation, Redwood City, California. Available: <http://www.adaptsoft.com>.
13. Design process using ADAPT-Builder platform. Technical Note 182, November 2004, ADAPT Corporation, Redwood City, California.

14. Design steps using ADAPT-Floor Pro. Technical Note 230, May 2007, ADAPT Corporation, Redwood City, California.
15. Aalami, B. O. Layout of post-tensioning and passive reinforcement in floor slabs. PTI Technical Notes, Issue 8, April 2000, Post-Tensioning Institute, Phoenix, Arizona, USA.
16. SFS-EN 1991-1-1. Eurocode 1: Actions on structures. Part 1-1: General actions. Densities, self-weight, imposed loads for buildings. Applied with the Finnish National annex.
17. SFS-EN 1990. Eurocode: Basis of structural design. Applied with the Finnish National annex.
18. National Building Code of Finland. Available: <http://www.ymparisto.fi>.
19. BY27. Tarunnattomat jänteet betonirakenteissa. Suunnittelu ja rakentamishjeet sekä pilarilaataston mitoitusmerkki. Concrete Association of Finland, 1988.
20. Siniluoto, S. Betonirakenteiden käyttörajatilatarkasteluiden vertailua eurokoodien käyttöönottoa valmisteltaessa.. Diplomityö. TKK Helsinki University of Technology, Department of Civil and Environmental Engineering. Espoo, Finland, 2007.
21. SFS-EN 1992-3. Eurocode 2: Design of concrete structures. Part 3: Liquid retaining and containment structures. Applied with the Finnish National annex.
22. BY16. Suunnittelun sovellusohjeet ja Betoninormien RakMK B4 suunnitteluosa, RakMK B1 ja B2. Concrete Association of Finland, 1984.
23. Wollman, P. G. & Roberts-Wollman, C. L. Anchorage zone design. Post-Tensioning Institute, Phoenix, Arizona, USA, 2000.
24. BY 3 B Käyttöseloste n:o 86. DYWIDAG-tarunnattomat jänteet. Concrete Association of Finland, 2006.

Additional references

- Bergmeister, K. & Wörner, J. D. BetonKalender 2005. Fertigteile, Tunnelbauwerke. Ernst & Sohn, 2005.
- Hemiö, T. Paikallavaletun tartunnattomin punoksin jännitetyn pilarilaattarakenteen mitoitus. Diplomityö. TKK Helsinki University of Technology, Department of Civil and Environmental Engineering. Espoo, Finland. 1994.

BY210. Betonirakenteiden suunnittelu ja mitoitus. Concrete Association of Finland, 2005.

Aalami, B. O. & Kelley, G. S. Structural design of post-tensioned floors. Concrete International, January 2001. American Concrete Institute.

Aalami, B.O. Design of post-tensioned floor slabs. Concrete International, June 1989. American Concrete Institute.

Aalami, B.O. Structural modeling of post-tensioned members. Journal of Structural Engineering, February 2000.

Aalami, B. O. Prestressing losses and elongation calculations. Technical Note 9, September 2004, ADAPT Corporation, Redwood City, California.

Aalami, B. O. Software for the design of concrete buildings. Concrete International, December 2001. American Concrete Institute.

Aalami, B. O. & Barth, F. G. Restraint cracks and their mitigation in unbonded post-tensioned building structures. Post-Tensioning Institute, Phoenix, Arizona, USA, 1989.

Aalami, B. O. Nonprestressed bonded reinforcement in post-tensioned building design. Technical Publication 2, February 2001, ADAPT Corporation, Redwood City, California.

Aalami, B. O. One-way and two-way post-tensioned floor systems. PTI Technical Notes, Issue 3, October 1993, Post-Tensioning Institute, Phoenix, Arizona, USA.

Tsang, N. EC2 code provisions on time dependent behaviour. Department of Civil and Environmental Engineering, Imperial College London, 2004.

Tsang, N. Time dependent behaviour and creep analysis for prestressed concrete beam/slab. Department of Civil and Environmental Engineering, Imperial College London, 2004.

ADAPT-PT, version 8, user manual. ADAPT Corporation, Redwood City, California, 2007.

ADAPT-Floor Pro, version EX 3.00, user manual. ADAPT Corporation, Redwood City, California, 2007.

www.adaptsoft.com

www.post-tensioning.org

www.eurocodes.fi

APPENDIX A – THE PRELIMINARY CALCULATIONS

Design solution 1

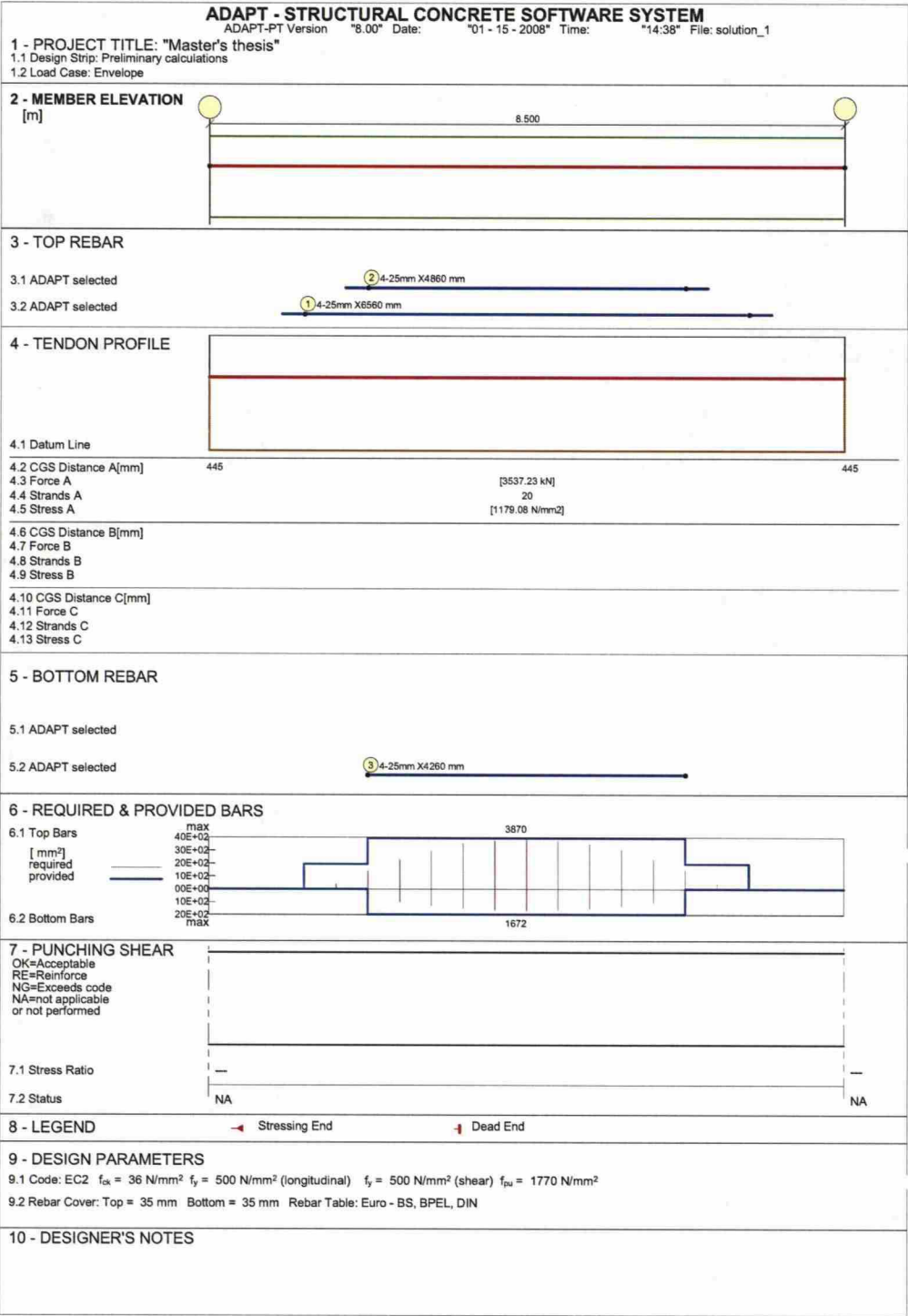


Figure 65. Adapt-PT summary report for design solution 1.

Table 13. Selected post-tensioning forces and tendon drape for design solution 1.

Span	Force	CGS Left	CSG C1	CGS C2	CGS Right	P/A	Wbal	WBal (%DL)
	kN	mm	mm	mm	mm	MPa	kN	
1	3537.228	445.00	---	---	445.00	1.25	0.000	0

Table 14. Number of tendons and stressing conditions for design solution 1.

Type	Num	Force	Right End	Left End	From	To	Extension
A	20	176.85	Dead	Live	1	1	---

Table 15. Required minimum post-tensioning forces for design solution 1.

Based on Stress Conditions				Based on Minimum P/A		
Type	Left	Center	Right	Left	Center	Right
	kN	kN	kN	kN	kN	kN
1	0.00	3526.34	0.00	2820.00	2820.00	2820.00

Table 16. Required rebar for design solution 1.

Span	Location	From	To	As Required	Ultimate	Minimum
		m	m	mm2	mm2	mm2
1	TOP	1.70	6.80	3870.00	3870.00	3216.00
1	BOT	2.55	5.95	1672.00	384.10	1672.00

Table 17. Adapt selected rebar for design solution 1.

Span	ID	Location	From	Quantity	Size	Length	Area
			m			m	mm2
1	1	TOP	0.97	4	25	6.56	1962.52
1	2	TOP	1.83	4	25	4.86	1962.52
1	3	BOT	2.13	4	25	4.26	1962.52

Design solution 2

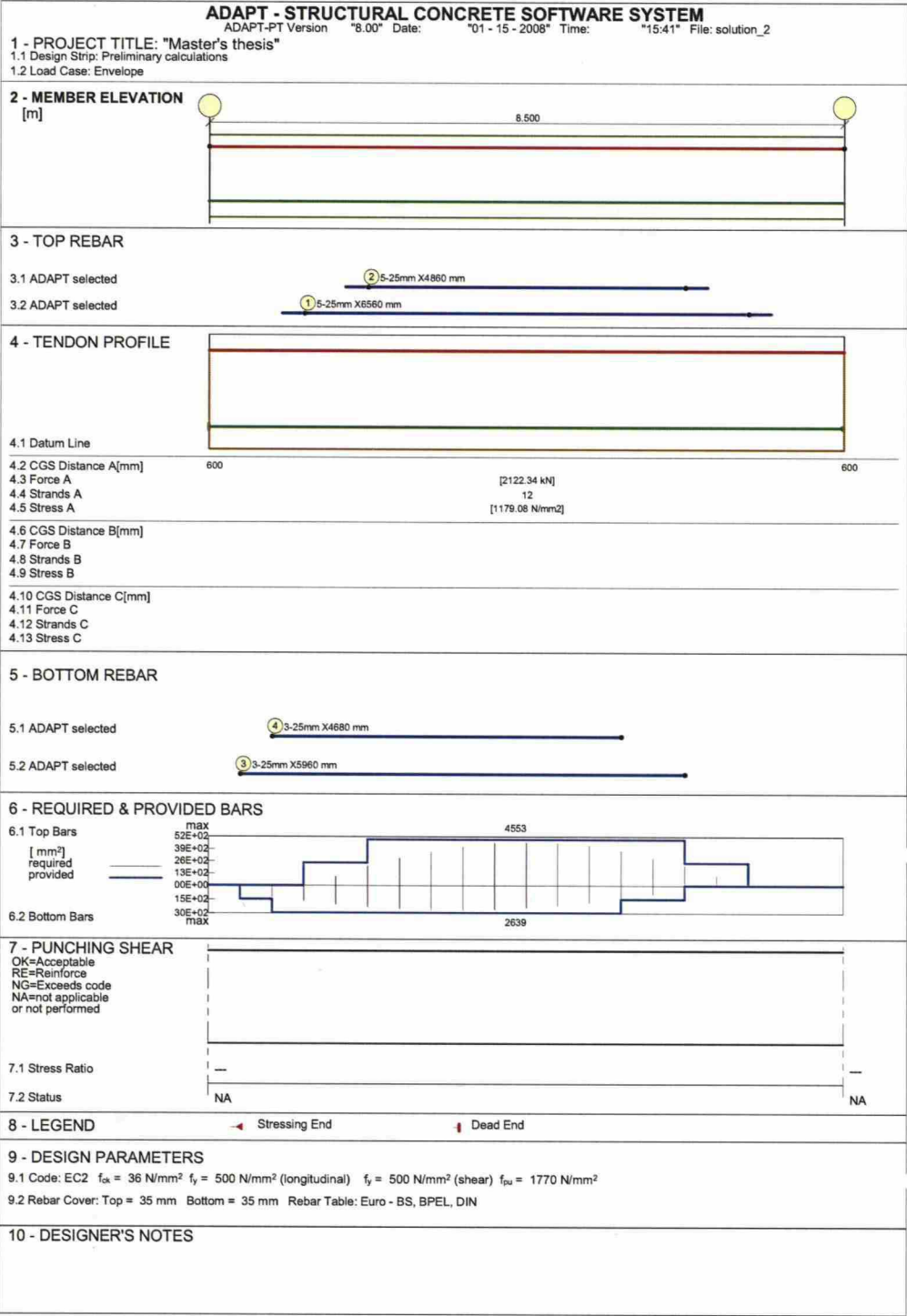


Figure 66. Adapt-PT summary report for design solution 2.

Table 18. Selected post-tensioning forces and tendon drape for design solution 2.
Tendon A

Span	Force	CGS Left	CSG C1	CGS C2	CGS Right	P/A	Wbal	WBal (%DL)
	kN	mm	mm	mm	mm	MPa	kN	
1	2122.337	600.00	---	---	600.00	0.75	0.000	0

Tendon B

Span	Force	CGS Left	CSG C1	CGS C2	CGS Right	P/A	Wbal	WBal (%DL)
	kN	mm	mm	mm	mm	MPa	kN	
1	1414.891	100.00	---	---	100.00	0.50	0.000	0

Table 19. Number of tendons and stressing conditions for design solution 2.

Type	Num	Force	Right End	Left End	From	To	Extension
A	12	176.85	Dead	Live	1	1	---
B	8	176.85	Dead	Live	1	1	0.00

Table 20. Required minimum post-tensioning forces for design solution 2.

Based on Stress Conditions			Based on Minimum P/A			
Type	Left	Center	Right	Left	Center	Right
	kN	kN	kN	kN	kN	kN
1	0.00	2892.02	0.00	2820.00	2820.00	2820.00

Table 21. Required rebar for design solution 2.

Span	Location	From	To	As Required	Ultimate	Minimum
		m	m	mm2	mm2	mm2
1	TOP	1.70	6.80	4553.00	4553.00	0.00
1	BOT	0.85	5.95	2639.00	0.00	2639.00

Table 22. Adapt selected rebar for design solution 2.

Span	ID	Location	From	Quantity	Size	Length	Area
			m			m	mm2
1	1	TOP	0.97	5	25	6.56	2453.15
1	2	TOP	1.83	5	25	4.86	2453.15
1	3	BOT	0.42	3	25	5.96	1471.89
1	4	BOT	0.85	3	25	4.68	1471.89

Design solution 3

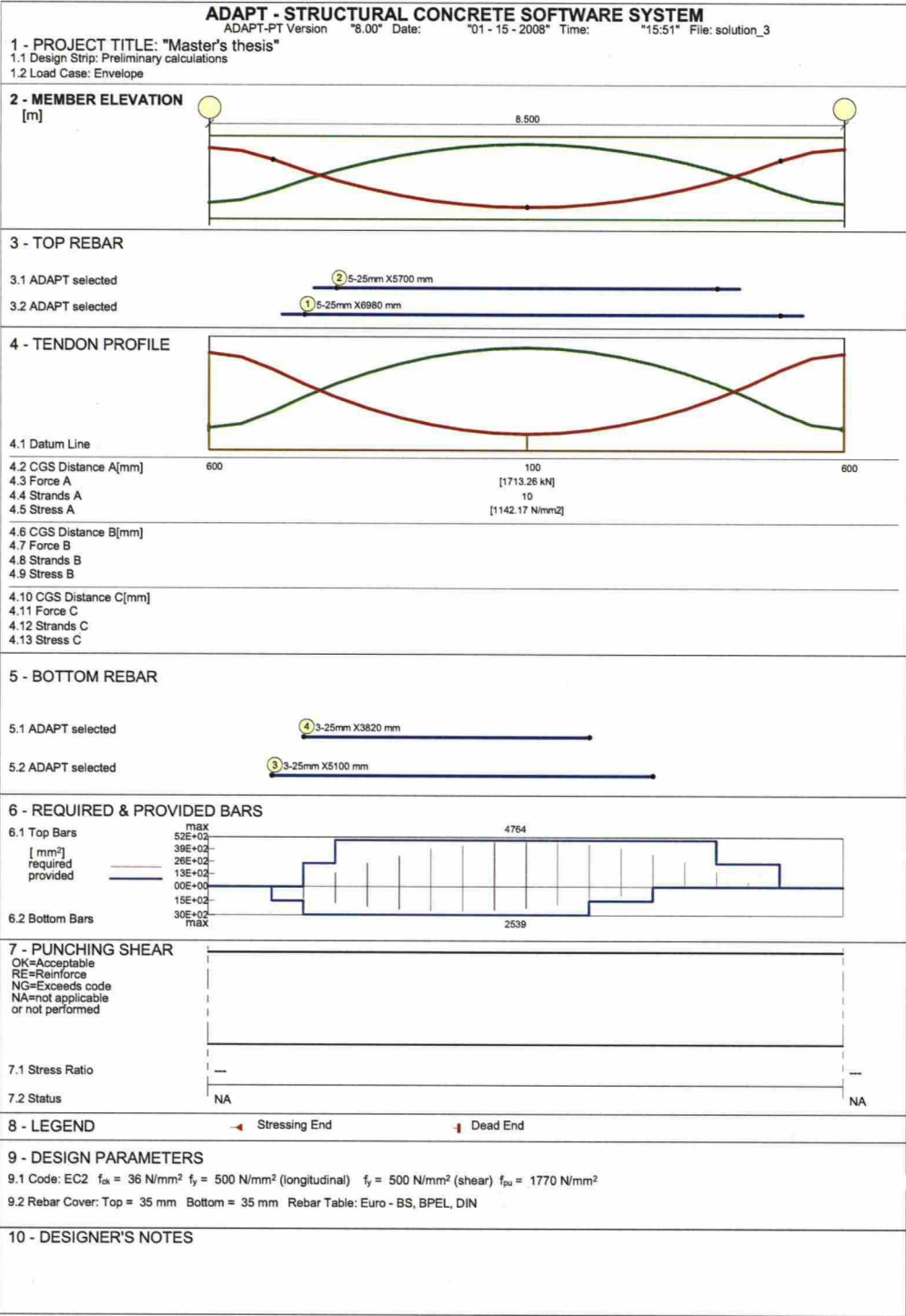


Figure 67. Adapt-PT summary report for design solution 3.

Table 23. Selected post-tensioning forces and tendon drape for design solution 3.
Tendon A

Span	Force	CGS Left	CSG C1	CGS C2	CGS Right	P/A	Wbal	WBal (%DL)
	kN	mm	mm	mm	mm	MPa	kN	
1	1713.259	600.00	---	100.00	600.00	0.61	94.852	-61

Tendon B

Span	Force	CGS Left	CSG C1	CGS C2	CGS Right	P/A	Wbal	WBal (%DL)
	kN	mm	mm	mm	mm	MPa	kN	
1	2055.910	100.00	---	600.00	100.00	0.73	-113.822	73

Table 24. Number of tendons and stressing conditions for design solution 3.

Type	Num	Force	Right End	Left End	From	To	Extension
A	10	171.19	Dead	Live	1	1	---
B	12	171.19	Dead	Live	1	1	0.00

Table 25. Required minimum post-tensioning forces for design solution 3.
Based on Stress Conditions Based on Minimum P/A

Type	Left	Center	Right	Left	Center	Right
	kN	kN	kN	kN	kN	kN
1	0.00	2916.80	0.00	2820.00	2820.00	2820.00

Table 26. Required rebar for design solution 3.

Span	Location	From	To	As Required	Ultimate	Minimum
		m	m	mm2	mm2	mm2
1	TOP	1.70	7.22	4764.00	4764.00	0.00
1	BOT	1.27	5.53	2539.00	0.00	2539.00

Table 27. Adapt selected rebar for design solution 3.

Span	ID	Location	From	Quantity	Size	Length	Area
			m			m	mm2
1	1	TOP	0.97	5	25	6.98	2453.15
1	2	TOP	1.40	5	25	5.70	2453.15
1	3	BOT	0.85	3	25	5.10	1471.89
1	4	BOT	1.27	3	25	3.82	1471.89

Design solution 4

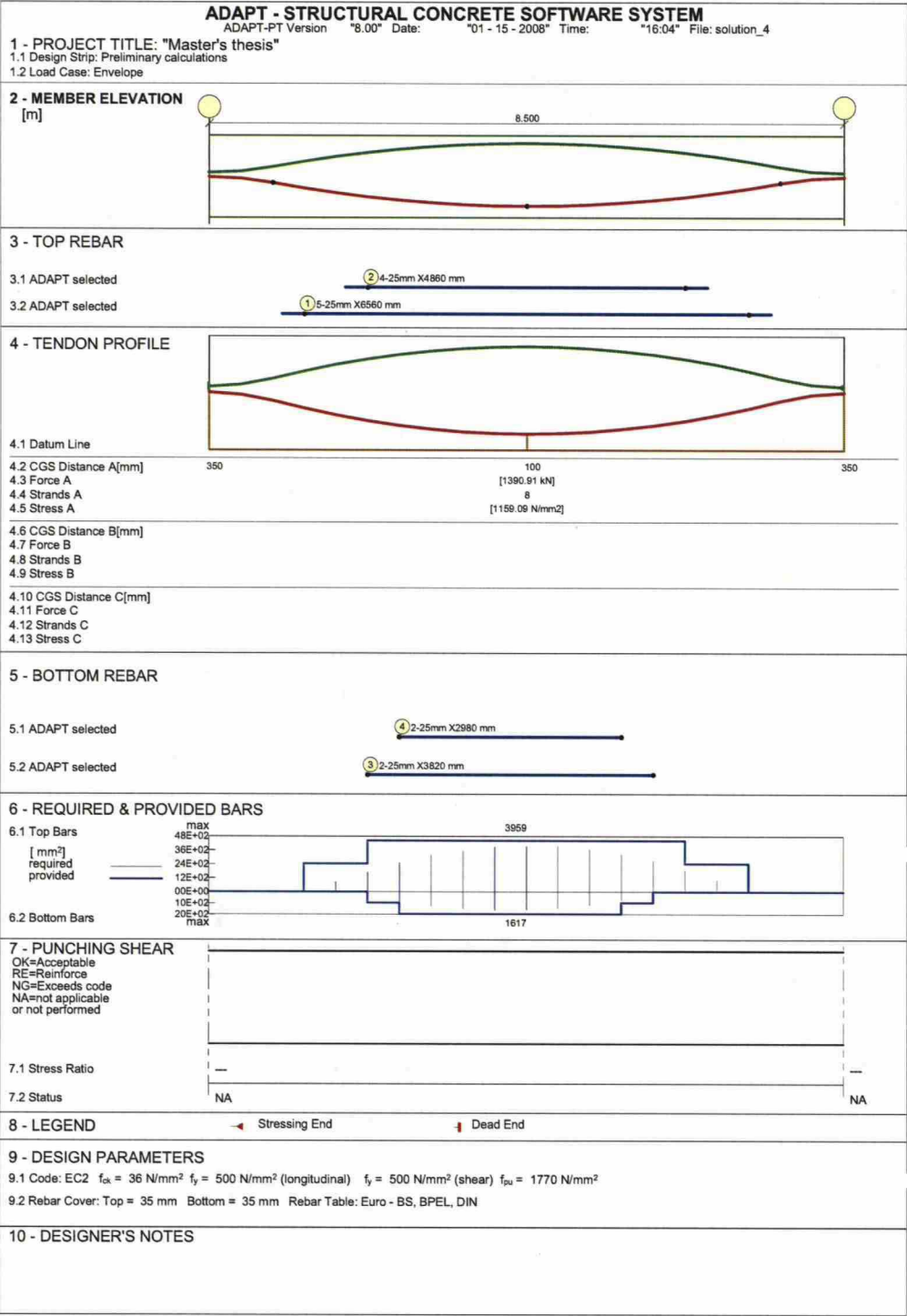


Figure 68. Adapt-PT summary report for design solution 4.

Table 28. Selected post-tensioning forces and tendon drape for design solution 4.
Tendon A

Span	Force	CGS Left	CSG C1	CGS C2	CGS Right	P/A	Wbal	WBal (%DL)
	kN	mm	mm	mm	mm	MPa	kN	
1	1390.914	350.00	---	100.00	350.00	0.49	38.503	-25

Tendon B

Span	Force	CGS Left	CSG C1	CGS C2	CGS Right	P/A	Wbal	WBal (%DL)
	kN	mm	mm	mm	mm	MPa	kN	
1	2434.099	350.00	---	600.00	350.00	0.86	-67.380	43

Table 29. Number of tendons and stressing conditions for design solution 4.

Type	Num	Force	Right End	Left End	From	To	Extension
A	8	173.79	Dead	Live	1	1	---
B	14	173.79	Dead	Live	1	1	0.00

Table 30. Required minimum post-tensioning forces for design solution 4.
Based on Stress Conditions Based on Minimum P/A

Type	Left	Center	Right	Left	Center	Right
	kN	kN	kN	kN	kN	kN
1	0.00	3390.84	0.00	2820.00	2820.00	2820.00

Table 31. Required rebar for design solution 4.

Span	Location	From	To	As Required	Ultimate	Minimum
		m	m	mm2	mm2	mm2
1	TOP	1.70	6.80	3959.00	3959.00	0.00
1	BOT	2.55	5.53	1617.00	0.00	1617.00

Table 32. Adapt selected rebar for design solution 4.

Span	ID	Location	From	Quantity	Size	Length	Area
			m			m	mm2
1	1	TOP	0.97	5	25	6.56	2453.15
1	2	TOP	1.83	4	25	4.86	1962.52
1	3	BOT	2.13	2	25	3.82	981.26
1	4	BOT	2.55	2	25	2.98	981.26

APPENDIX B – VERIFICATION BY CODE-BASED METHODS

The alternating parameters are highlighted in yellow and the central results in green.

Preliminary section – midspan – top

The National Building Code of Finland

$h = 700\text{mm}$	
$b = 1400\text{mm}$	
$M = (2004.97 - 599.63)\text{kN m}$	$M = 1.405 \times 10^3 \text{ kN m}$
$M_d = (1.2 \cdot 2004.97 - 0.9 \cdot 599.63)\text{kN m}$	$M_d = 1.866 \times 10^3 \text{ kN m}$
$P = 176.8\text{kN}$	
$n_{p1} = 8$	
$e_1 = 100\text{mm}$	
$n_{p2} = 12$	
$e_2 = 600\text{mm}$	
$n_p = n_{p1} + n_{p2}$	$n_p = 20$
$e_p = 400\text{mm}$	
$P_{\text{tot}} = n_p \cdot P$	$P_{\text{tot}} = 3.537 \times 10^3 \text{ kN}$
$P_d = 0.9 \cdot P_{\text{tot}}$	$P_d = 3.183 \times 10^3 \text{ kN}$
$c = 35\text{mm}$	
$d = h - c$	$d = 665\text{mm}$
$e = d - e_p$	$e = 265\text{mm}$
$f_y = 500 \frac{\text{N}}{\text{mm}^2}$	$\gamma_s = 1.20$
$f_{yd} = \frac{f_y}{\gamma_s}$	$f_{yd} = 416.667 \frac{\text{N}}{\text{mm}^2}$
$\phi_s = 25\text{mm}$	
$n_s = 10$	

$$A_{s1} = \pi \left(\frac{\phi_s}{2} \right)^2$$

$$A_{s1} = 490.874 \text{ mm}^2$$

$$A_s = A_{s1} n_s$$

$$A_s = 4.909 \times 10^{-3} \text{ m}^2$$

$$F_{sd} = A_s f_{yd}$$

$$F_{sd} = 2.045 \times 10^3 \text{ kN}$$

$$f_{ck} = 36 \frac{\text{N}}{\text{mm}^2}$$

$$\gamma_c = 1.50$$

$$f_{cd} = \frac{f_{ck}}{\gamma_c}$$

$$f_{cd} = 24 \frac{\text{N}}{\text{mm}^2}$$

$$F_{cd} = P_d + F_{sd}$$

$$y = \frac{F_{cd}}{f_{cd} b}$$

$$y = 0.156 \text{ m}$$

$$M_d = 1.866 \times 10^3 \text{ kN m}$$

$$M_u = F_{sd} \left(d - \frac{y}{2} \right) + P_d \left(d - e - \frac{y}{2} \right)$$

$$M_u = 2.227 \times 10^3 \text{ kN m}$$

$$n_s = 7$$

$$A_{s1} = \pi \left(\frac{\phi_s}{2} \right)^2$$

$$A_{s1} = 490.874 \text{ mm}^2$$

$$A_s = A_{s1} n_s$$

$$A_s = 3.436 \times 10^{-3} \text{ m}^2$$

$$F_{sd} = A_s f_{yd}$$

$$F_{sd} = 1.432 \times 10^3 \text{ kN}$$

$$M_d = 1.866 \times 10^3 \text{ kN m}$$

$$M_u = F_{sd} \left(d - \frac{y}{2} \right) + P_d \left(d - e - \frac{y}{2} \right)$$

$$M_u = 1.866 \times 10^3 \text{ kN m}$$

$$A_{s, \text{req}} = \frac{M_d - P_d \left(d - e - \frac{y}{2} \right)}{f_{yd} \left(d - \frac{y}{2} \right)}$$

$$A_{s, \text{req}} = 3.436 \times 10^3 \text{ mm}^2$$

The Eurocodes

$$h = 700\text{mm}$$

$$b = 1400\text{mm}$$

$$M = (2004.97 - 599.63)\text{kN m}$$

$$M_d = (1.35 \cdot 2004.97 - 0.9 \cdot 599.63)\text{kN m}$$

$$f_y = 500 \frac{\text{N}}{\text{mm}^2}$$

$$\gamma_s = 1.15$$

$$f_{yd} = \frac{f_y}{\gamma_s}$$

$$\phi_s = 25\text{mm}$$

$$n_s = 10$$

$$A_{s1} = \pi \left(\frac{\phi_s}{2} \right)^2$$

$$A_s = A_{s1} n_s$$

$$F_{sd} = A_s f_{yd}$$

$$f_{ck} = 36 \frac{\text{N}}{\text{mm}^2}$$

$$\gamma_c = 1.5$$

$$f_{cd} = \frac{f_{ck}}{\gamma_c}$$

$$F_{cd} = P_d + F_{sd}$$

$$y = \frac{F_{cd}}{f_{cd} b}$$

$$M_d = 2.167 \times 10^3 \text{ kN m}$$

$$M_u = F_{sd} \left(d - \frac{y}{2} \right) + P_d \left(d - e - \frac{y}{2} \right)$$

$$M = 1.405 \times 10^3 \text{ kN m}$$

$$M_d = 2.167 \times 10^3 \text{ kN m}$$

$$f_{yd} = 434.783 \frac{\text{N}}{\text{mm}^2}$$

$$A_{s1} = 490.874 \text{ mm}^2$$

$$A_s = 4.909 \times 10^{-3} \text{ m}^2$$

$$F_{sd} = 2.134 \times 10^3 \text{ kN}$$

$$f_{cd} = 24 \frac{\text{N}}{\text{mm}^2}$$

$$y = 0.158 \text{ m}$$

$$M_u = 2.272 \times 10^3 \text{ kN m}$$

$$n_s = 10$$

$$A_{s1} = \pi \left(\frac{\phi_s}{2} \right)^2$$

$$A_{s1} = 490.874 \text{ mm}^2$$

$$A_s = A_{s1} n_s$$

$$A_s = 4.909 \times 10^{-3} \text{ m}^2$$

$$F_{sd} = A_s f_{yd}$$

$$F_{sd} = 2.134 \times 10^3 \text{ kN}$$

$$M_d = 2.167 \times 10^3 \text{ kN m}$$

$$M_u = F_{sd} \left(d - \frac{y}{2} \right) + P_d \left(d - e - \frac{y}{2} \right)$$

$$M_u = 2.272 \times 10^3 \text{ kN m}$$

$$A_{s, \text{req}} = \frac{M_d - P_d \left(d - e - \frac{y}{2} \right)}{f_{yd} \left(d - \frac{y}{2} \right)}$$

$$A_{s, \text{req}} = 4.497 \times 10^3 \text{ mm}^2$$

Preliminary section – midspan – bottom

The National Building Code of Finland

$$b = 1400 \text{ mm}$$

$$h = 700 \text{ mm}$$

$$A_c = b h$$

$$A_c = 9.8 \times 10^5 \text{ mm}^2$$

$$f_y = 500 \frac{\text{N}}{\text{mm}^2}$$

$$\phi_s = 25 \text{ mm}$$

$$K = 45$$

$$f_{ctk} = 0.2 (K)^{\frac{2}{3}} \frac{\text{N}}{\text{mm}^2}$$

$$f_{ctk} = 2.53 \frac{\text{N}}{\text{mm}^2}$$

$$A_{s, \text{min}} = 0.5 A_c \frac{f_{ctk}}{f_y}$$

$$A_{s, \text{min}} = 2.48 \times 10^3 \text{ mm}^2$$

$$n_s = 6$$

$$A_{s1} = \pi \left(\frac{\phi_s}{2} \right)^2$$

$$A_{s1} = 490.874 \text{ mm}^2$$

$$A_s = A_{s1} n_s$$

$$A_s = 2.945 \times 10^{-3} \text{ m}^2$$

Stress losses

Initial data

$$f_{puk} = 1770 \frac{N}{mm^2}$$

$$f_{p0.2k} = 1570 \frac{N}{mm^2}$$

$$A_{p1} = 150mm^2$$

$$E_p = 200000 \frac{N}{mm^2}$$

$$P_1 = 0.8 \cdot f_{puk} \cdot A_{p1}$$

$$P_1 = 212.4kN$$

$$P_2 = 0.7 \cdot f_{puk} \cdot A_{p1}$$

$$P_2 = 185.85kN$$

$$\sigma_{p1} = 0.8 \cdot f_{puk}$$

$$\sigma_{p1} = 1.416 \times 10^3 \frac{N}{mm^2}$$

$$\sigma_{p2} = 0.7 \cdot f_{puk}$$

$$\sigma_{p2} = 1.239 \times 10^3 \frac{N}{mm^2}$$

Losses due to friction

$$\mu = 0.07$$

$$\beta = 0.00459 \frac{rad}{m}$$

$$k = e^{-\mu \left[\left(\sum_n \alpha \right) + \beta \cdot x \right]}$$

$$\alpha = 0$$

$$L = 8.5m$$

$$x_1 = 0m$$

$$x_2 = \frac{L}{2}$$

$$x_2 = 4.25m$$

$$x_3 = L$$

$$x_3 = 8.5m$$

$$k_1 = e^{-\mu \cdot \beta \cdot x_1}$$

$$k_1 = 1$$

$$k_2 = e^{-\mu \cdot \beta \cdot x_2}$$

$$k_2 = 0.999$$

$$k_3 = e^{-\mu \cdot \beta \cdot x_3}$$

$$k_3 = 0.997$$

Losses at anchorage

$$\delta_{mm} = \frac{(1 - k_1) \cdot \sigma_p \cdot x_1}{E_p}$$

$$\delta_{anch_1} = \frac{(1 - k_1) \cdot \sigma_{p1} \cdot x_1}{E_p}$$

$$\delta_{anch_1} = 0 \text{ m}$$

$$\delta_{anch_2} = \frac{(1 - k_2) \cdot \sigma_{p1} \cdot x_2}{E_p}$$

$$\delta_{anch_2} = 0.041 \text{ mm}$$

$$\delta_{anch_3} = \frac{(1 - k_3) \cdot \sigma_{p1} \cdot x_3}{E_p}$$

$$\delta_{anch_3} = 0.164 \text{ mm}$$

$$x_{\text{test}} = 52 \text{ m}$$

$$k_{\text{test}} = e^{-\mu \beta x_{\text{test}}}$$

$$k_{\text{test}} = 0.983$$

$$\delta_{\text{anch}_{\text{test}}} = \frac{(1 - k_{\text{test}}) \cdot \sigma_{p1} \cdot x_{\text{test}}}{E_p}$$

$$\delta_{\text{anch}_{\text{test}}} = 6.1 \text{ mm}$$

Final losses due to friction including losses at anchorage

$$k_{1.\text{tot}} = k_1 - 2 \cdot \frac{(1 - k_{\text{test}})}{x_{\text{test}}} \cdot (x_{\text{test}} - x_1)$$

$$k_{1.\text{tot}} = 0.967$$

$$k_{2.\text{tot}} = k_2 - 2 \cdot \frac{(1 - k_{\text{test}})}{x_{\text{test}}} \cdot (x_{\text{test}} - x_2)$$

$$k_{2.\text{tot}} = 0.968$$

$$k_{3.\text{tot}} = k_3 - 2 \cdot \frac{(1 - k_{\text{test}})}{x_{\text{test}}} \cdot (x_{\text{test}} - x_3)$$

$$k_{3.\text{tot}} = 0.97$$

$$k_{\text{ave}} = \frac{k_{1.\text{tot}} + k_{2.\text{tot}} + k_{3.\text{tot}}}{3}$$

$$k_{\text{ave}} = 0.968$$

$$k_{\text{max}} = \max(k_{1.\text{tot}}, k_{2.\text{tot}}, k_{3.\text{tot}})$$

$$k_{\text{max}} = 0.97$$

$$P_{\text{ave}} = P_2 \cdot \frac{k_{\text{ave}}}{k_{\text{max}}}$$

$$P_{\text{ave}} = 185.592 \text{ kN}$$

$$n_p = 20$$

$$P_{\text{ave.tot}} = P_{\text{ave}} \cdot n_p$$

$$P_{\text{ave.tot}} = 3.712 \times 10^3 \text{ kN}$$

$$\frac{P_{\text{ave}}}{k_{\text{ave}}} = 191.687 \text{ kN}$$

Losses due to instantaneous deformation of concrete

$$\Delta P = P_{ave} \cdot \frac{E_p \cdot A_{p1}}{E_c \cdot L \cdot h}$$

$$K_j = 27$$

$$E_{cj} = 5000 \sqrt{K_j} \frac{N}{mm^2}$$

$$E_{cj} = 2.598 \times 10^4 \frac{N}{mm^2}$$

$$h = 700mm$$

$$\Delta P = P_{ave} \cdot \frac{E_p \cdot A_{p1}}{E_{cj} \cdot L \cdot h}$$

$$\Delta P = 0.036kN$$

$$\Delta P_{tot} = \frac{(n_p - 1)}{2} \cdot n_p \cdot \Delta P$$

$$\Delta P_{tot} = 6.843kN$$

$$P_0 = P_{ave} \cdot n_p - \Delta P_{tot}$$

$$P_0 = 3.705 \times 10^3 kN$$

$$P_{0.1} = \frac{P_0}{n_p}$$

$$P_{0.1} = 185.25kN$$

$$\sigma_{p,0.1} = \frac{P_{0.1}}{A_{p1}}$$

$$\sigma_{p,0.1} = 1.235 \times 10^3 \frac{N}{mm^2}$$

Losses due to creep and shrinkage

$$\Delta \sigma_p = \left(1 - e^{-\kappa \cdot \phi_{inf}}\right) \cdot \frac{A_c}{A_p} \cdot \left(\frac{P_0}{A_c} + \frac{\epsilon_{cs} \cdot E_c}{\phi_{inf}}\right)$$

$$b = 6m$$

$$b_w = 1400mm$$

$$h_f = 400mm$$

$$h_w = 300mm$$

$$A_c = b \cdot h_f + b_w \cdot h_w$$

$$A_c = 2.82m^2$$

$$A_p = A_{p1} \cdot n_p$$

$$A_p = 3 \times 10^3 mm^2$$

$$h_e = \frac{A_c}{\left[\frac{b + 2 \cdot h_f + 2 \cdot h_w + b_w + (b - b_w)}{2}\right]}$$

$$h_e = 0.421m$$

$$K = 45$$

$$E_c = 5000 \sqrt{K} \frac{N}{mm^2}$$

$$E_c = 3.354 \times 10^4 \frac{N}{mm^2}$$

$$\kappa = \frac{E_p \cdot A_p}{E_p \cdot A_p + E_c \cdot A_c}$$

$$\kappa = 6.303 \times 10^{-3}$$

$$\varepsilon_{cs0} = 0.1 \text{ promille}$$

$$k_{sh} = 0.55$$

$$k_{sn} = 1.0$$

$$k_{si} = 0.15$$

$$\varepsilon_{cs} = k_{sh} \cdot \varepsilon_{cs0} \cdot (k_{sn} - k_{si})$$

$$\varepsilon_{cs} = 0.047 \text{ promille}$$

$$k_t = \max \left(2.5 - 1.5 \frac{K_j}{K}, 1.0 \right)$$

$$k_t = 1.6$$

$$k_{ch} = 0.72$$

$$\phi_0 = 1.25$$

$$\phi_{inf} = k_t \cdot k_{ch} \cdot \phi_0$$

$$\phi_{inf} = 1.44$$

$$\Delta\sigma_p = \left(1 - e^{-\kappa \phi_{inf}} \right) \cdot \frac{A_c}{A_p} \cdot \left(\frac{P_0}{A_c} + \frac{\varepsilon_{cs} \cdot E_c}{\phi_{inf}} \right)$$

$$\Delta\sigma_p = 20.408 \frac{\text{N}}{\text{mm}^2}$$

Losses due to steel relaxation

$$\Delta\sigma_{p,rel} = \Delta\sigma_{p,rel,inf} \left(1 - \frac{2 \cdot \Delta\sigma_p}{\sigma_{p0}} \right)$$

$$\sigma_{p0} = \frac{P_0}{A_p}$$

$$\sigma_{p0} = 1.235 \times 10^3 \frac{\text{N}}{\text{mm}^2}$$

$$\Delta\sigma_{p,rel,inf} = 3 \cdot 2.5\% \sigma_{p0}$$

$$\Delta\sigma_{p,rel,inf} = 92.625 \frac{\text{N}}{\text{mm}^2}$$

$$\Delta\sigma_{p,rel} = \Delta\sigma_{p,rel,inf} \left(1 - \frac{2 \cdot \Delta\sigma_p}{\sigma_{p0}} \right)$$

$$\Delta\sigma_{p,rel} = 89.564 \frac{\text{N}}{\text{mm}^2}$$

Total time dependent loss

$$\Delta\sigma_{p,tot} = \Delta\sigma_p + \Delta\sigma_{p,rel}$$

$$\Delta\sigma_{p,tot} = 109.972 \frac{\text{N}}{\text{mm}^2}$$

$$\frac{\Delta\sigma_{p,tot}}{\sigma_{p0}} = 8.905\%$$

$$P_0 = 3.705 \times 10^3 \text{ kN}$$

$$P_{\text{inf}} = P_0 - P_0 \cdot \frac{\Delta\sigma_{\text{p.tot}}}{\sigma_{\text{p0}}}$$

$$P_{\text{inf}} = 3.375 \times 10^3 \text{ kN}$$

$$P_{\text{inf.1}} = P_{0.1} - P_{0.1} \cdot \frac{\Delta\sigma_{\text{p.tot}}}{\sigma_{\text{p0}}}$$

$$P_{\text{inf.1}} = 168.754 \text{ kN}$$

$$\sigma_{\text{p.inf.1}} = \frac{P_{\text{inf.1}}}{A_{\text{p1}}}$$

$$\sigma_{\text{p.inf.1}} = 1.125 \times 10^3 \frac{\text{N}}{\text{mm}^2}$$

APPENDIX C – SEPARATE BEAM AND SLAB ANALYSIS

Separate beam analysis

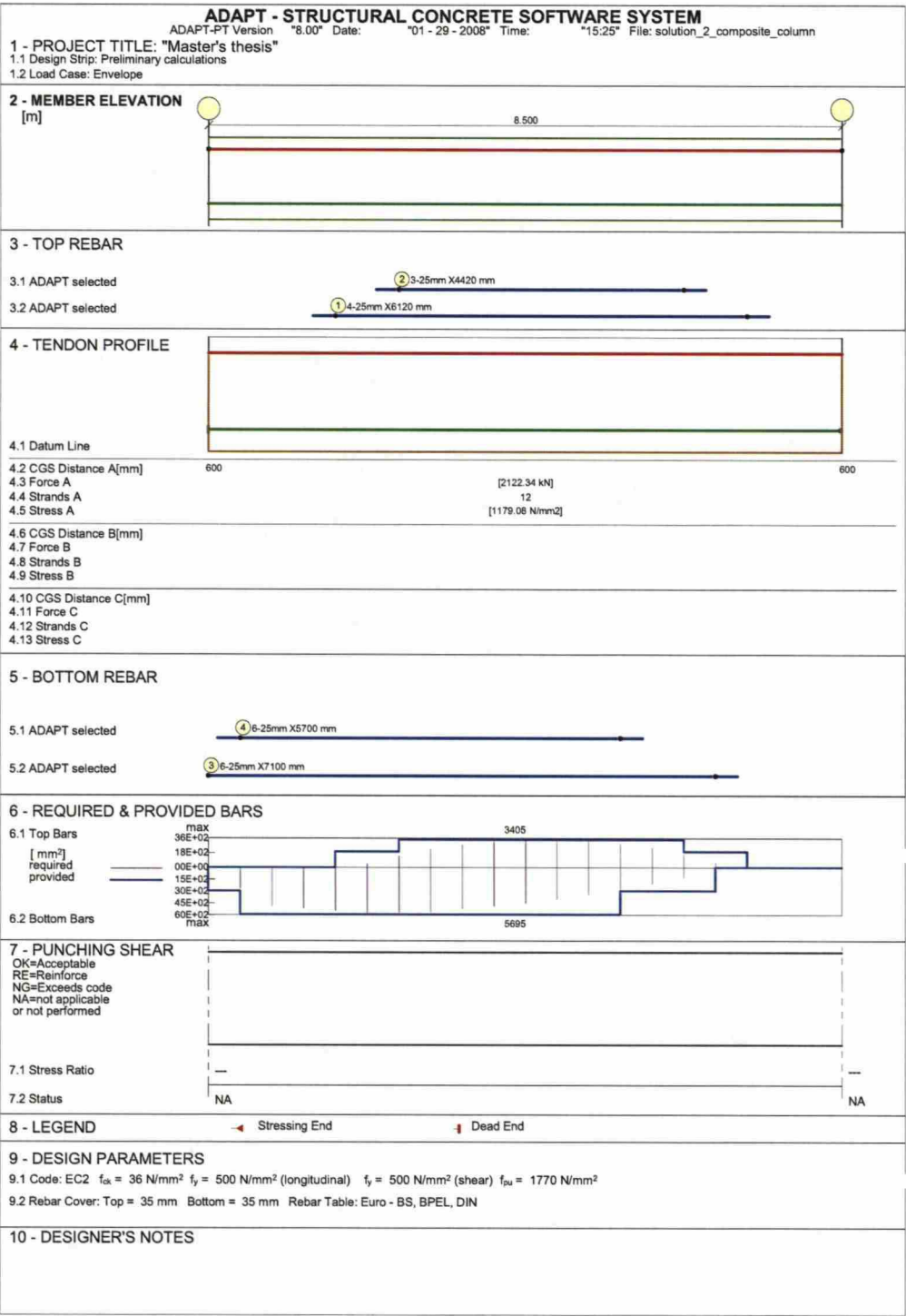


Figure 69. Adapt-PT summary report for the beam carrying the point load.

Table 33. Selected post-tensioning forces and tendon drape for the beam carrying the point load.

Tendon A

Span	Force	CGS Left	CSG C1	CGS C2	CGS Right	P/A	Wbal	WBal (%DL)
	kN	mm	mm	mm	mm	MPa	kN	
1	2122.337	600.00	---	---	600.00	0.75	0.000	0

Tendon B

Span	Force	CGS Left	CSG C1	CGS C2	CGS Right	P/A	Wbal	WBal (%DL)
	kN	mm	mm	mm	mm	MPa	kN	
1	1414.891	100.00	---	---	100.00	0.50	0.000	0

Table 34. Number of tendons and stressing conditions for design the beam carrying the point load.

Type	Num	Force	Right End	Left End	From	To	Extension
A	12	176.85	Dead	Live	1	1	---
B	8	176.85	Dead	Live	1	1	0.00

Table 35. Required minimum post-tensioning forces for design the beam carrying the point load.

Type	Based on Stress Conditions			Based on Minimum P/A		
	Left	Center	Right	Left	Center	Right
	kN	kN	kN	kN	kN	kN
1	0.00	11938.12	0.00	2820.00	2820.00	2820.00

Table 36. Required rebar for the beam carrying the point load.

Span	Location	From	To	As Required	Ultimate	Minimum
		m	m	mm2	mm2	mm2
1	TOP	2.13	6.80	3405.00	3405.00	0.00
1	BOT	0.42	6.38	5695.00	2039.00	5695.00

Table 37. Adapt selected rebar for the beam carrying the point load.

Span	ID	Location	From	Quantity	Size	Length	Area
			m			m	mm2
1	1	TOP	1.40	4	25	6.12	1962.52
1	2	TOP	2.25	3	25	4.42	1471.89
1	3	BOT	0.00	6	25	7.10	2943.78
1	4	BOT	0.13	6	25	5.70	2943.78

Slab

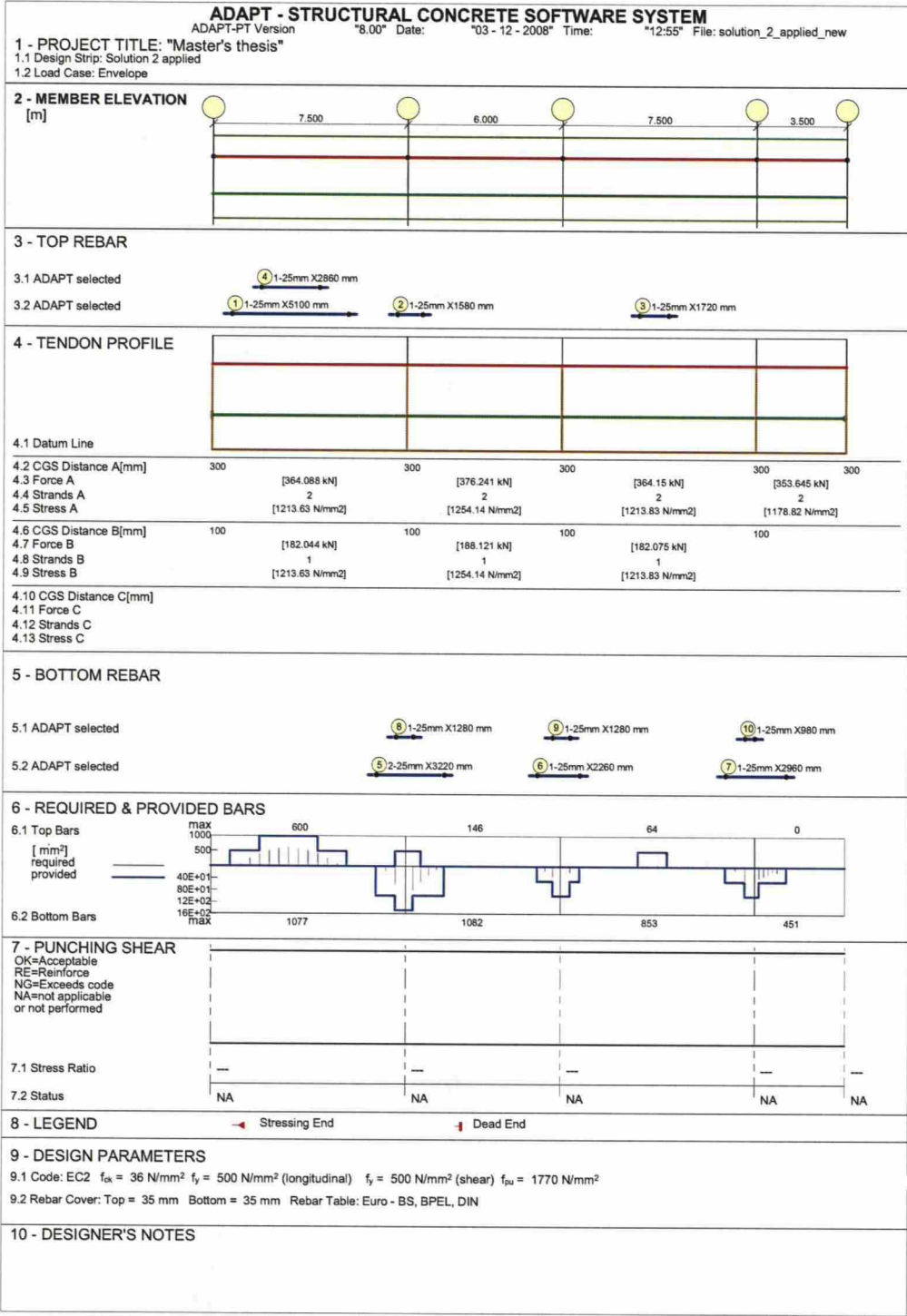


Figure 70. Adapt-PT summary report for the slab section.

Table 38. Selected post-tensioning forces and tendon drape for the slab section.
Tendon A

Span	Force	CGS Left	CSG C1	CGS C2	CGS Right	P/A	Wbal	WBal (%DL)
	kN	mm	mm	mm	mm	MPa	kN	
1	364.088	300.00	---	---	300.00	0.91	0.000	0
2	376.241	300.00	---	---	300.00	0.94	0.000	0
3	364.150	300.00	---	---	300.00	0.91	0.000	0
4	353.645	300.00	---	---	300.00	0.88	0.000	0

Tendon B

Span	Force	CGS Left	CSG C1	CGS C2	CGS Right	P/A	Wbal	WBal (%DL)
	kN	mm	mm	mm	mm	MPa	kN	
1	182.044	100.00	---	---	100.00	0.46	0.000	0
2	188.121	100.00	---	---	100.00	0.47	0.000	0
3	182.075	100.00	---	---	100.00	0.46	0.000	0
4	176.822	100.00	---	---	100.00	0.44	0.000	0

Table 39. Number of tendons and stressing conditions for design the slab section.

Type	Num	Force	Right End	Left End	From	To	Extension
A	2	182.49	Dead	Live	1	4	---
B	1	182.49	Dead	Live	1	4	0.00

Table 40. Required minimum post-tensioning forces for design the slab section.

Type	Based on Stress Conditions			Based on Minimum P/A		
	Left	Center	Right	Left	Center	Right
	kN	kN	kN	kN	kN	kN
1	0.00	295.19	0.00	400.00	400.00	700.00
2	0.00	0.00	0.00	700.00	400.00	700.00
3	0.00	0.00	0.00	700.00	400.00	700.00
4	0.00	0.00	0.00	700.00	400.00	400.00

Table 41. Required rebar for the slab section.

Span	Location	From	To	As Required	Ultimate	Minimum
		m	m	mm2	mm2	mm2
1	TOP	1.13	4.88	600.20	600.20	0.00
1	TOP	7.50	7.50	141.50	141.50	0.00
2	TOP	0.00	0.30	145.90	145.90	0.00
3	TOP	3.38	3.75	47.18	47.18	0.00
1	BOT	6.75	7.50	1077.00	1077.00	0.00
2	BOT	0.00	1.20	1082.00	1082.00	0.00
2	BOT	5.40	6.00	558.10	558.10	0.00
3	BOT	0.00	0.38	553.00	553.00	0.00
3	BOT	6.75	7.50	853.20	853.20	0.00
4	BOT	0.00	1.05	450.70	450.70	0.00

Table 42. Adapt selected rebar for the slab section.

Span	ID	Location	From	Quantity	Size	Length	Area
			m			m	mm2
1	1	TOP	0.45	1	25	5.10	490.63
1	2	TOP	6.83	1	25	1.58	490.63
3	3	TOP	2.70	1	25	1.72	490.63
1	4	TOP	1.58	1	25	2.86	490.63
1	5	BOT	6.08	2	25	3.22	981.26
2	6	BOT	4.80	1	25	2.26	490.63
3	7	BOT	6.07	1	25	2.96	490.63
1	8	BOT	6.83	1	25	1.28	490.63
2	9	BOT	5.40	1	25	1.28	490.63
3	10	BOT	6.82	1	25	0.98	490.63

APPENDIX D – CRACK WIDTH CALCULATIONS

The alternating parameters are highlighted in yellow and the central results in green.

Preliminary section- midspan- bottom

$$w_k = [s_{r,max}(\epsilon_{sm} - \epsilon_{cm})]$$

$$h = 700\text{mm}$$

$$b_w = 1400\text{mm}$$

$$b_0 = 6\text{m}$$

$$c = 35\text{mm}$$

$$c_p = 100\text{mm}$$

$$\phi_s = 25\text{mm}$$

$$x_s = 6$$

$$A_s = \pi \left(\frac{\phi_s}{2} \right)^2 x_s$$

$$A_s = 2.945 \times 10^3 \text{ mm}^2$$

$$A_{p1} = 150\text{mm}^2$$

$$E_s = 200000 \frac{\text{N}}{\text{mm}^2}$$

$$E_{cm} = 34000 \frac{\text{N}}{\text{mm}^2}$$

$$M_k = (599.63 + 135.47) \text{ kN m}$$

$$M_k = 735.1 \text{ kN m}$$

$$P_1 = 1414.8 \text{ kN}$$

$$P_2 = 2122.34 \text{ kN}$$

$$P = P_1 + P_2$$

$$P = 3.537 \times 10^3 \text{ kN}$$

$$d_{p1} = 600\text{mm}$$

$$d_{p2} = 100\text{mm}$$

$$d_p = \frac{d_{p1} P_1 + d_{p2} P_2}{P}$$

$$d_p = 0.3\text{m}$$

$$d_s = h - c$$

$$d_s = 665\text{mm}$$

$$h_f = 400\text{mm}$$

$$K_p = \frac{M_k - P d_p}{P d_s} \quad K_p = -0.139$$

$$\rho = \frac{A_s}{b_w d_s} \quad \rho = 3.164 \times 10^{-3}$$

$$\alpha_e = \frac{E_s}{E_{cm}} \quad \alpha_e = 5.882$$

$$a_1 = \frac{h_f}{d_s} \quad a_1 = 0.602$$

$$a_2 = \frac{b_w}{b_0} \quad a_2 = 0.233$$

$$K_1 = 6 \alpha_e \rho (1 + K_p) \quad K_1 = 0.096$$

$$K_2 = 3 a_1 (a_1 + 2 K_p) \quad K_2 = 0.585$$

$$K_3 = a_1^2 (2 a_1 + 3 K_p) \quad K_3 = 0.285$$

$$\xi^3 + 3 K_p \xi^2 + \left(\frac{K_1 + K_2}{a_2} - K_2 \right) \xi + \left(K_3 - \frac{K_3 + K_1}{a_2} \right) = 0$$

$$\xi = 0.558$$

$$x = \xi d_s \quad x = 371.277 \text{ mm}$$

$$\sigma_c = \frac{P}{b_w d_s} \left[\frac{2 \xi}{a_1 (2 \xi - a_1) + a_2 (\xi - a_1)^2 - 2 \alpha_e \rho (1 - \xi)} \right] \quad \sigma_c = 14.438 \frac{\text{N}}{\text{mm}^2}$$

$$\sigma_s = \sigma_c \left(\frac{1 - \xi}{\xi} \right) \alpha_e$$

$$\sigma_s = 67.189 \frac{\text{N}}{\text{mm}^2}$$

$$s_{r,max} = k_3 c + k_1 k_2 k_4 \frac{\phi}{\rho_{p,eff}}$$

$$k_1 = 0.8$$

$$k_2 = 0.5$$

$$k_3 = 3.4$$

$$k_4 = 0.425$$

$$A_{wire} = \frac{A_{p1}}{7} \quad \phi_{wire} = 2 \sqrt{\frac{A_{wire}}{\pi}}$$

$$\phi_{wire} = 5.223 \text{ mm}$$

$$\phi_p = 1.75 \phi_{wire}$$

$$\phi_p = 9.141 \text{ mm}$$

$$\xi = 0.7$$

$$\xi_1 = \sqrt{\xi \frac{\phi_s}{\phi_p}}$$

$$\xi_1 = 1.384$$

$$d = h - \left(\frac{c_p - c}{2} + c \right)$$

$$d = 632.5 \text{ mm}$$

$$h_{c,eff} = \min \left[2.5 (h - d), \frac{(h - x)}{3}, \frac{h}{2} \right]$$

$$h_{c,eff} = 0.11 \text{ m}$$

$$A_{c,eff} = h_{c,eff} b_w$$

$$A_{c,eff} = 1.534 \times 10^5 \text{ mm}^2$$

$$n_p = 8$$

$$A'_p = A_{p1} n_p$$

$$A'_p = 1.2 \times 10^3 \text{ mm}^2$$

$$\rho_{p,eff} = \frac{(A_s + \xi_1^2 A'_p)}{A_{c,eff}}$$

$$\rho_{p,eff} = 0.034$$

$$s_{r,max} = k_3 c + k_1 k_2 k_4 \frac{\phi_s}{\rho_{p,eff}}$$

$$s_{r,max} = 243.359 \text{ mm}$$

$$\varepsilon_{sm} - \varepsilon_{cm} = \frac{\sigma_s - k_t \frac{f_{ct,eff}}{\rho_{p,eff}} (1 + \alpha_e \rho_{p,eff})}{E_s} \geq 0.6 \frac{\sigma_s}{E_s}$$

$$k_t = 0.4$$

$$f_{ct,eff} = 3.2 \frac{N}{mm^2}$$

$$\varepsilon = 2.016 \times 10^{-4}$$

$$w_k = s_{r,max} \varepsilon$$

$$w_k = 0.049 mm$$

$$A_{s,min} = \frac{k_c k f_{ct,eff} A_{ct}}{\sigma_s}$$

$$h_{area} = 300 mm$$

$$h' = \begin{cases} h & \text{if } h < 1.0m \\ (1.0m) & \text{if } h \geq 1.0m \end{cases}$$

$$h' = 0.7m$$

$$h_{tens} = \min[h_{area}, h_{area} - (x - 400mm)]$$

$$h_{tens} = 0.3m$$

$$A_{ct} = b_w h_{tens}$$

$$A_{ct} = 4.2 \times 10^5 mm^2$$

$$k_1 = 1.5$$

$$\sigma_c = \frac{P_1}{b_w h_{area}}$$

$$\sigma_c = 3.369 \frac{N}{mm^2}$$

$$k_c = \min \left[1, 0.4 \left[1 - \frac{\sigma_c}{k_1 \left(\frac{h}{h'} \right) f_{ct,eff}} \right] \right]$$

$$k_c = 0.119$$

$$k = 0.9$$

$$\sigma_s = 500 \frac{N}{mm^2}$$

$$A_{s,min} = \frac{k_c k f_{ct,eff} A_{ct}}{\sigma_s}$$

$$A_{s,min} = 288.533 mm^2$$

Preliminary section – midspan – top

$$n_s = 10$$

$$\phi_s = 25\text{mm}$$

$$A_s = \pi \left(\frac{\phi_s}{2} \right)^2 n_s$$

$$A_s = 4.909 \times 10^3 \text{ mm}^2$$

$$M_k = (2004.97 - 599.63) \text{ kN m}$$

$$M_k = 1.405 \times 10^3 \text{ kN m}$$

$$P_1 = 2122.34 \text{ kN}$$

$$P_2 = 1414.89 \text{ kN}$$

$$P = P_1 + P_2$$

$$P = 3.537 \times 10^3 \text{ kN}$$

$$\sigma_c = 19.21 \frac{\text{N}}{\text{mm}^2}$$

$$\sigma_s = 129.223 \frac{\text{N}}{\text{mm}^2}$$

$$s_{r,\max} = 211.528 \text{ mm}$$

$$\varepsilon = 4.691 \times 10^{-4}$$

$$w_k = 0.099 \text{ mm}$$

$$A_{s,\min} = 1.244 \times 10^4 \text{ mm}^2$$

$$\frac{A_{s,\min}}{b} = 2.074 \times 10^3 \frac{\text{mm}^2}{\text{m}}$$

Beam including the point load – midspan – bottom

$$\phi_s = 25\text{mm}$$

$$n_s = 12$$

$$A_s = \pi \left(\frac{\phi_s}{2} \right)^2 n_s$$

$$A_s = 5.89 \times 10^3 \text{ mm}^2$$

$$M_k = (599.63 + 264.01 + 285.47) \text{ kN m}$$

$$M_k = 1.149 \times 10^3 \text{ kN m}$$

$$P_1 = 1414.89 \text{ kN}$$

$$P_2 = 2122.34 \text{ kN}$$

$$P = P_1 + P_2$$

$$P = 3.537 \times 10^3 \text{ kN}$$

$$\sigma_c = 19.924 \frac{\text{N}}{\text{mm}^2}$$

$$\sigma_s = 125.343 \frac{\text{N}}{\text{mm}^2}$$

$$s_{r,\max} = 210.724 \text{ mm}$$

$$\varepsilon = 4.509 \times 10^{-4}$$

$$w_k = 0.095 \text{ mm}$$

$$A_{s,\min} = 288.533 \text{ mm}^2$$

Beam including the point load – midspan – top

$$x_s = 7$$

$$\phi_s = 25 \text{ mm}$$

$$A_s = \pi \left(\frac{\phi_s}{2} \right)^2 x_s$$

$$A_s = 3.436 \times 10^3 \text{ mm}^2$$

$$M_k = (2004.97 - 599.63 - 264.0) \text{ kN m}$$

$$M_k = 1.141 \times 10^3 \text{ kN m}$$

$$P_1 = 2122.34 \text{ kN}$$

$$P = 3.537 \times 10^3 \text{ kN}$$

$$P_2 = 1414.89 \text{ kN}$$

$$P = P_1 + P_2$$

$$\sigma_c = 15.266 \frac{\text{N}}{\text{mm}^2}$$

$$\sigma_s = 77.915 \frac{\text{N}}{\text{mm}^2}$$

$$s_{r,\max} = 218.118 \text{ mm}$$

$$\varepsilon = 2.337 \times 10^{-4}$$

$$w_k = 0.051 \text{ mm}$$

$$A_{s,\min} = \frac{k_c k_{f_{ct,eff}} A_{ct}}{\sigma_s}$$

$$A_{s,\min} = 1.244 \times 10^4 \text{ mm}^2$$

$$\frac{A_{s,\min}}{b} = 2.074 \times 10^3 \frac{\text{mm}^2}{\text{m}}$$

Slab section – midspan – bottom

$$n_s = 2$$

$$\phi_s = 25\text{mm}$$

$$A_s = \pi \left(\frac{\phi_s}{2} \right)^2 n_s$$

$$A_s = 981.748\text{mm}^2$$

$$M_k = (17.57 + 7.22)\text{kN m} \quad \text{Span 1}$$

$$M_k = 24.79\text{kN m}$$

$$P_1 = 178.144\text{kN}$$

$$P_2 = 356.288\text{kN}$$

$$P = P_1 + P_2$$

$$P = 534.432\text{kN}$$

$$d_{p1} = 300\text{mm}$$

$$d_{p2} = 100\text{mm}$$

$$d_p = \frac{d_{p1} P_1 + d_{p2} P_2}{P}$$

$$d_p = 0.167\text{m}$$

$$d_s = h - c$$

$$d_s = 365\text{mm}$$

$$K_p = \frac{M_k - P d_p}{P d_s}$$

$$K_p = -0.33$$

$$\rho = \frac{A_s}{b_w d_s}$$

$$\rho = 2.69 \times 10^{-3}$$

$$\alpha_e = \frac{E_s}{E_{cm}}$$

$$\alpha_e = 5.882$$

$$K_1 = 6 \alpha_e \rho (1 + K_p)$$

$$K_1 = 0.064$$

$$\xi^3 + 3 K_p \xi^2 + K_1 \xi - K_1 = 0$$

$$\xi = 0.989$$

$$x = \xi d_s$$

$$x = 361.097\text{mm}$$

$$a_1 = \left(\frac{1 - \xi}{\xi} \right) \alpha_e$$

$$a_1 = 0.064$$

$$\sigma_c = \frac{P}{b_w d_s} \left(\frac{2}{\xi - 2 a_1 \rho} \right)$$

$$\sigma_c = 2.961 \frac{\text{N}}{\text{mm}^2}$$

$$\sigma_s = a_1 \sigma_c$$

$$\sigma_s = 0.188 \frac{\text{N}}{\text{mm}^2}$$

$$s_{r,\max} = 162.433\text{mm}$$

$$\varepsilon = 5.648 \times 10^{-7}$$

$$w_k = 9.175 \times 10^{-5} \text{ mm}$$

$$A_{s,\min} = 81.317 \text{ mm}^2$$

Slab section – midspan – top

$$n_s = 1$$

$$\phi_s = 25 \text{ mm}$$

$$A_s = \pi \left(\frac{\phi_s}{2} \right)^2 n_s$$

$$A_s = 490.874 \text{ mm}^2$$

$$M_k = (68.93 - 17.57) \text{ kN m} \quad \text{Span 1}$$

$$M_k = 51.36 \text{ kN m}$$

$$P_1 = 356.28 \text{ kN}$$

$$P_2 = 178.144 \text{ kN}$$

$$P = P_1 + P_2$$

$$P = 534.432 \text{ kN}$$

$$d_{p1} = 300 \text{ mm}$$

$$d_{p2} = 100 \text{ mm}$$

$$d_p = \frac{d_{p1} P_1 + d_{p2} P_2}{P}$$

$$d_p = 0.233 \text{ m}$$

$$d_s = h - c$$

$$d_s = 365 \text{ mm}$$

$$K_p = \frac{M_k - P d_p}{P d_s}$$

$$K_p = -0.376$$

$$\rho = \frac{A_s}{b_w d_s}$$

$$\rho = 1.345 \times 10^{-3}$$

$$\alpha_e = \frac{E_s}{E_{cm}}$$

$$\alpha_e = 5.882$$

$$K_1 = 6 \alpha_e \rho (1 + K_p)$$

$$K_1 = 0.03$$

$$\xi^3 + 3 K_p \xi^2 + K_1 \xi - K_1 = 0$$

$$\xi = 1.125$$

$$x = \xi d_s$$

$$x = 410.626 \text{ mm} \quad x > h$$

Slab section – support – bottom

$$n_s = 3$$

$$\phi_s = 25 \text{ mm}$$

$$A_s = \pi \left(\frac{\phi_s}{2} \right)^2 n_s$$

$$A_s = 1.473 \times 10^3 \text{ mm}^2$$

$$M_k = (152.21 - 40.43) \text{ kN m} \quad \text{Span 1}$$

$$M_k = 111.78 \text{ kN m}$$

$$P_1 = 178.144 \text{ kN}$$

$$P_2 = 356.288 \text{ kN} \quad P = P_1 + P_2$$

$$P = 534.432 \text{ kN}$$

$$\sigma_c = 10.032 \frac{\text{N}}{\text{mm}^2}$$

$$\sigma_s = 99.604 \frac{\text{N}}{\text{mm}^2}$$

$$s_{r,\max} = 331.692 \text{ mm}$$

$$\varepsilon = 2.988 \times 10^{-4}$$

$$w_k = 0.099 \text{ mm}$$

$$A_{s,\min} = 552.254 \text{ mm}^2$$

Slab section – support – top

$$n_s = 2$$

$$\phi_s = 25 \text{ mm}$$

$$A_s = \pi \left(\frac{\phi_s}{2} \right)^2 n_s$$

$$A_s = 981.748 \text{ mm}^2$$

$$M_k = (40.43 + 11.92) \text{ kN m} \quad \text{Span 1}$$

$$M_k = 52.35 \text{ kN m}$$

$$P_1 = 356.288 \text{ kN}$$

$$P_2 = 178.144 \text{ kN} \quad P = P_1 + P_2$$

$$P = 534.432 \text{ kN}$$

$$d_{p1} = 300 \text{ mm}$$

$$d_{p2} = 100 \text{ mm}$$

$$d_p = \frac{d_{p1} P_1 + d_{p2} P_2}{P}$$

$$d_p = 0.233 \text{ m}$$

$$d_s = h - c$$

$$d_s = 365 \text{ mm}$$

$$K_p = \frac{M_k - P d_p}{P d_s}$$

$$K_p = -0.371$$

$$\rho = \frac{A_s}{b_w d_s}$$

$$\rho = 2.69 \times 10^{-3}$$

$$\alpha_e = \frac{E_s}{E_{cm}}$$

$$\alpha_e = 5.882$$

$$K_1 = 6 \alpha_e \rho (1 + K_p)$$

$$K_1 = 0.06$$

$$\xi^3 + 3 K_p \xi^2 + K_1 \xi - K_1 = 0$$

$$\xi = 1.107$$

$$x = \xi d_s$$

$$x = 404.227 \text{ mm} \quad x > h$$

APPENDIX E – JOINT REINFORCEMENT CALCULATIONS

The alternating parameters are highlighted in yellow and the central results in green.

Lateral loads

$$h_{\text{earth}} = 3750\text{mm}$$

$$h_{\text{water}} = 3700\text{mm}$$

$$b = 6000\text{mm}$$

$$q = 10 \frac{\text{kN}}{\text{m}^2}$$

$$k_{0w} = 1.0$$

$$\gamma_w = 10 \frac{\text{kN}}{\text{m}^3}$$

$$H_w = k_{0w} \gamma_w h_{\text{water}} b$$

$$H_w = 222 \frac{\text{kN}}{\text{m}}$$

$$\phi = 36\text{deg}$$

$$k_0 = 1 - \sin(\phi)$$

$$k_0 = 0.412$$

$$\gamma_{\text{gr}} = 18 \frac{\text{kN}}{\text{m}^3} - \gamma_w$$

$$\gamma_{\text{gr}} = 8 \frac{\text{kN}}{\text{m}^3}$$

$$H_g = k_0 \gamma_{\text{gr}} h_{\text{earth}} b$$

$$H_g = 74.199 \frac{\text{kN}}{\text{m}}$$

$$H_q = k_0 q b$$

$$H_q = 24.733 \frac{\text{kN}}{\text{m}}$$

Reinforcement calculations

Strength analysis

$$h = 300\text{mm}$$

$$b = 1\text{m}$$

$$c = 35\text{mm}$$

$$d = h - c$$

$$d = 265\text{mm}$$

$$f_{ck} = 35 \frac{\text{N}}{\text{mm}^2}$$

$$\gamma_c = 1.5$$

$$f_{cd} = \frac{f_{ck}}{\gamma_c}$$

$$f_{cd} = 23.333 \frac{\text{N}}{\text{mm}^2}$$

$$f_{ctm} = 3.2 \frac{\text{N}}{\text{mm}^2}$$

$$E_{cm} = 34000 \frac{\text{N}}{\text{mm}^2}$$

$$f_{yk} = 500 \frac{\text{N}}{\text{mm}^2}$$

$$\gamma_s = 1.15$$

$$f_{yd} = \frac{f_{yk}}{\gamma_s}$$

$$f_{yd} = 434.783 \frac{\text{N}}{\text{mm}^2}$$

$$E_s = 200000 \frac{\text{N}}{\text{mm}^2}$$

$$M_d = \frac{433.6 \text{ kN m}}{6}$$

$$M_d = 72.267 \text{ kN m}$$

$$\mu = \frac{M_d}{b d^2 f_{cd}}$$

$$\mu = 0.044$$

$$\beta = 1 - \sqrt{1 - 2\mu}$$

$$\beta = 0.045$$

$$z = d \left(1 - \frac{\beta}{2} \right)$$

$$z = 259.021 \text{ mm}$$

$$A_{s, \text{req}} = \frac{M_d}{z f_{yd}}$$

$$A_{s, \text{req}} = 641.697 \text{ mm}^2$$

$$A_{s, \text{min}} = 0.26 \frac{f_{ctm}}{f_{yk}} b d$$

$$A_{s, \text{min}} = 440.96 \text{ mm}^2$$

$$A_{s, \text{req}} = \max(A_{s, \text{req}}, A_{s, \text{min}})$$

$$A_{s, \text{req}} = 641.697 \text{ mm}^2$$

$$\phi_s = 16 \text{ mm}$$

$$A_{s1} = \pi \left(\frac{\phi_s}{2} \right)^2$$

$$A_{s1} = 201.062 \text{ mm}^2$$

$$n_s = 4$$

$$A_s = n_s A_{s1}$$

$$A_s = 804.248 \text{ mm}^2$$

Crack control

$$n_s = 7$$

$$A_s = n_s A_{s1}$$

$$A_s = 1.407 \times 10^3 \text{ mm}^2$$

$$\sigma_s = \frac{M_d}{A_s z}$$

$$\sigma_s = 198.232 \frac{\text{N}}{\text{mm}^2}$$

$$k_1 = 0.8$$

$$k_2 = 0.5$$

$$k_3 = 3.4$$

$$k_4 = 0.425$$

$$\alpha_e = \frac{E_s}{E_{cm}}$$

$$\alpha_e = 5.882$$

$$\rho = \frac{A_s}{b d}$$

$$\rho = 5.311 \times 10^{-3}$$

$$x = \alpha_e \rho \left(-1 + \sqrt{1 + \frac{2}{\alpha_e \rho}} \right) d$$

$$x = 58.477 \text{ mm}$$

$$h_{c,ef} = \min \left[2.5 (h - d), \frac{(h - x)}{3}, \frac{h}{2} \right]$$

$$h_{c,ef} = 0.081 \text{ m}$$

$$A_{c,eff} = h_{c,ef} b$$

$$A_{c,eff} = 8.051 \times 10^4 \text{ mm}^2$$

$$\rho_{p,eff} = \frac{A_s}{A_{c,eff}}$$

$$\rho_{p,eff} = 0.017$$

$$s_{r,max} = k_3 c + k_1 k_2 k_4 \frac{\phi_s}{\rho_{p,eff}}$$

$$s_{r,max} = 274.588 \text{ mm}$$

$$\varepsilon_{sm} - \varepsilon_{cm} = \frac{\sigma_s - k_t \frac{f_{ct,eff}}{\rho_{p,eff}} (1 + \alpha_e \rho_{p,eff})}{E_s} \geq 0.6 \frac{\sigma_s}{E_s}$$

$$k_t = 0.4$$

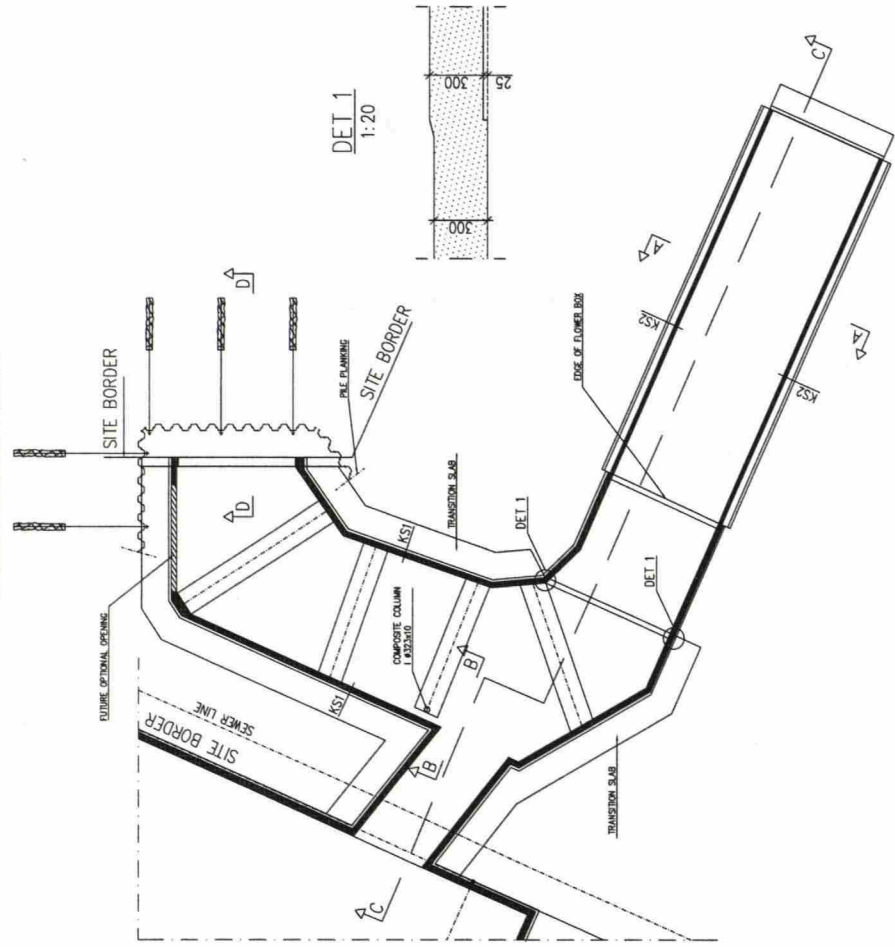
$$f_{ct,eff} = 3.2 \frac{\text{N}}{\text{mm}^2}$$

$$\varepsilon = 5.947 \times 10^{-4}$$

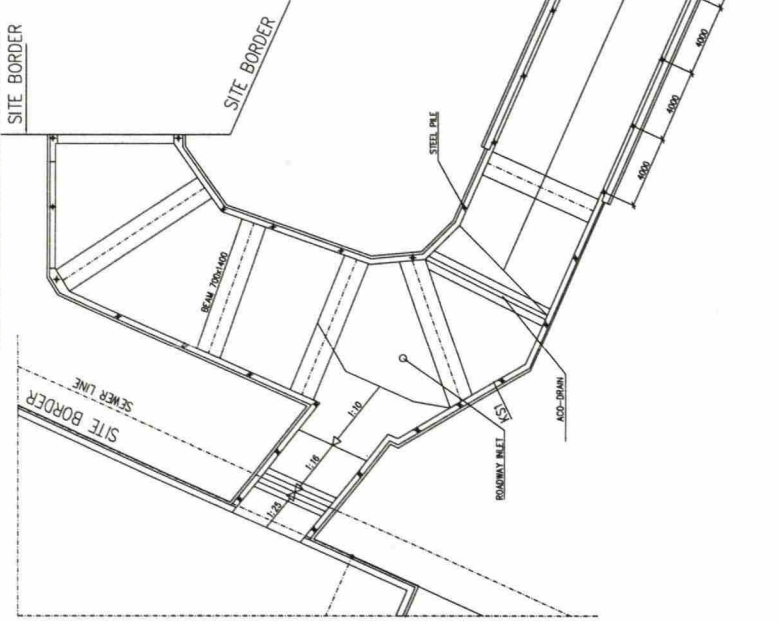
$$w_k = s_{r,max} \varepsilon$$

$$w_k = 0.163 \text{ mm}$$

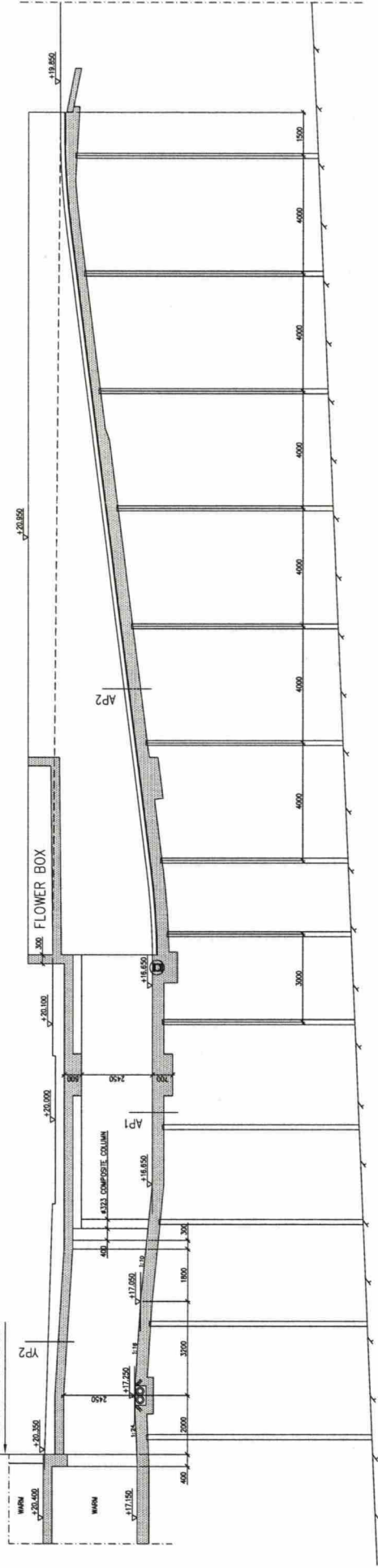
PLAN DRAWING 1:200



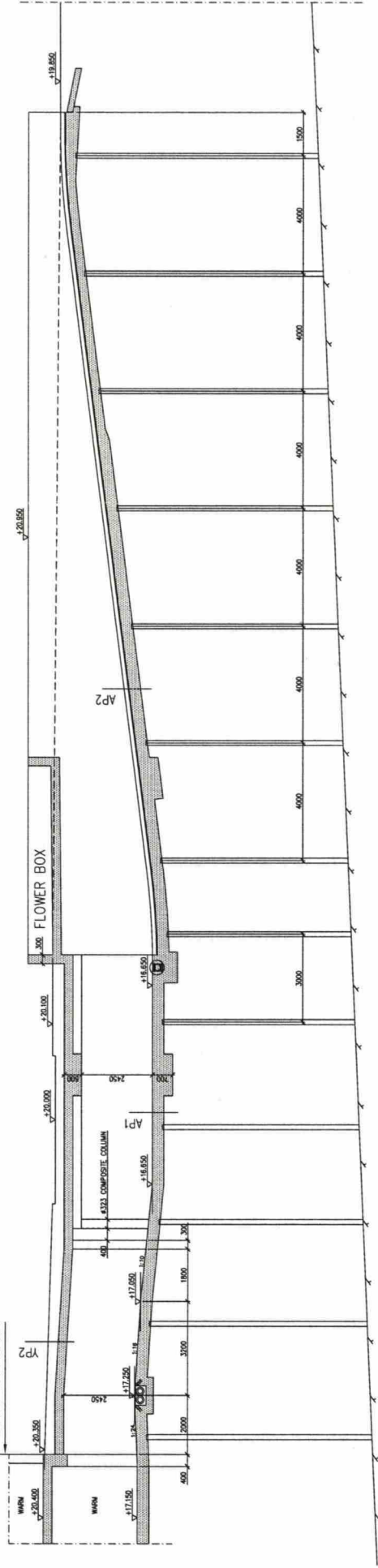
BOTTOM STRUCTURES 1:200



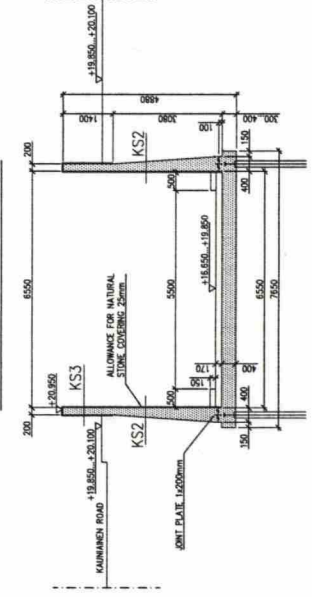
SECTION A - A 1:100



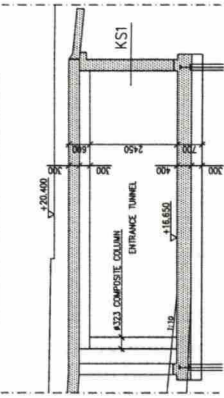
SECTION C - C 1:100



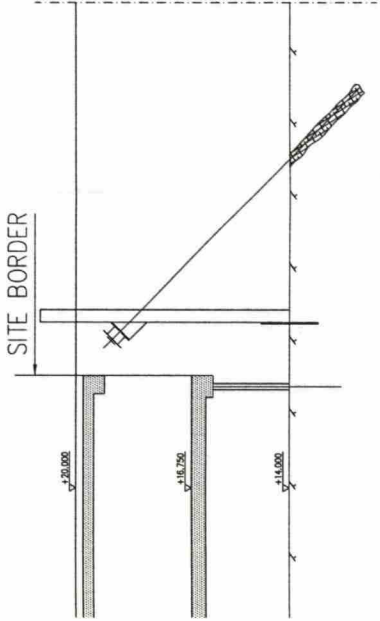
SECTION A - A 1:100



SECTION B - B 1:100



SECTION D - D 1:100



APPENDIX F. PRELIMINARY DRAWING

		KOSKIMÄKI 2 02210 ESPOO Puh. 09-887 91 fax 09-883 7715	
District 2	Quarter 250	Site 6	Archive number
Action NEW CONSTRUCTION	Document kind STRUCTURAL DRAWING	Document number	Consecutive number
Project PARKING STRUCTURE ENTRANCE TUNNEL	Title ENTRANCE TUNNEL AND RAMP	Scale	Scale
Client KAUNIAINEN CITY CENTRE	PLAN AND SECTION DRAWING		
Drawn JBL/G	Reference drawings	Document number	RAK 92-1102-0101 /
Checked JBL		Design Tero Merilinen	Client document number
Approved TBL		Date 05.09.2007	